

**DEVELOPMENT OF HIGH NATURAL FREQUENCY  
LOAD CELL FOR YARN TENSION SENSORS**

**Mohamad Yazan SADOON**



T.C.  
BURSA ULUDAĞ UNIVERSITY  
GRADUATE SCHOOL OF NATURAL AND APPLIED SCIENCES

**DEVELOPMENT OF HIGH NATURAL FREQUENCY LOAD CELL FOR  
YARN TENSION SENSORS**

Mohamad Yazan Sadoun  
0000-0002-7869-4212

Prof. Dr. Recep EREN  
(Supervisor)

MSc THESIS  
DEPARTMENT OF TEXTILE ENGINEERING

BURSA – 2020  
**All Rights Reserved**

## THESIS APPROVAL

This thesis titled "DEVELOPMENT OF HIGH NATURAL FREQUENCY LOAD CELL FOR YARN TENSION SENSORS" and prepared by Mohamad Yazan SADOON has been accepted as a **MSc THESIS** in Bursa Uludağ University Graduate School of Natural and Applied Sciences, Department of Textile Engineering following a unanimous vote of the jury below.

**Supervisor** : Prof. Dr. Recep EREN

**Head** : Prof. Dr. Recep EREN  
0000-0001-9389-0281  
Bursa Uludağ University,  
Faculty of Engineering,  
Department of Textile Engineering

Signature

**Member:** Prof. Dr. Hasan Basri KOÇER  
0000-0003-2612-6712  
Bursa Technical University,  
Faculty of Engineering and Natural Sciences,  
Department of Polymer Materials Engineering

Signature

**Member:** Asst.Prof. Dr. Özge ÇELİK  
0000-0002-3558-9068  
Bursa Uludağ University,  
Faculty of Engineering,  
Department of Textile Engineering

Signature

**I approve the above result**

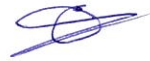
**Prof. Dr. Hüseyin Aksel EREN**  
**Institute Director**  
**19/01/2021**

**I declare that this thesis has been written in accordance with the following thesis writing rules of the U.U Graduate School of Natural and Applied Sciences;**

- All the information and documents in the thesis are based on academic rules,
- audio, visual and written information and results are in accordance with scientific code of ethics,
- in the case that the works of others are used, I have provided attribution in accordance with the scientific norms,
- I have included all attributed sources as references,
- I have not tampered with the data used,
- and that I do not present any part of this thesis as another thesis work at this university or any other university.

**19/01/2021**

**Mohamad Yazan SADOON**



## ÖZET

Yüksek Lisans Tezi

### İPLİK GERGINLİK SENSÖRLERİ İÇİN YÜKSEK DOĞAL FREKANSLI YÜK HÜCRESİ GELİŞTİRİLMESİ

**Mohamad Yazan SADOUN**

Bursa Uludağ Üniversitesi  
Fen Bilimleri Enstitüsü  
Tekstil Mühendisliği Anabilim Dalı

**Danışman:** Prof. Dr. Recep EREN

Bu yüksek lisans tezinde, yük hücresi tabanlı iplik gerginlik sensörleri tasarlanmış, üretilmiş ve deneysel olarak test edilmiştir. Tasarım süreci, yük hücresinin fiziksel ve matematiksel temellerini inceleyerek, çalışma prensiplerini inceleyerek ve bilimsel bir literatür taraması yaparak başladı. Geliştirme aşamasında, yük hücreleri bir CAD programı (Solidworks) tarafından tasarlandı ve tüm tasarım özellikleri bir FEA programında (ANSYS) çalışıldı. Analiz sürecinde odaklanılan özellikler arasında doğal frekans ve gerinim seviyeleri vardı. Farklı geometriye sahip üç yük hücresi tasarımı seçildi ve tasarım parametrelerinin özelliklerine etkisi ile ilgili daha fazla analiz yapıldı. Son olarak, tasarlanan çizimlere göre CNC tezgahında üretim gerçekleştirildi. Üç yük hücresinin üretiminde alüminyum alaşım 6013 kullanıldı. Yüksek gerinim alanları ANSYS analizinde işaretlendi, uygun gerinim ölçerler seçildi ve kuruldu.

Deneysel testlerle ilgili olarak, geliştirilen sensörler, bir bobin askısı ve bir sarım ünitesi kullanılarak test edildi. Sensörler, çağlığın çıkışına aynı anda yerleştirildi ve iplik gerginliği izleri, dört farklı sarım hızında ve üç farklı alçak geçiren filtre frekansında kaydedildi. Daha sonra gerilim seviyeleri değerlendirildi ve piyasada bulunan sensörden elde edilen sonuçlarla karşılaştırıldı. Son olarak, elde edilen sinyalleri iyileştirmek ve analiz etmek amacıyla MATLAB aracılığıyla verilere Dijital Sinyal İşleme (DSP) uygulandı. Deneysel veriler, geliştirilen yük hücrelerini kullanan gerginlik sensörlerinin tekstil prosesi için dinamik iplik gerginlik ölçümünün ölçülmesinde kullanılabileceğini gösterdi.

**Anahtar Kelimeler:** İplik gerginliği, doğal frekans, yük hücresi, gerginlik sensörü, filtreleme frekansı

**2020, ix + 86 sayfa.**

## **ABSTRACT**

MSc Thesis

### **DEVELOPMENT OF HIGH NATURAL FREQUENCY LOAD CELL FOR YARN TENSION SENSORS**

**Mohamad Yazan SADOUN**

Bursa Uludağ University  
Graduate School of Natural and Applied Sciences  
Department of Textile Engineering

**Supervisor:** Prof. Dr. Recep EREN

In this MSc thesis, load cell based yarn tension sensors were designed, manufactured, and tested experimentally. The design process started by examining the load cell's physical and mathematical fundamentals, studying its working principles, and conducting a scientific literature review. In the development stage, load cells were designed by a CAD program (SOLIDWORKS), and the design properties were studied in a FEA program (ANSYS). Among the properties focused on in the analysis process were the Natural frequency and Strain. Three load cell designs with different geometry were chosen, and further analysis was done regarding the effect of the design parameters on their properties. Finally, they were manufactured in a CNC machine according to the designed drawings. Aluminum alloy was used in the manufacturing of the three load cells. The high strain areas were marked in ANSYS analysis, and the strain gauges were chosen and installed.

Regarding the experimental tests, the developed sensors were tested using a bobbin creel and a winding unit. The sensors were positioned simultaneously on the creel's outlet, and the yarn tension traces were recorded at four different winding speeds and three different low pass filter frequencies. Then the tension levels were evaluated and compared with results acquired from commercially available sensor. Finally, Digital signal processing (DSP) was applied to the data through MATLAB to improve and analyze the resulting signals. Experimental data showed that the tension sensors using the developed load cells could be used for dynamic yarn tension measurement in the textile processes.

**Key words:** Yarn tension, natural frequency, load cell, tension sensor, filtering frequency

**2020, ix + 86 pages.**

## ACKNOWLEDGEMENT

"Whoever does not thank people has not thanked Allah." I am thankful and grateful to every one assisted and helped me throughout my project especially:

To Prof. Dr. Recep EREN, some debts are life-debts because you can't pay them no matter what you do, and that how much I owe Prof. Dr. Recep; he was beside me throughout the project; he shared with me the hardships and the happy moments, he was patient with my shortcomings and with all my mistakes, and He always brought out the best in me.

To Asst.Prof. Dr. Özge ÇELİK, for all the help, support, encouragement, and guidance she gave me, and her great kindness.

To Every teacher who educated and taught me throughout my journey.

To my friends who were beside me throughout my project, who supported and made me feel like home.

To My Father, My Mother, Moutamn, and Hoomam, who have done everything they could to assist and help me finish my study. Who stands by me in every step of my journey. To my biggest blessing in life.

Finally, I'd also like to thank electronic engineer Nuri ÇOŞKUN from PULS ELEKTRONİK company for their help in installing the strain gauges.

Mohamad Yazan SADOON  
29/12/2020

## CONTENTS

	<b>Page</b>
ÖZET.....	i
ABSTRACT.....	ii
ACKNOWLEDGEMENT .....	iii
ABBREVIATIONS .....	v
FIGURES .....	vi
TABLES.....	ix
1. INTRODUCTION.....	1
2. THEORETICAL BASICS AND LITERATURE REVIEW .....	4
2.1. Theoretical Basics .....	4
2.1.1. Strain and strain gauges .....	8
2.1.2. Wheatstone bridge.....	15
2.1.3. Mathematical modelling of the tension sensor.....	19
2.2. Literature Review.....	24
3. MATERIALS AND METHODS .....	40
3.1. Materials.....	40
3.2. Methods.....	48
4. RESULTS AND DISCUSSION .....	59
5. CONCLUSION .....	81
REFERENCES.....	83
RESUME .....	86



## ABBREVIATIONS

<b>Abbreviation</b>	<b>Definition</b>
---------------------	-------------------

CAD	Computer Aided Design
DSP	Digital Signal Processing
FEA	Finite Element Analysis
FIR	Finite Impulse Response
FFT	Fast Fourier Transform

## FIGURES

	<b>Page</b>
Figure 2.1. Analyzing different designs of the spring element to study their strain level	4
Figure 2.2. The physical deformation of a spring element .....	5
Figure 2.3. Different load cell designs .....	6
Figure 2.4. A section in a S type load cell and its parts .....	7
Figure 2.5. A section in a shear beam load cell and its parts .....	7
Figure 2.6. Strain gauge load cell .....	8
Figure 2.7. Load cell with strain gauges under force P.....	8
Figure 2.8. Strain types in a spring element with a strain gauge example.....	9
Figure 2.9. Strain gauge structure .....	10
Figure 2.10. Averaging of the strain by a strain gauge .....	11
Figure 2.11. Different Strain gauge patterns.....	12
Figure 2.12. Commercially available strain gauge patterns.....	12
Figure 2.13. The strain gauge installing steps.....	14
Figure 2.14. A Wheatstone bridge circuit .....	15
Figure 2.15. Quarter-Bridge Circuit.....	16
Figure 2.16. Using dummy gauge to compensate for temperature effect .....	16
Figure 2.17. Half-Bridge Circuit.....	17
Figure 2.18. Full-Bridge Circuit .....	17
Figure 2.19. State of strain gauges in full bridge circuit under a load.....	18
Figure 2.20. State of strain gauges in full bridge circuit in a load cell under a load .....	18
Figure 2.21. Load cell measurement system.....	19
Figure 2.22. The sensor (stiff spring element) under force.....	19
Figure 2.23. The spring-mass system.....	20
Figure 2.24. The deviation from accuracy plot.....	23
Figure 2.25. A schematic view of the measuring system.....	24
Figure 2.26. The used system to capture the yarn tension .....	25
Figure 2.27. The optical system tension results in comparison with a resistance tension sensor .....	25
Figure 2.28. A schematic of the developed system.....	26
Figure 2.29. The wireless yarn tension sensor working concept .....	27
Figure 2.30. The developed yarn tension sensor.....	27
Figure 2.31. The design of the yarn tension sensor.....	28
Figure 2.32. The natural frequency of the first five modal shapes before and after the optimization .....	29
Figure 2.33. A schematic of the SAW sensor .....	30
Figure 2.34. (a) The developed sensor. (b) The system schematic. (c) The schematic of the yarn tension F.....	30
Figure 2.35. (a) The fabricated sensor and (b) The IDT design schematic.....	31
Figure 2.36. The ANSYS simulation results of the substrate .....	31
Figure 2.37. Some design parameters used for the SAW yarn tension sensor.....	32
Figure 2.38. (a) The manufactured SAW sensor (b) a schematic of the SAW sensor....	32
Figure 2.39. The curve between temperature change $\Delta T$ and oscillation frequency $\Delta f_T$ .....	33
Figure 2.40. (a) The developed measuring apparatus (b) Quartz Crystal Resonator .....	34
Figure 2.41. A detailed schematic of the developed yarn tension measuring system.....	35
Figure 2.42. A schematic of the invented yarn tension meter.....	36

Figure 2.43 Different rotary guides can be used in the sensor.....	36
Figure 2.44. The schematic of the developed sensor .....	37
Figure 2.45. The developed optic sensor .....	38
Figure 2.46. (a) The yarn and the optical device (b) The optical device schematic (c) The complete developed system.....	39
Figure 3.1. SOLIDWORKS user interface .....	40
Figure 3.2. ANSYS user interface .....	41
Figure 3.3. SGA/A analog strain gauge signal conditioner .....	42
Figure 3.4. Strain gauge – amplifier connections .....	42
Figure 3.5. The Arduino Uno.....	43
Figure 3.6. The Arduino programming software .....	43
Figure 3.7. The creel and winding unit .....	44
Figure 3.8. The sensor positioning.....	44
Figure 3.9. Sensor #1 .....	45
Figure 3.10. Sensor #2 .....	45
Figure 3.11. Sensor #3 .....	45
Figure 3.12. The complete yarn tension sensor .....	46
Figure 3.13. MATLAB user interface.....	46
Figure 3.14. Fourier Transform.....	47
Figure 3.15. The design in ANSYS .....	49
Figure 3.16. Selecting the analysis.....	49
Figure 3.17. Adding Modal and Static Structural analyses.....	50
Figure 3.18. Material and material properties selection.....	50
Figure 3.19. Selecting the sensor design.....	51
Figure 3.20. Selecting the sensor material .....	51
Figure 3.21. Meshing and selecting mesh properties.....	52
Figure 3.22. The sensor after the mesh process .....	52
Figure 3.23. Adding the boundary conditions.....	53
Figure 3.24. Adding the solutions .....	53
Figure 3.25. The designed sensors .....	54
Figure 3.26. The sensor assembly .....	55
Figure 3.27. The maximum strain zones.....	55
Figure 3.28. The bridge connection of the sensor #1 .....	56
Figure 3.29. The bridge connection of the sensor #2 and #3 .....	56
Figure 3.30 The analog reading code.....	57
Figure 3.31. The Fast Fourier Transform (FFT) code.....	57
Figure 3.32. The FIR filter code.....	58
Figure 3.33. Sensors calibration curves .....	58
Figure 4.1. Tested yarn tension sensors shapes.....	59
Figure 4.2. Variation in designs for studying different specifications.....	62
Figure 4.3. ANSYS report for Sensor #1 .....	66
Figure 4.4. ANSYS report for Sensor #2 .....	67
Figure 4.5. ANSYS report for Sensor #3 .....	68
Figure 4.6. The effect of amplifier filter cut-off frequency on the signal shape at a speed of 50 m/min.....	70
Figure 4.7. The effect of amplifier filter cut-off frequency on the signal shape at a speed of 200 m/min.....	71

Figure 4.8. The effect of amplifier filter cut-off frequency on the signal shape at a speed of 500 m/min .....	72
Figure 4.9. The effect of amplifier filter cut-off frequency on the signal shape at a speed of 800 m/min .....	73
Figure 4.10. The developed sensors and control sensor signal shapes at a speed of 200 m/min .....	74
Figure 4.11. The developed sensors and control sensor signal shapes at a speed of 500 m/min .....	75
Figure 4.12. The developed sensors and control sensor signal shapes at a a speed of 800 m/min .....	76
Figure 4.13. Frequency and time domains for the control sensor at a speed of 800 m/min .....	77
Figure 4.14. Frequency and time domains for sensors #1 and #3 with a 1000 Hz analog filter, at a speed of 800 m/min .....	78
Figure 4.15. Frequency and time domains for the sensor #1 and #3 with a 100 Hz analog filter at a speed of 800 m/min .....	79
Figure 4.16. Frequency and time domains for the sensor #1 and #3 with a 100 Hz digital filter at a speed of 800 m/min .....	80

## TABLES

	<b>Page</b>
Table 2.1. The deviation from accuracy.....	23
Table 4.1. The width effect on strain and natural frequency .....	60
Table 4.2. The height effect on strain and natural frequency.....	60
Table 4.3. The length effect on strain and natural frequency.....	61
Table 4.4. The rollers effect on strain and natural frequency .....	61
Table 4.5. Offsetting the high strain zone effect.....	63
Table 4.6. The high strain zone length effect 1.....	63
Table 4.7. The high strain zone length effect 2.....	64
Table 4.8. The High strain zone thickness effect.....	64
Table 4.9. Yarn tension sensors properties. ....	65
Table 4.10. The averages of 1000 sample for the sensors .....	69

## 1. INTRODUCTION

Tension sensors play an essential role in the textile industry and have a wide range of applications in many different industry areas, from weaving looms to winding, warping and finishing machines.

Because the tension is one of the most critical parameters in the production setup, it is crucial to have it measured at all times and provide correct measurements.

In textile machines, there are many processes that depends on the feedback signal coming from the tension sensors; this signal is used in the control loop to provide the system with the required information to adjust its parameters and stay stable under different conditions, for example in weaving the tension signal is used to synchronize the take-up and let-off motions and adjust warp beam angular velocity.

Yarn or fabric tension sensors are used for mainly two purposes. These are;

- Measuring the tension for forming a feedback tension control system.
- Measuring the tension for data evaluation and recording.

On the other hand, dynamic yarn tension measurement is required to analyze effect of machine mechanisms on tension variation for high speed machine running and optimization of operation of its mechanisms. From design point, there are some critical points in dynamic tension measurement sensors compared to static tension measurement.

There are three-cylinder systems used for tension measurement. In this system, fabric passes around middle cylinder with certain angle and applies a resultant downward pressure. As the fabric wrapping angle remains constant, resultant downward pressure only changes if fabric tension changes. This pressure is detected and then converted to an electrical signal by a sensor called load cell. This is most widely used in yarn or fabric measurement method in industry. A feedback tension control system is formed by using this tension sensor signal. A controller continuously reads tension sensor signals and compares it with the set tension value. Depending on the difference, breaking by powder

brake is adjusted so that fabric is fed with constant tension despite the decrease in fabric roll diameter.

Tension sensors are designed and manufactured to measure the tension at different intervals, from 0-20 cN to 0-... kN levels. For yarn tension measurements, tension sensors are designed mostly at 0-20 cN, 0-100 cN, 0-500 cN, etc. One application for yarn tension measurement can be seen in a bobbin winding machine. Here the pressure applied to the sensor by the yarn is detected and converted to electrical signal. This is used for tension control in yarn feeding system as well as for winding process evaluation.

There are portable tension measurement sensors produced by different manufacturers. They can be carried to spinning, knitting, winding, warping, weaving and sewing machines with their stand and individual yarn tensions are recorded and evaluated.

In the textile industry, there are many sensor types (tension detection methods) to measure the tension. Among them, strain gauges, piezoelectric sensors, hall effect sensors, and capacitive and optical sensors are widely employed. They differ in their measuring concept, used area, and production cost.

Strain gauges or resistance load cells are among the most used sensors types for tension measurements, not only in textile machines but in many other industries. Strain gauge load cells are ideal for static tension measurements. They can also be used for dynamic tension measurements up to frequencies sufficient for many textile processes.

Dynamic yarn tension measurements transducers are not manufactured in Turkey and imported from different countries. In this MSc thesis, it is aimed at designing, manufacturing and testing a dynamic yarn tension transducer based on strain gauge principle. Mechanical design and optimization were carried out by using ANSYS program. These mechanical designs were manufactured using CNC machine tools and then strain gauges were glued on the most deforming parts to form a full bridge load cell measurement system. These load cells were used as part of tension transducer and their

performance was tested on a bobbin winding unit up to 900 meter per minutes yarn unwinding speeds.



## 2. THEORETICAL BASICS AND LITERATURE REVIEW

### 2.1. Theoretical Basics

In a strain gauge type load cell, there are three main parts in addition to its amplifier and filtering circuits. These are;

- Spring element
- Strain gauges
- Wheatstone bridge circuit

One of the main elements in the tension measurement system is the spring element. The force or torque causes deformation in this spring element. Elasticity theory enables the designer to establish the required relation between load (force or torque) and strain. Strain analysis is carried out for different spring elements constructions and load cells types. Strain analysis by ANSYS program will be a good help for the load cell designer. As strain gauges will be subjected to the same strain as the spring element when they are bonded, the maximum strain cannot exceed the maximum allowed strain of the strain gauges. Therefore, there will be an upper limit for the strain of spring element (dictated by strain gauge allowed maximum strain). This requires that more rigid spring elements are designed for higher forces. Also, steel material is preferred in measuring higher forces rather than aluminum in the design of the spring element. Figure 2.1 Shows an example from literature of using ANSYS to analyze the spring element.

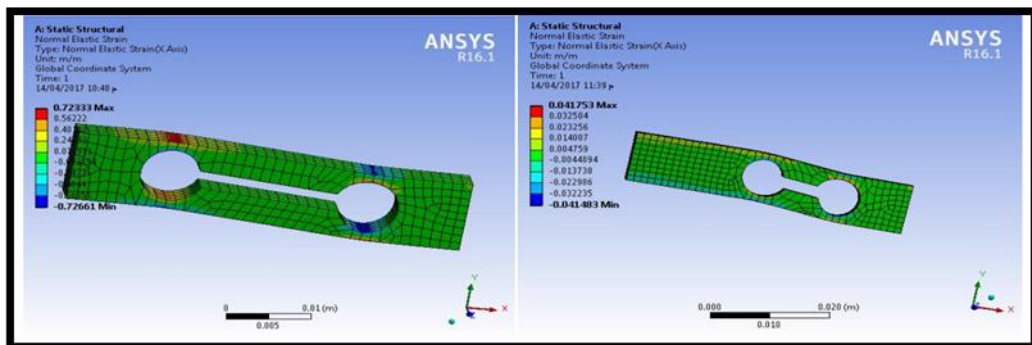


**Figure 2.1.** Analyzing different designs of the spring element to study their strain levels (Hamed and Abdullah 2017)

When a spring element is under a load or force its different section deforms under in a micro-level scale, If the load is small it may not be observed by the human eye.

Figure 2.2 shows the most four deformed areas in a spring element. Two parts endure compression and the other two endure tension. This micro-physical deformation can be converted to a useful data and used to measure different forces and loads.

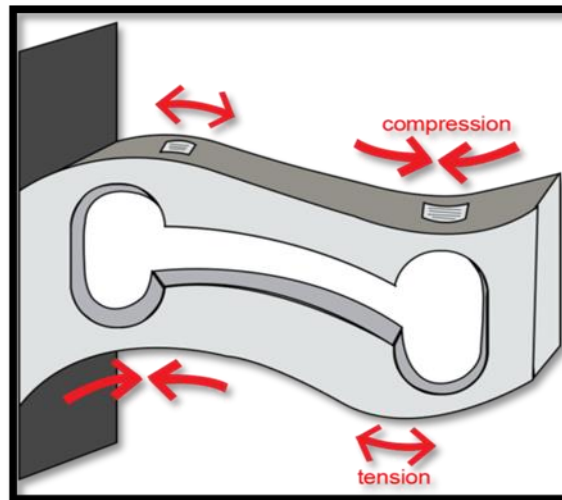


**Figure 2.2.** The physical deformation of a spring element (Anonymous 2016a)

Load cells can come in multiple measurement concepts including hydraulic, pneumatic, strain gauge, piezoelectric, and capacitance and may come in different shapes, lengths and suitable for different types of forces. Figure 2.3 shows different load cells designs. They are preferred for different applications and force measurement intervals.



**Figure 2.3.** Different load cell designs (Anonymous 2014)

Bending beam load cell works by measuring the strain caused by bending moment, while the load pressure deforms the loadcell metal spring element and causes strain.

Compression load cell is fixed from the bottom side and generally is objected to a pushing force along a single axis, and deforms accordingly. This is measured by the strain gauges bonded on its deforming spring element.

Double ended beam load cell is used to centralize the loading position and minimize sensitivity to off-center forces. It provides high sensitivity measurements. Force affects from the middle and strains occurring from right and left sides are measured to determine the force.

S type load cell working principle is similar to single point load cell but the S shape and the placement of the upper and lower limbs ensure that the central axis and the mounting holes are totally aligned and the spring element is deformed at both ends by compression or tension. Figure 2.4 shows a section in S type load cell. Strain gauges are bonded on the most deforming surfaces.

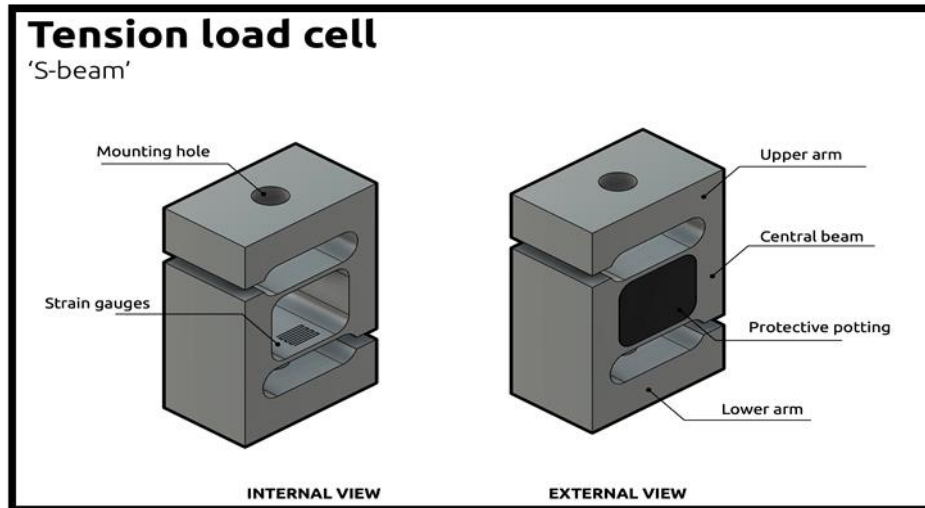


**Figure 2.4.** A section in a S type load cell and its parts (Anonymous 2020a)

In shear beam load cells, the strain gauges are placed at 45-degree angles to detect strain and mostly they are used for medium to high capacity applications. Figure 2.5 shows a section and strain gauges in a shear beam load cell.

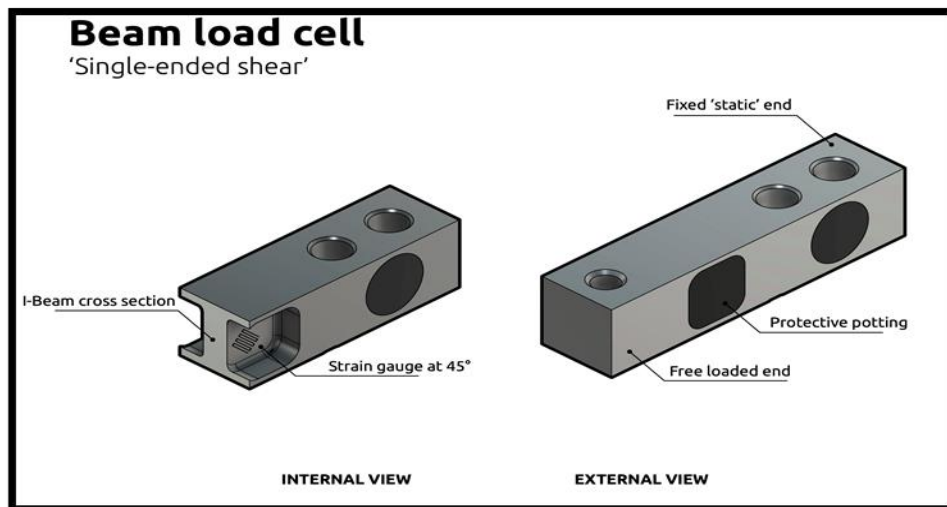


**Figure 2.5.** A section in a shear beam load cell and its parts (Anonymous 2020b)

Single point load cell is one of the most used load cell types. It is mostly used in weighing applications and has high accuracy in measurements.

One of the most common type and used load cells are the strain gauge load cells. Strain gauge load cells help converting the load into a proportionally changing electrical signal

that will be changed later to a value, a value that can be used to understand the current load. The force is translated into a voltage by the resistance change in the strain gauges, which are bonded to the spring element. Amount of change in resistance correlates to the deformation in the spring element structure (strain) and hence the load applied. Figure 2.6 shows a strain gauge load cell.

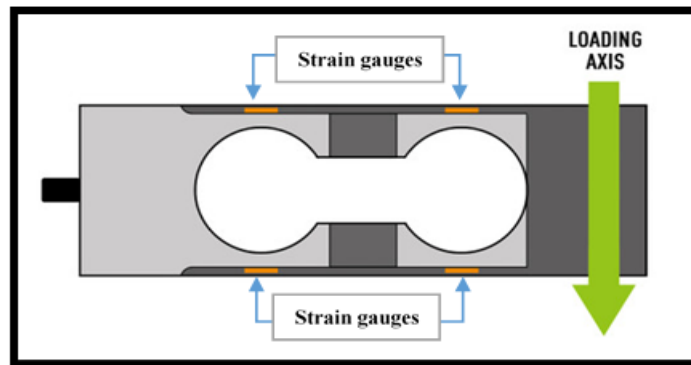


**Figure 2.6.** Strain gauge load cell (Anonymous 2019, changes were made)

### 2.1.1. Strain and strain gauges

Strain is the amount of deformation of a unit length in a body due to an applied force, strain can be positive as tensile or elongation and negative as compressive or contraction, It is expressed in units like mm/mm and in"/in". But because the magnitude of the measured strain is small, the strain is often expressed as micro strain ( $\mu\epsilon$ ). In load cells it takes values like 50  $\mu\epsilon$ , 100  $\mu\epsilon$ , 200  $\mu\epsilon$ , 500  $\mu\epsilon$ ... etc. As seen simply in the Figure 2.7 a metal bar is subjected to forces that elongates it.

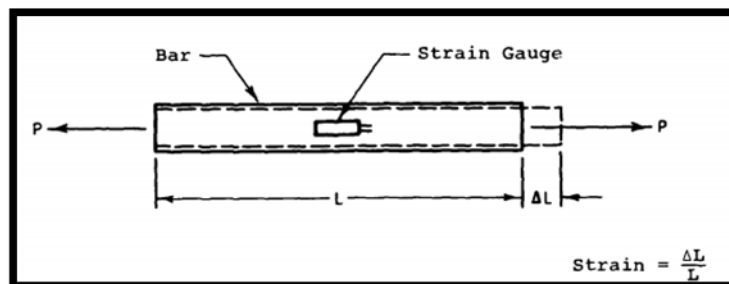


**Figure 2.7.** Load cell with strain gauges under force P (Gee and Conder 1984)

As strain gauge is fixed on this metal bar, it also elongates the same amount as the metal bar. If the original length of the sensor is  $L$  and its length is increased by  $DL$  under the load  $P$ , the tensile strain equals to  $\frac{\Delta L}{L}$ .

Likewise, if a strain gauge was installed on the sensor body having a resistance of  $R$ , it would also be under a change of  $DR$  due the load  $P$  (Force). As a result, the fractional resistance change would equal to  $\frac{\Delta R}{R}$ .

Fractional resistance in a strain gauge is related to the strain by a proportional constant  $K$  as shown in Equation 2.1.

$$\frac{\Delta R}{R} = k \cdot \frac{\Delta L}{L} \quad (2.1)$$

$K$  in this equation is called gauge factor, which is provided from the strain gauge manufacturers. The gauge factor can be seen as the conversion factor of strain to fractional resistance change. Figure 2.8 shows a strain gauge structure. It is formed by a resistive material on a polyimide foil in grid form.

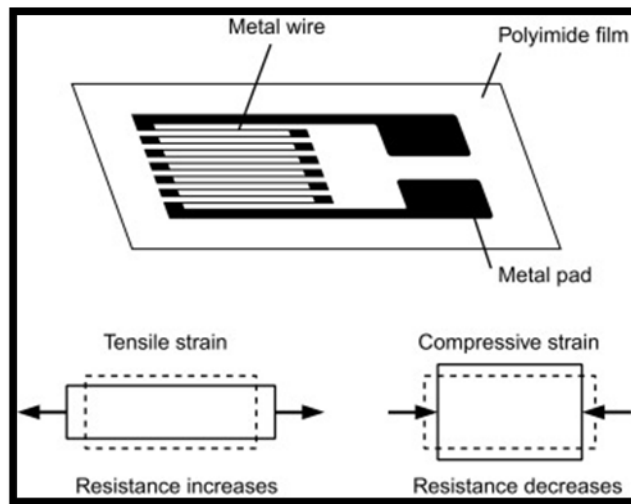


**Figure 2.8.** Strain types in a spring element with a strain gauge example (Anonymous 2015a)

They are manufactured at different resistance values. For smaller size strain gauges, the resistance is smaller and it can be made larger with increasing sizes. The strain gauge

consists of an active grid which is the elongated part, a carrier, and solder tabs to connect it to the cables. (Figure 2.9)

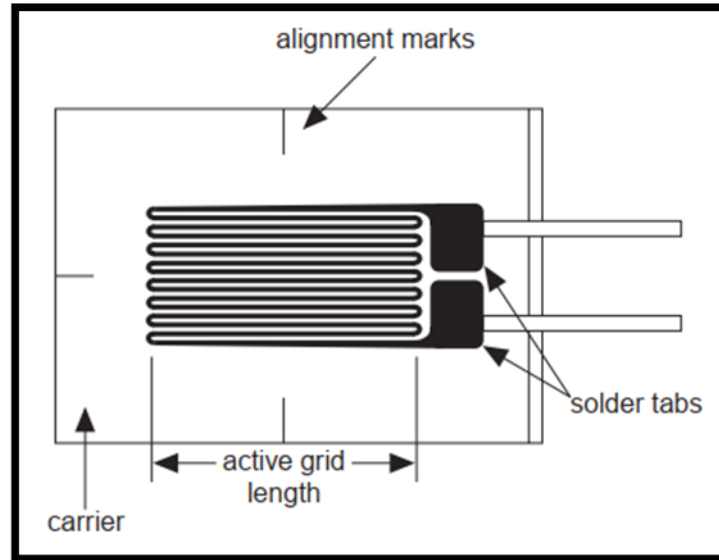


**Figure 2.9.** Strain gauge structure (Anonymous 1998)

There are certain criteria to select a strain gauge for a specific application. This can be listed and explained as follows.

- Gauge length
- Gauge pattern
- The gauge resistance
- Strain-sensitive alloy

#### *Gauge length*

The gauge length of a strain gauge is the strain-sensitive length of the grid as seen in Figure 2.9. The solder tabs are considered insensitive to strain because of their relatively large cross-sectional area and low electrical resistance. Strain gauges have wide range of gauge lengths from millimeters to centimeters, but the smaller the strain gauge the harder it gets to handle and work with.

Gauge length is an important factor in determining the gage performance under a certain force. The strain gradient is quite steep and the area of maximum strain is restricted to a small region. The strain gauges try to average the strain over the area covered by the grid

and because the average of any nonuniform strain is always less than the maximum, a strain gage which is larger than the maximum strain region will indicate a strain magnitude which is much smaller than the real value. Figure 2.10 explains this phenomenon and demonstrates the error in strain indicated by a gage which is too long with respect to the zone of the peak strain (Anonymous 1992).

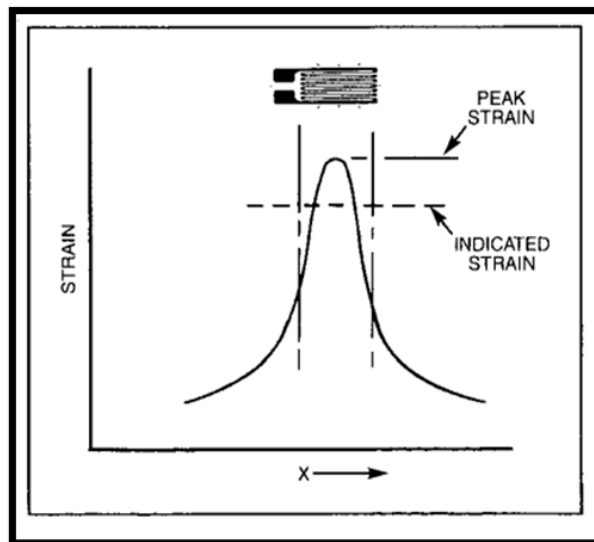


**Figure 2.10.** Averaging of the strain by a strain gauge (Anonymous 1992)

### *Gauge pattern*

Linear strain gauges are used for all general-purpose applications where the directions of the principle strains are known and the gauges can be aligned in the correct directions to the applied force accurately. Shear gauges are used to measure shear strain when the directions of the principle strains are known and the elements of the gauge can be aligned at 45 degrees to these directions. Rosette gauges are employed when the principle strain directions are not known as magnitude and direction of the principle strains, the strains in the 3 axes, have been measured separately. Figure 2.11 shows the simple gauge patterns and, Figure 2.12 shows strain gauges with different patterns from HBM.



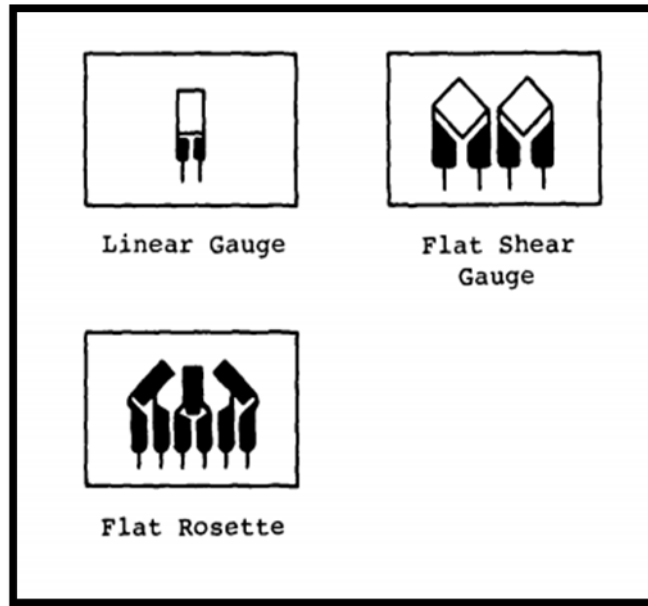


**Figure 2.11.** Different strain gauge patterns (Gee and Conder 1984)

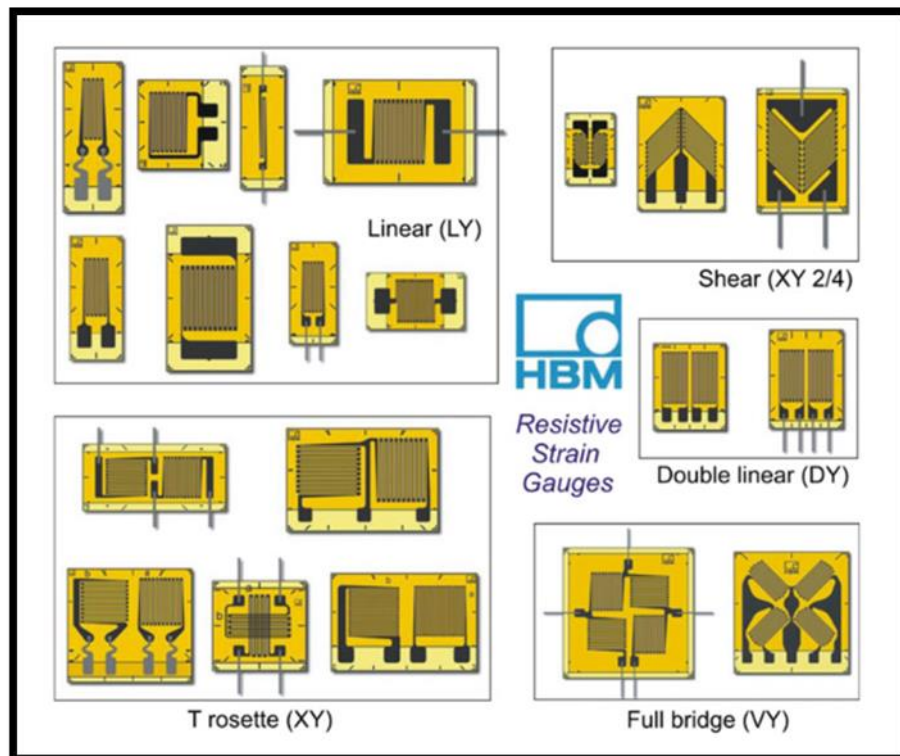


**Figure 2.12.** Commercially available strain gauge patterns (Ștefănescu 2020)

### *The gauge resistance*

The most commonly available gauges have a resistance of 120, 350 or 1000 Ohms. To prevent heating problem of strain gauges, a higher possible resistance is preferred as a moderate voltage levels can be used. For small resistance values of strain gauges, a smaller voltage sources are required. Otherwise, heating will cause problems of resistance change and affects the measurement adversely.

### *Strain-sensitive alloy*

The strain-sensitive alloy is the main component which is responsible for the operating characteristics of the strain gauge. It is selected by the manufacturing company and every alloy has different behavior under force. Among the most used alloys are;

- Constantan in self-temperature compensated form
- Annealed constantan
- Isoelastic
- Nickel-chromium alloy, a modified Karma in self-temperature-compensated form

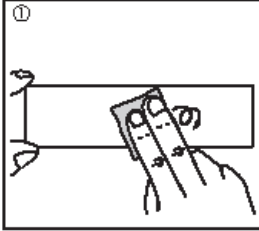
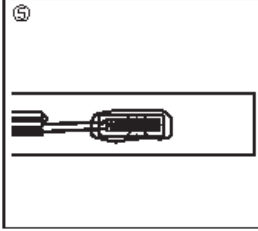
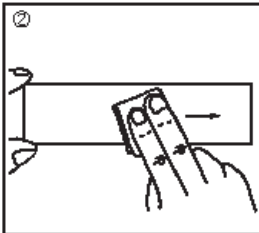
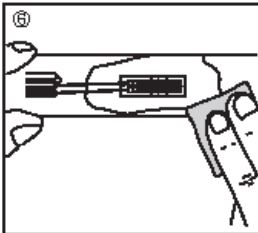
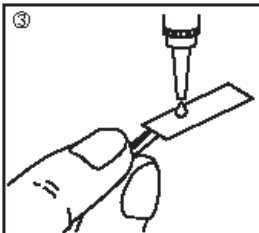
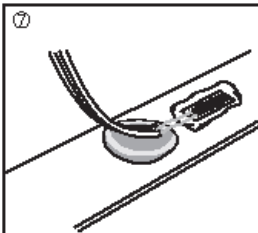
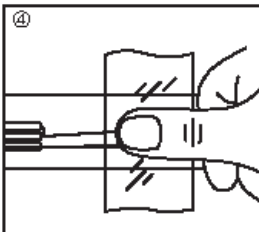
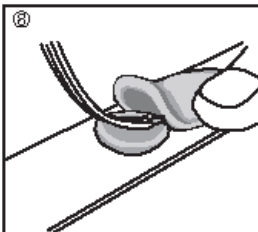
### *Installing strain gauges*

Before installing a strain gauge on a spring element, many things should be considered, like choosing and marking the maximum strain areas and using the appropriate adhesives and cleaning agents.

Figure 2.13 shows the steps of installing the strain gauge on a spring element (from strain gauge manufacturer KYOWA).

● **Typical Bonding Procedures and Dampproof Treatment**

The bonding procedures for strain gages differ depending on the type of the adhesive applied. The description below applies to a case where the lead-wire-equipped KFG5 gage is bonded to a mild steel test piece with a typical cyanoacrylate adhesive, CC-33A. The dampproof treatment shows a scenario using a butyl rubber coating agent.

	<p>Using sandpaper (#320 grade or similar), polish the bonding site with circular motions across a considerably wider area than the strain gage size.</p> <p>(If the measuring object is a practical structure, wipe off paint, rust and plating with a grinder or sand blast. Then, polish with sandpaper.)</p>		<p>When the adhesive is cured, remove the polyethylene sheet and check the bonding condition. Ideally, the adhesive should be protruding slightly from around the strain gage.</p>
	<p>Using an absorbent cotton, gauze or SILBON paper dipped in a highly volatile solvent that dissolves oils and fats such as acetone, strongly wipe the bonding site in a single direction to remove oils and fats. Repeated wiping does not clean the surface. After cleaning, mark the strain gage bonding position.</p>		<p>If the adhesive is protruding excessively from around the gage base, remove the protruding adhesive with a cutter or sandpaper. Place the gage leads in a slightly slackened condition.</p>
	<p>Make sure of the front (metal foil part) and the rear of the strain gage. Apply a drop of adhesive to the rear face and immediately put the strain gage on the bonding site. (Do not spread the adhesive over the rear face, as doing so may cause the adhesive to cure too quickly to adhere to the bonding site.)</p>		<p>Lift up the lead wire to the point where the adhesive is applied. Place a block of the coating agent below the lead wire with the gage leads slightly loose.</p>
	<p>Cover the strain gage with the accessory polyethylene sheet and strongly press the strain gage over the sheet with a thumb for approximately 1 minute (Do not remove your thumb partway through). Perform steps 3 and 4 quickly, or the adhesive will cure prematurely. Once the strain gage is put on the bonding site, do not put lift up to adjust the position.</p>		<p>Completely cover the strain gage, protruding adhesive and part of the lead wires with another block of the coating agent. Without tearing the block into small pieces, slightly flatten it with a finger to fully cover the strain gage and part of the lead wires. Completely hide protrusions including gage leads behind the coating agent.</p>

**Figure 2.13.** The strain gauge installing steps (Anonymous 2018a)

### 2.1.2. Wheatstone bridge

The strain levels in the elastic element are very small, therefore the resistance change will be tiny and it is hard to convert it to a readable voltage. To measure small resistance differences, Wheatstone bridge configuration is the most widely used electrical circuit. Apart from converting resistance change in strain gauges due to strain formation, Wheatstone Bridge circuits can also compensate the adverse effect of temperature change on the measurement signal. Figure 2.14 shows a typical Wheatstone bridge.

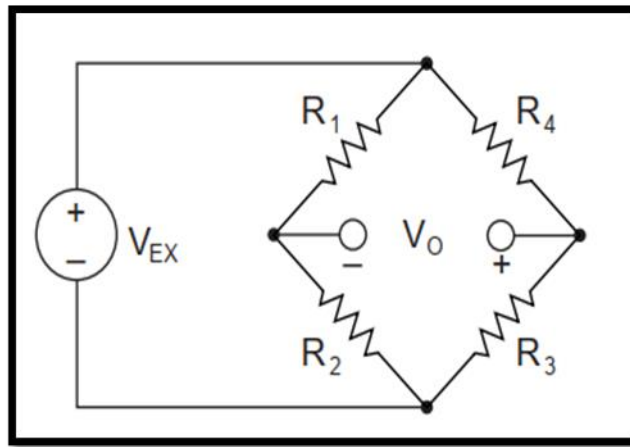


**Figure 2.14.** A Wheatstone bridge circuit (Anonymous 1998)

The Wheatstone bridge circuit is formed by four resistive elements (bridge arms), and a supply Dc voltage source. Dc supply voltage is applied to the circuit between R2-R3 and R1-R4. Output voltage representing the measured signal is measured as  $V_0$  between R1-R2 and R4-R3. If the 4 resistances are equal, then a balanced bridge circuit is obtained and the output voltage becomes zero. If a change in resistance happens in any bridge arm a nonzero output voltage will result. From electrical circuit solutions Wheatstone bridge circuit output voltage can be expressed by the following equation.

$$V_0 = \left[ \frac{R_3}{R_3 + R_4} - \frac{R_2}{R_1 + R_2} \right] \cdot V_{EX} \quad (2.2)$$

Wheatstone bridge circuit can function to convert resistance changes to electrical signal if all the resistances are equal or there is a relation among them as follows. In most of Wheatstone bridge circuit resistances are equal,  $R_1 = R_2 = R_3 = R_4$ .

The number of active arms or resistances subjected to deformation can differ. If only one strain gauge is used in one of the bridge arms for measurement this circuit is called a Quarter-Bridge circuit Figure 2.15 shows a Quarter-Bridge circuit in which  $R_G$  ( $R_4$ ) is subjected to strain and caused a resistance change of  $\Delta R$ . The other three resistances will not get affected by the measured load. In this circuit, output voltage is obtained by the equation under the Figure 2.15 where  $V_{EX}$  is supply Dc voltage, GF is gauge factor (K) and  $\epsilon$  represents the strain.

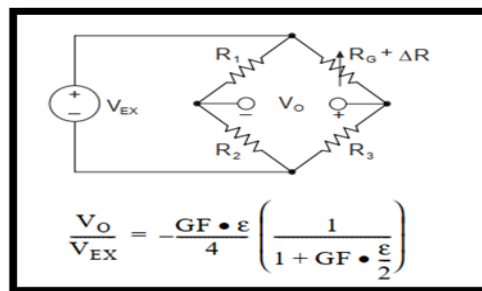


**Figure 2.15.** Quarter-bridge circuit (Anonymous 1998)

If a dummy strain gauge (not subjected to deformation) is used, it can compensate for the effect of temperature as seen in Figure 2.16.

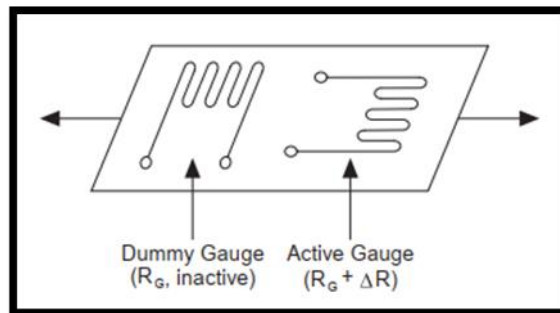


**Figure 2.16.** Using dummy gauge to compensate for temperature effect (Anonymous 1998)

Although it makes it easy to construct a load cell with a single active gauge, it reduces the sensitivity of a load cell. The sensitivity of a load cell would be doubled if a bridge circuit with 2 active resistances is employed as seen in Figure 2.17 this type of bridge circuit is called Half-Bridge Circuit; one strain gauge is bonded on the upper surface of a beam and the other to the lower surface at the same position. When a downward force

affects the beam is bent and its upper surface is tensioned (elongated) and the bottom surface is compressed (contracted). As a result, resistance on the upper surface increases its value because of its increasing length and the resistance of the bottom surface's strain gauge is decreased due to its compression. This resistance changes are indicated as  $\Delta R$  in Figure 2.17. Therefore; upper surface strain gauge resistance becomes  $R_G + \Delta R$  and bottom surface strain gauge resistance  $R_G - \Delta R$ . As resistance change is doubled, output voltage is also approximately doubled and sensitivity increases.

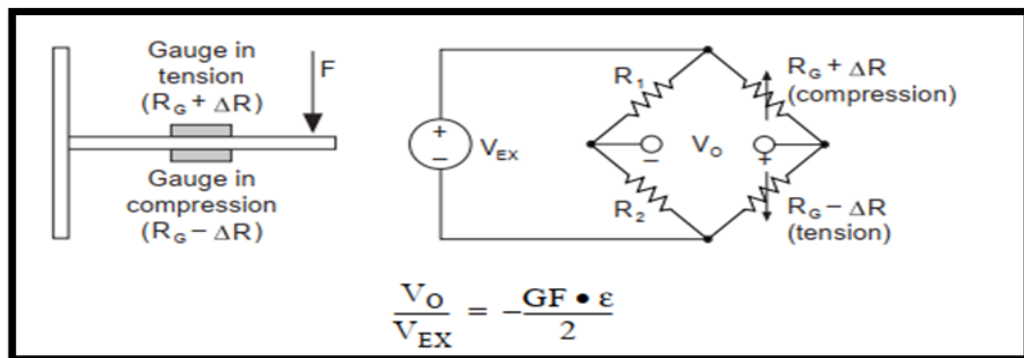


**Figure 2.17.** Half-bridge circuit (Anonymous 1998)

Highest measurement sensitivity is obtained from a Wheatstone bridge circuit if four active strain gauges are employed. This is called Full-Bridge circuit. As shown in the Figure 2.18 two of the strain gauges are subjected to tensioning and other two compression. Therefore, depending on the load, two strain gauge resistances increase as  $\Delta R$  and other two decrease the same amount. In this case, output voltage is given by the equation below the Figure 2.18. Sensitivity is four times higher than Quarter-Bridge circuit and twice of the Half-Bridge circuit.

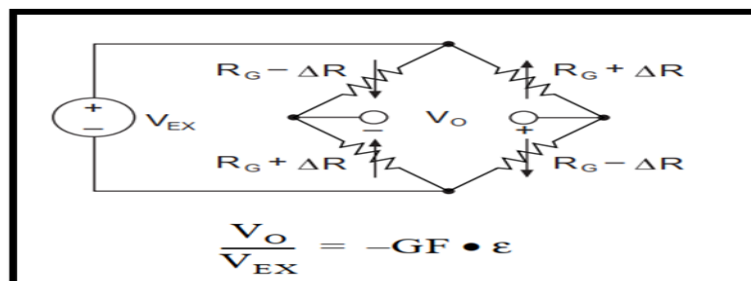


**Figure 2.18.** Full-bridge circuit (Anonymous 1998)

An example of Full-Bridge circuit used in a bending beam loadcell is shown in Figure 2.19. Weight represent the force affecting in bending beam. As seen in the figure, two places are compressed and other two are tensioned. Four strain gauges are bonded to these positions and Wheatstone Full-Bridge circuit is formed as presented in Figure 2.20. Two tensioned and two compressed strain gauges are placed in opposite arms of the Full-Bridge circuit. Output voltage is obtained with highest sensitivity in this circuit.

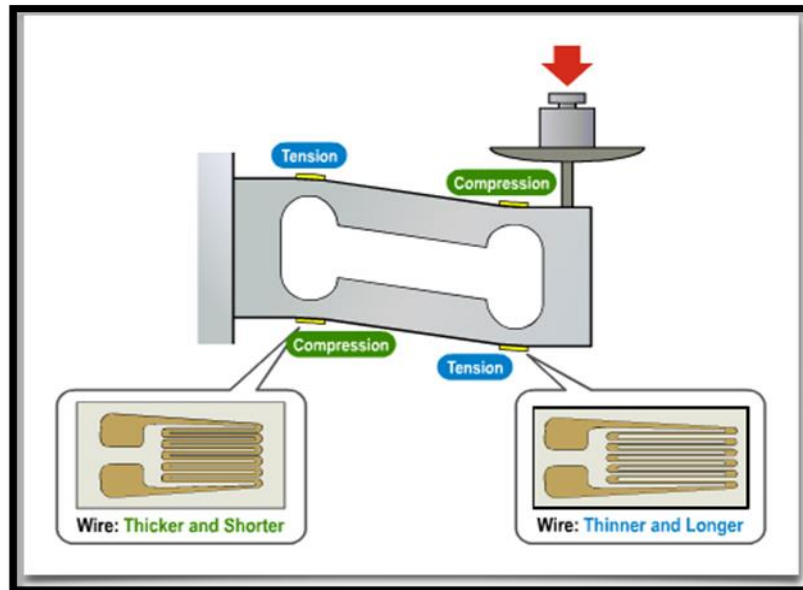


**Figure 2.19.** State of strain gauges in full bridge circuit under a load (Anonymous 2015b)

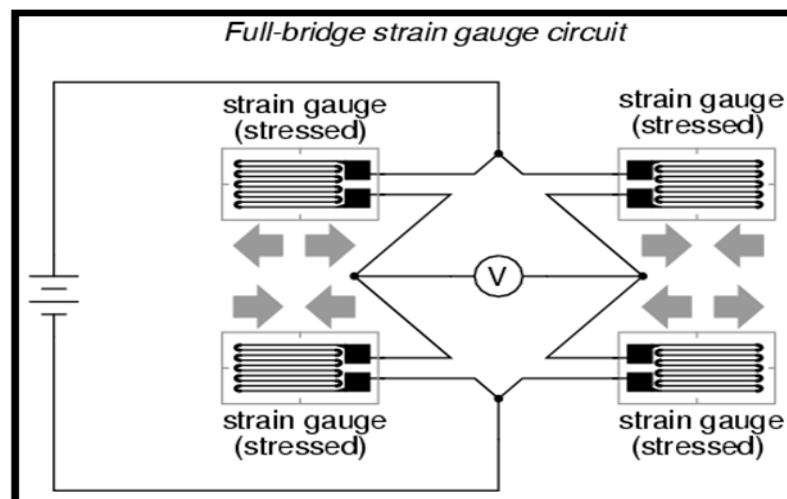


**Figure 2.20.** State of strain gauges in full bridge circuit in a load cell under a load (Anonymous 2008)

The output signal obtained from a Wheatstone Bridge circuit is very small and at the level of 10-20 mV levels and cannot drive any circuit for reading. Therefore, amplifiers are used following bridge circuits to amplify the signal from mV levels to 5-10 V levels. Then this signal can be read easily by a computer, recorder or any type of controller. A load cell measurement system can be shown with all its units as follows in Figure 2.21.

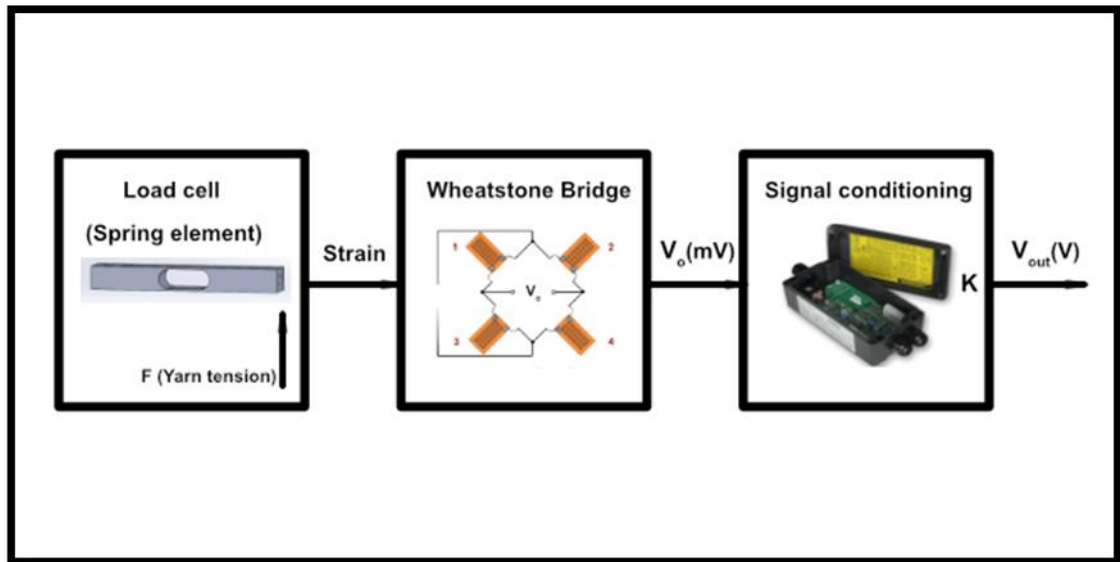


**Figure 2.21.** Load cell measurement system

### 2.1.3. Mathematical modelling of the tension sensor

The designed yarn tension sensors are like a stiff spring system, and can be modeled as one, Figure 2.22 shows the designed sensor under a force. Figure 2.23 shows mass spring system.

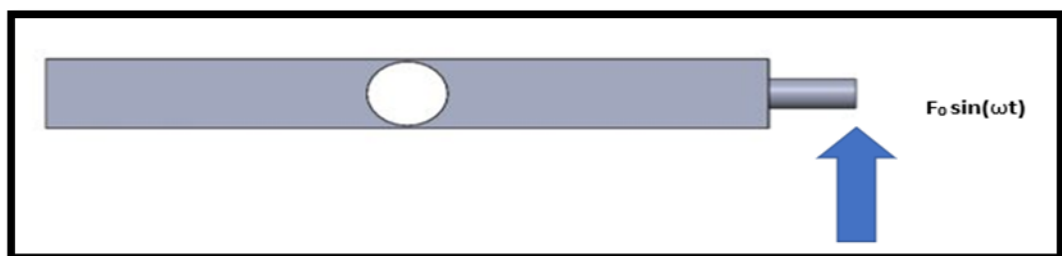


**Figure 2.22.** The sensor (stiff spring element) under force



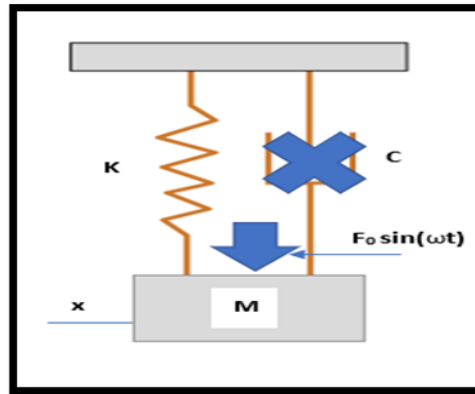


**Figure 2.23.** The spring-mass system

The describing equation of the system can be written as Equation 2.3.

$$m\ddot{x} + c\dot{x} + kx = f_0 \sin(\omega t) \quad (2.3)$$

The effect of the damping factor is neglectable due to the miniature displacement of the sensor and with simple operations Equation 2.4 can be obtained, and the natural frequency is equal to:

$$\omega_n = \frac{k}{m}$$

$$\ddot{x} + \omega_n x = \frac{f_0}{m} \sin(\omega t) \quad (2.4)$$

The model represents a Second-Order Non-Homogeneous Differential Equation  
It's general solution (Equation 2.5):

$$x_g = x_h + x_s \quad (2.5)$$

For the homogeneous solution (Equation 2.7):

$$\ddot{x} + \omega_n x = 0 \quad (2.6)$$

$$\lambda_{1,2} = \pm i\omega_n$$

$$x_h = c_1 \cos(\omega_n t) + c_2 \sin(\omega_n t) \quad (2.7)$$

For calculating the general solution (Equation 2.8), the special solution can as follow:

$$\begin{aligned}x_s &= A \cdot \cos(\omega t) + B \sin(\omega t) \\ \dot{x}_s &= -A \cdot \omega \sin(\omega t) + B \cdot \omega \cos(\omega t) \\ \ddot{x}_s &= -A \cdot \omega^2 \cos(\omega t) + B \cdot \omega^2 \sin(\omega t)\end{aligned}$$

After replacing in Equation 2.6 A and B can be calculated as follows.

$$\begin{aligned}A &= 0 \\ B &= \frac{\frac{f_0}{m}}{\omega_n^2 - \omega^2} \\ x_s &= \frac{\frac{f_0}{m}}{\omega_n^2 - \omega^2} \cdot \sin(\omega t) \\ x_s &= \frac{\frac{f_0}{k}}{\left(1 - \frac{\omega^2}{\omega_n^2}\right)} \cdot \sin(\omega t) \\ x_g &= c_1 \cos(\omega_n t) + c_2 \sin(\omega_n t) + \frac{\frac{f_0}{k}}{\left(1 - \frac{\omega^2}{\omega_n^2}\right)} \cdot \sin(\omega t)\end{aligned}$$

We can use the initial conditions to solve c1 and c2.

$$\begin{aligned}t=0 &\rightarrow x=0 \\ t=0 &\rightarrow \dot{x}=0 \\ \rightarrow c_1 &= 0 \quad \rightarrow c_2 = -\frac{\frac{f_0}{k}}{\left(1 - \frac{\omega^2}{\omega_n^2}\right)} \cdot \frac{\omega}{\omega_n} \\ x_g &= -\frac{\frac{f_0}{k}}{\left(1 - \frac{\omega^2}{\omega_n^2}\right)} \cdot \frac{\omega}{\omega_n} \cdot \sin(\omega_n t) + \frac{\frac{f_0}{k}}{\left(1 - \frac{\omega^2}{\omega_n^2}\right)} \cdot \sin(\omega t)\end{aligned} \quad (2.8)$$

$\omega$  angular frequency

$k$  spring constant (stiffness).

$\omega_n$  Natural frequency

$F_0$  Force

$t$  Time

From the solution, it can be concluded that the sensor's displacement decreases with the increment of the stiffness and is closely related to the natural frequency, and the relation between the angular frequency  $\omega$  and the natural frequency  $\omega_n$  has a significant effect on the accuracy of the measurements.

From  $(1 - \frac{\omega^2}{\omega_n^2})$  multiple states can be observed.

If the sensor's natural frequency is equal or near the frequency of vibrating force, the displacement is not accurate at all, and the system is in a resonance state.

If the natural frequency of the sensor is smaller than the frequency of vibrating force, the displacement is amplified, and the accuracy of the system is hugely compromised.

If the natural frequency of the sensor is bigger than the frequency of vibrating force, the accuracy of the system increases with the increment of the natural frequency; for example, a sensor has a vibrating force frequency, which is smaller than the sensor's natural frequency with ten folds, has measurement errors of  $\approx 1\%$ .

$$\text{Ex: } \omega = 100 \quad \omega_n = 1000 \rightarrow \left(1 - \frac{\omega^2}{\omega_n^2}\right) = \frac{99}{100}$$

Table 2.1 and Figure 2.24 show the relation between frequency of vibrating force and the measurements accuracy at 1000 Hz natural frequency.

**Table 2.1.** The deviation from accuracy

$\omega$	$\omega_n$	Deviation from accuracy
1	1000	0.0001
10	1000	0.01
20	1000	0.04
50	1000	0.25
100	1000	1
250	1000	6.25
500	1000	25
750	1000	56.25
900	1000	81

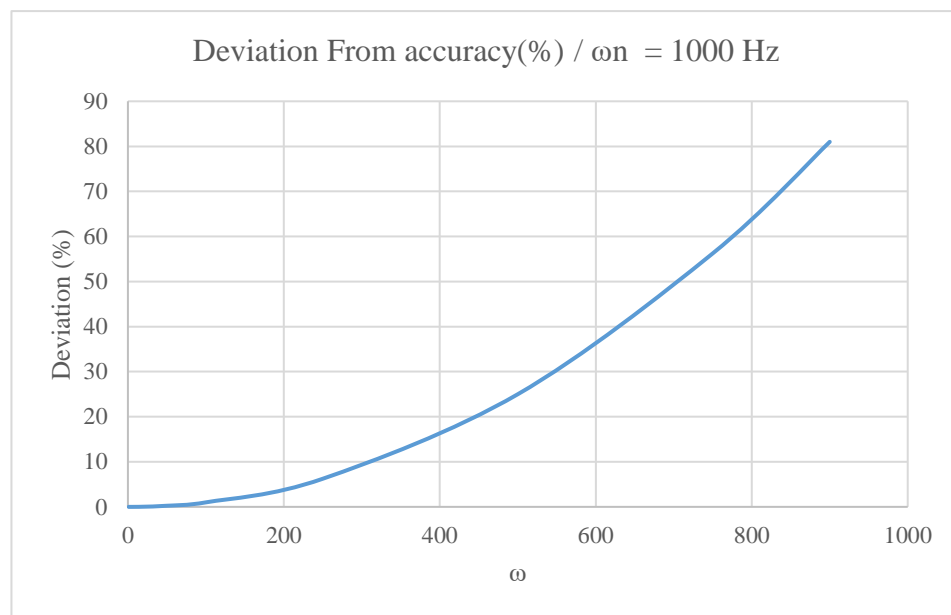


**Figure 2.24.** The deviation from accuracy plot

## 2.2. Literature Review

In this chapter a literature review of the yarn tension sensors was conducted. Wang et al. (2016) measured the yarn tension in a winding system through an optical method and they tried to analyze the captured images to get the strain values. Figure 2.25 shows a schematic of the used system.

The used method is insensitive to yarn diameter unevenness and can be applied to varieties of subjects like cords, braiding, cables and yarns. Figure 2.26 shows the system and the tension sensing mechanism, the line laser and the linear array camera are perpendicular to the axis of yarn in the same plane. The laser source forms the light on the yarn and its reflection is captured by the linear CCD camera (charged-coupled device), then the camera is linked to the PC which processes and stores the data. The yarn speed used in the experiment was 32 m/min.

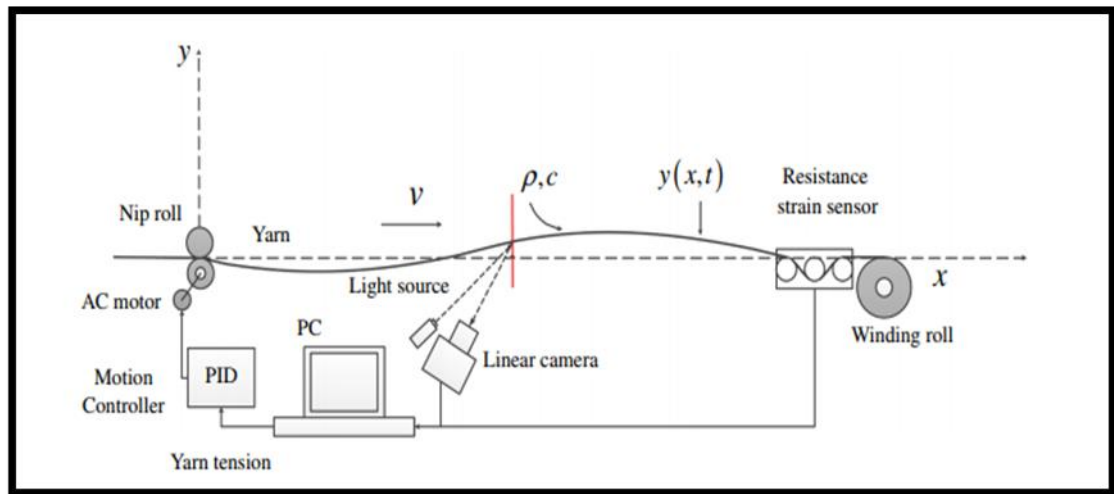


**Figure 2.25.** A schematic view of the measuring system (Wang et al. 2016)

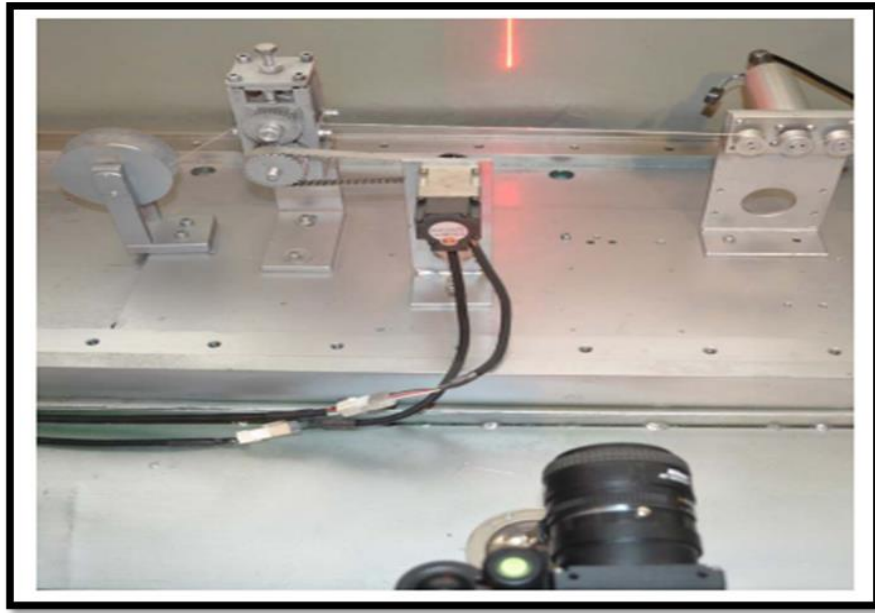


**Figure 2.26.** The used system to capture the yarn tension (Wang et al. 2016)

The tension measured by optical method as explained above is compared with the tension measured by strain gauge tension sensor. A near perfect match between the two-tension measuring system is found as shown in Figure 2.27.

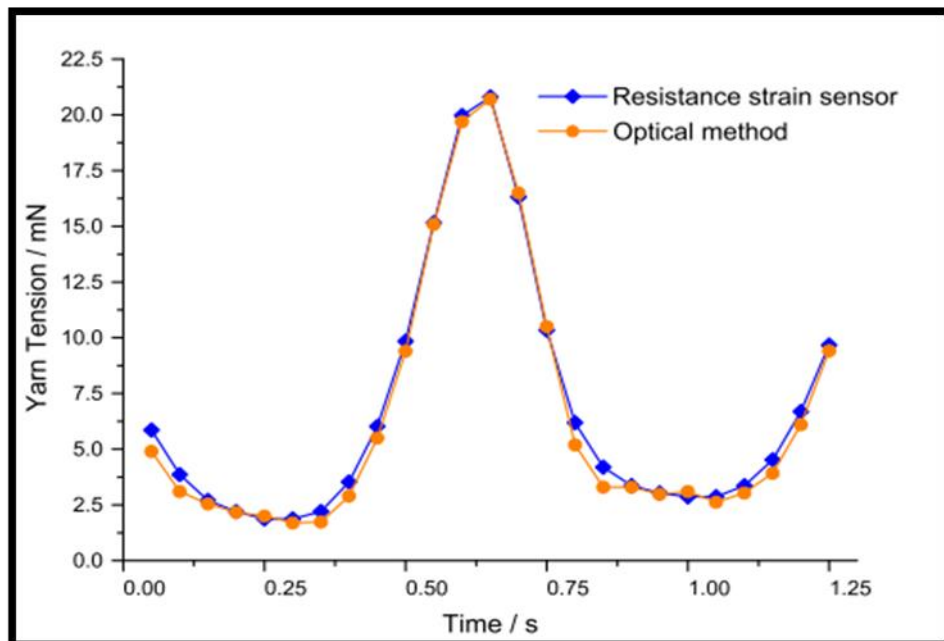


**Figure 2.27.** The optical system tension results in comparison with a resistance tension sensor (Wang et al. 2016)

Another method of measuring the yarn tension is using the MEMS and RF to measure the tension wirelessly. Shankam et al. (2009) designed and developed a system to measure and control the yarn tension wirelessly. The measurement was done by Micro-Electro-Mechanical Systems (MEMS) technology with radio frequency (RF) transmission. The system included two modules: 1. A wireless yarn tension sensor: this sensor is deployed in the track of the yarn and tension is measured by strain gauges and then it is transmitted wirelessly to the computer. 2. A control module that will change the yarn tension in according to the tension sensed by the first module (the wireless sensor) and the initial value of the tension. Figure 2.28 shows a schematic of the developed system.

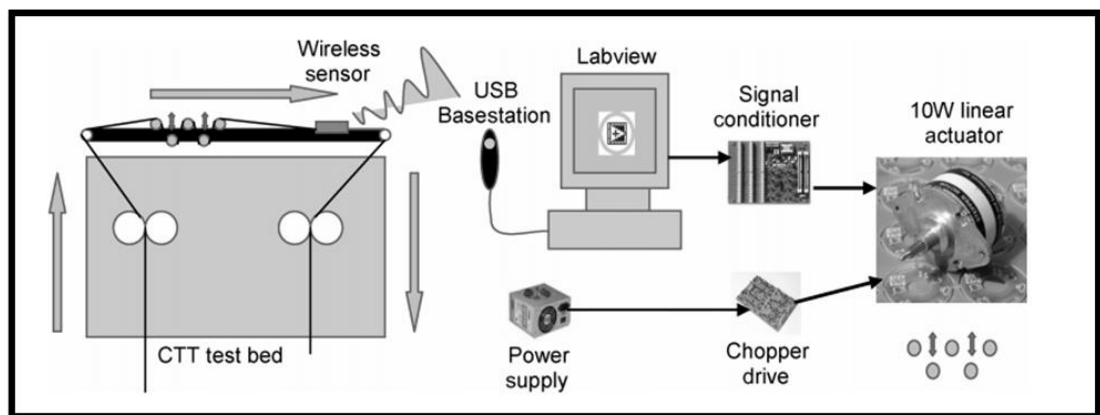


**Figure 2.28.** A schematic of the developed system (Shankam et al. 2009)

The sensing concept is to install two sensors in each of the component yarn tracks that the control system gets a signal pertaining to tension values in each component yarns T1 and T2. Figure 2.29 shows the working concept of the wireless tension sensor. There are two semiconductor strain gauges embedded on the ceramic dowels, and these ceramic dowels act as the transducer in the sensor. These strain gauges are connected to a radio frequency (RF) transceiver. A battery system was used to power the system. Experimental work was carried out at 20, 30, 40, 50 and 60 m/min speeds.

The yarns used are polyester, nylon, dyneema, spectra, and the sensor showed a good linearity. Therefore, it was commented that it could be used effectively to measure the yarn tension. Figure 2.30 shows the developed sensor.

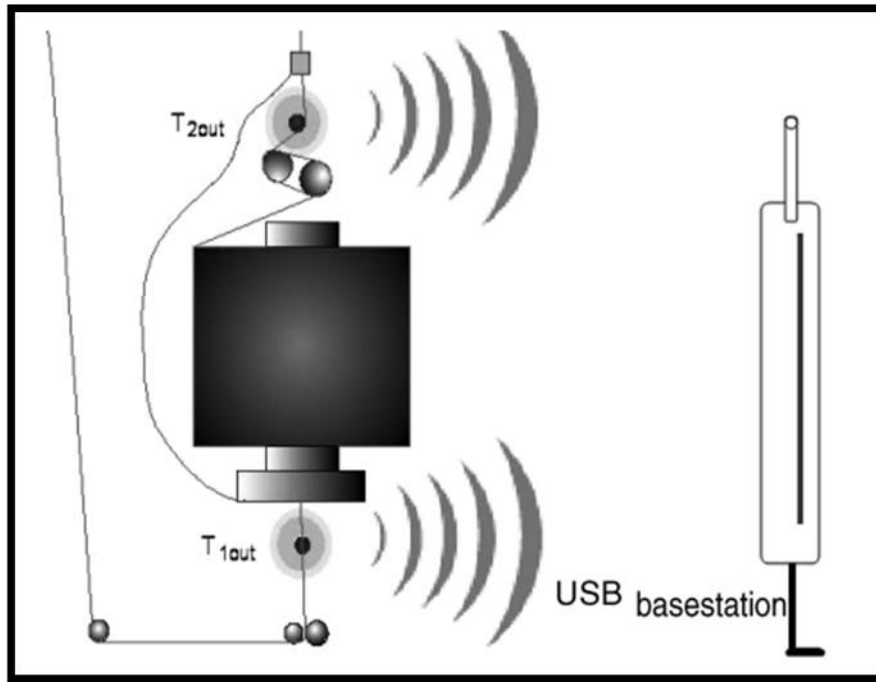


**Figure 2.29.** The wireless yarn tension sensor working concept (Shankam et al. 2009)

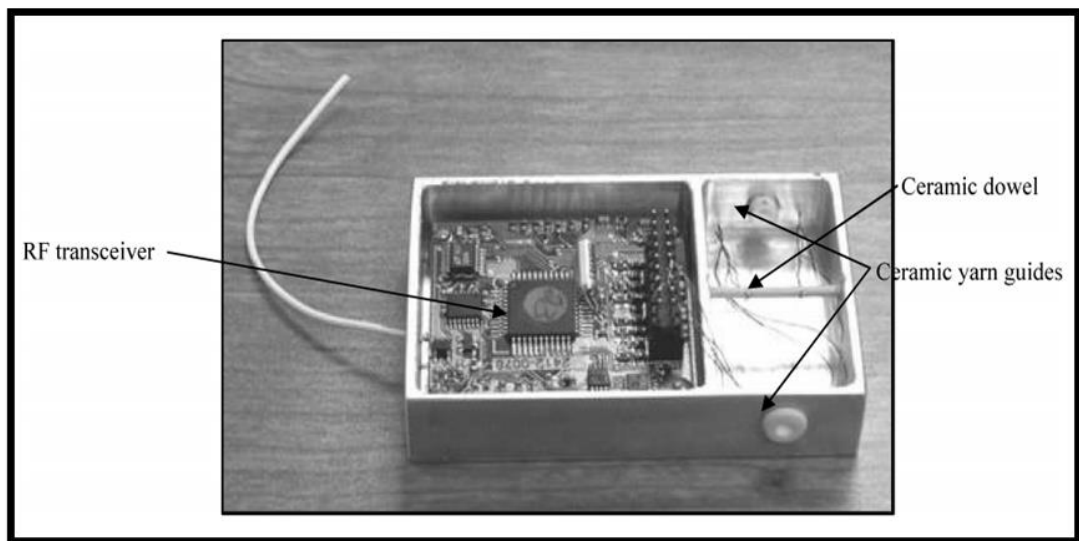


**Figure 2.30.** The developed yarn tension sensor (Shankam et al. 2009)



The dynamic characteristics of the sensor elastic element are critical to the accuracy of the measurements, it affects the accuracy and reliability of the tension sensor.

Xiang-lin, and Xiao-ping (2008) worked on optimization of the yarn tension sensor where they built a finite element model of the sensor and analyzed the vibration characteristics of the elastic spring before and after the optimization. The modal shapes and the natural frequency of every modal shape were calculated. The analysis was done through a computer simulation program ANSYS.

Due to minimal effect, the damping factor was ignored in this study. The results depended on the mass distribution, stiffness and fixed support. Figure 2.31 shows the design of the yarn tension sensor.

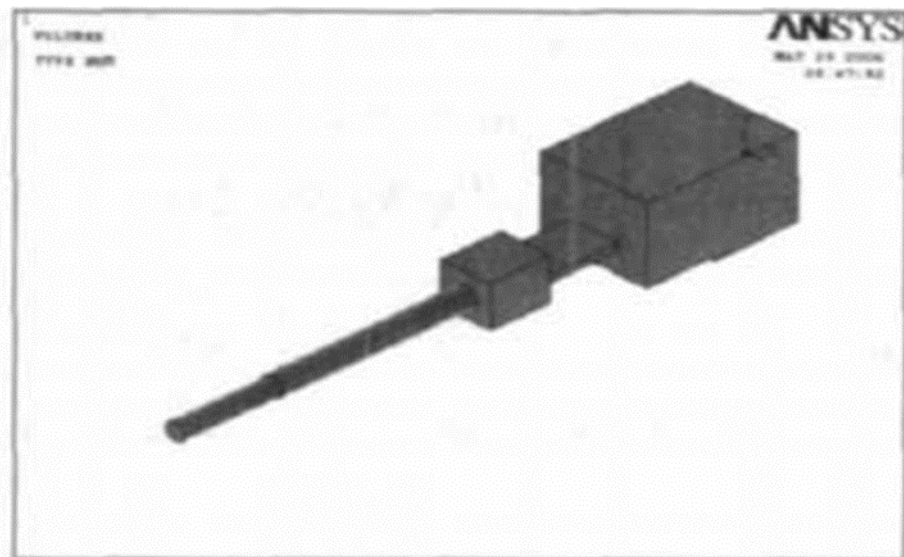


**Figure 2.31.** The design of the yarn tension sensor (Xiang-lin, and Xiao-ping 2008)

In order to increase the natural frequency of the sensor and avoid resonance and improve the sensor's structure, multiple tests were done and it was found that by reducing the mass of the free end cylinder a better result would be achieved so the cylinder was shelled and designed in a hollow structure. The optimized model has a better natural frequency and its stability was improved.

The natural frequency of the first five modal shapes before and after optimization is shown in the Figure 2.32.

Before the optimization		After the optimization	
1	236	1	425
2	1092	2	1628
3	2855	3	3038
4	4725	4	4953
5	4988	5	6325

**Figure 2.32.** The natural frequency of the first five modal shapes before and after the optimization (Xiang-lin, and Xiao-ping 2008, changes were made)

Another method developed to measure yarn tension is using the surface acoustic wave (SAW), Lu et al. (2012) used the surface acoustic wave (SAW) oscillators to create a yarn tension sensor. The new sensor can overcome the problems of the existing sensors. Its main working principle is that when the yarn is under tension, the piezoelectric substrate of the SAW oscillator will oscillate with oscillation frequency changing with yarn tension. The developed yarn tension sensor has the good properties of the SAW oscillator, which are good reliability, stability, small size and fast response time, and the output signal of the developed sensor is a frequency signal not an analog one which improve the anti-interference of the sensor and delivers less noise in addition to low production cost. And a linear relation between the yarn tension and the output frequency shift of the yarn tension sensor was deduced. Figure 2.33 shows a schematic of the developed sensor, and Figure 2.34 shows the developed sensor and its working principle, the oscillator 2 is used to compensate for the temperature effect of the first oscillator.

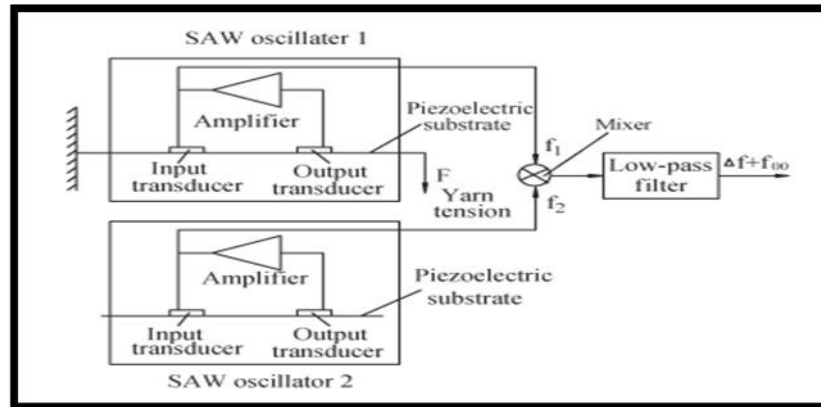


**Figure 2.33.** A schematic of the SAW sensor (Lu et al. 2012)

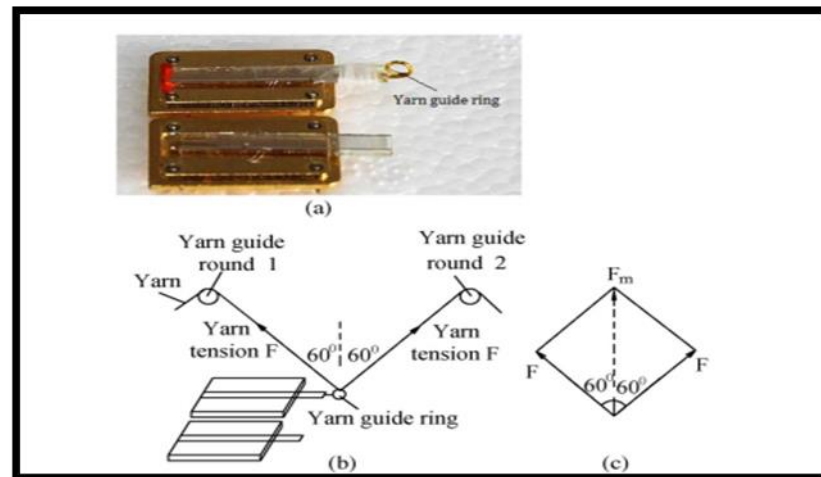


**Figure 2.34.** (a) The developed sensor. (b) The system schematic. (c) The schematic of the yarn tension  $F$  (Lu et al. 2012)

Another paper for the SAW sensor by Lei et al. The effect of the interdigital transducer (interlocking comb-shaped arrays of metallic electrodes) position on the SAW sensor sensitivity and the characteristics of the sensor substrate were studied by FEA program ANSYS and regression analysis. An optimal solution was reached and tension sensor with the optimal dimensions was manufactured and tested. The force used in the finite element analysis on the substrate is 1 g. Figure 2.35 (a) shows the fabricated sensor and (b) the IDT design schematic.

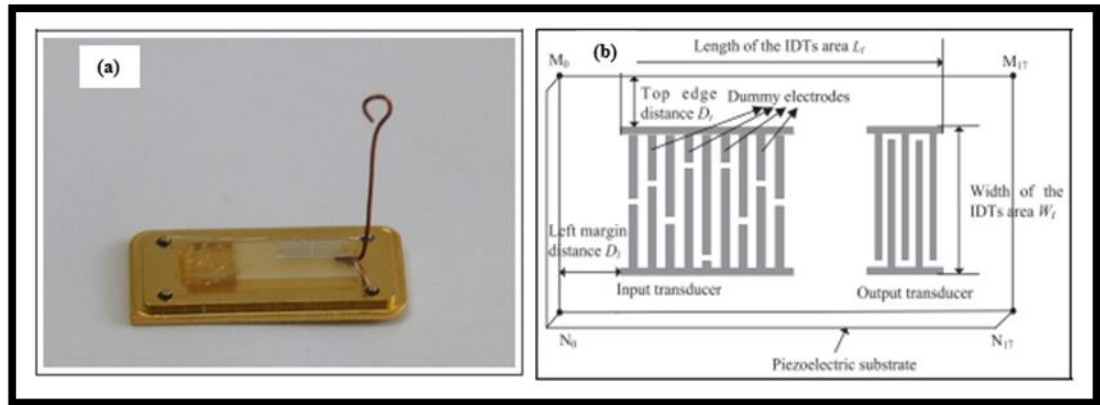


**Figure 2.35.** (a) The fabricated sensor and (b) The IDT design schematic (Lei et al. 2020)

When the yarn tension force  $F$  deforms the piezoelectric substrate, it creates a change in the properties of the substrate (strain). This will change the SAW propagation velocity and the interdigital transducer wavelength and will shift the oscillation frequency of the first oscillator accordingly. By measuring the output frequency shift of the oscillator, the yarn tension could be obtained. Figure 2.36 shows the strain simulation results on the substrate.

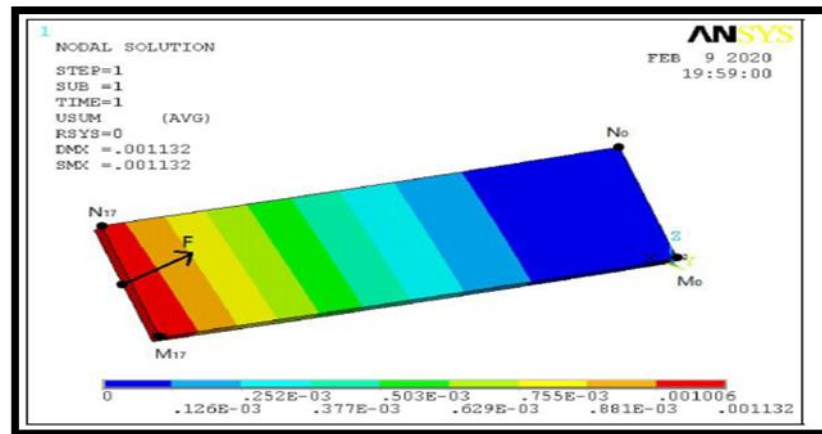


**Figure 2.36.** The ANSYS simulation results of the substrate (Lei et al. 2020)

Another paper by Lei et al. (2015) focused on optimizing the sensitivity of the SAW sensor, they tried to optimize the sensitivity by improving the strain rate of the piezoelectric substrate. This optimization process was done by using regression analysis, FEA (ANSYS analysis) and by establishing linear programming model. The built regression model between the strain of the sensor substrate and its size indicated that by

optimizing the substrate size design, the piezoelectric substrate strain increased. And in order to get the optimal results a linear programming model was created. Figure 2.37 shows some design parameters of the SAW yarn tension sensor. Figure 2.38. shows (a) the manufactured SAW sensor (b) a schematic of the SAW sensor.

Yarn tension sensor	SAW1	SAW2	SAW3	SAW4	SAW5	SAW6
Substrate length (mm)	7	10	13	9	15	9
Substrate width (mm)	3	3	3	4.5	4.5	6
Spacer length (mm)	3	3	3	4.5	4.5	6
Spacer width (mm)	2.5	2.5	2.5	2.5	2.5	2.5
Left margin (mm)	0.1	1.2	1.2	1.2	1.2	1.2
Top margin (mm)	0.3	0.3	0.3	0.3	0.3	0.3

**Figure 2.37.** Some design parameters used for the SAW yarn tension sensor (Lei et al. 2015)

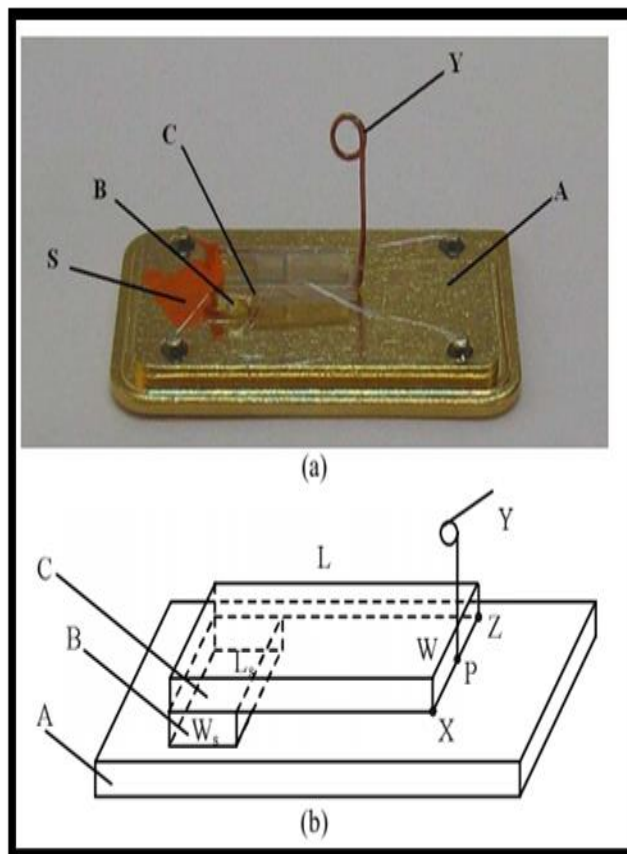


**Figure 2.38.** (a) The manufactured SAW sensor (b) a schematic of the SAW sensor (Lei et al. 2015)

The sensor parts are described as following;

- Yarn guide: Y
- Sensor substrate: C
- Metal pedestal: A
- Quartz spacer: B

A and B are bonded together and P is the center of X-Z and the spot where the sensor substrate and yarn guide are glued together. The length of the SAW sensor substrate is L its width is W. The length of the quartz spacer is  $L_s$  and its width is  $W_s$ .

To compensate for the temperature effect on the SAW yarn tension sensor, another study was conducted by Lu et al. (2017) In this study, a functional relationship was deduced. It describes the shift of the oscillation frequency with respect to temperature change. Then the calculated shift was used to compensate for the temperature effect on the SAW yarn tension measurement. Figure 2.39 shows the curve between the temperature change  $\Delta T$  and the oscillation frequency  $\Delta f_T$ .

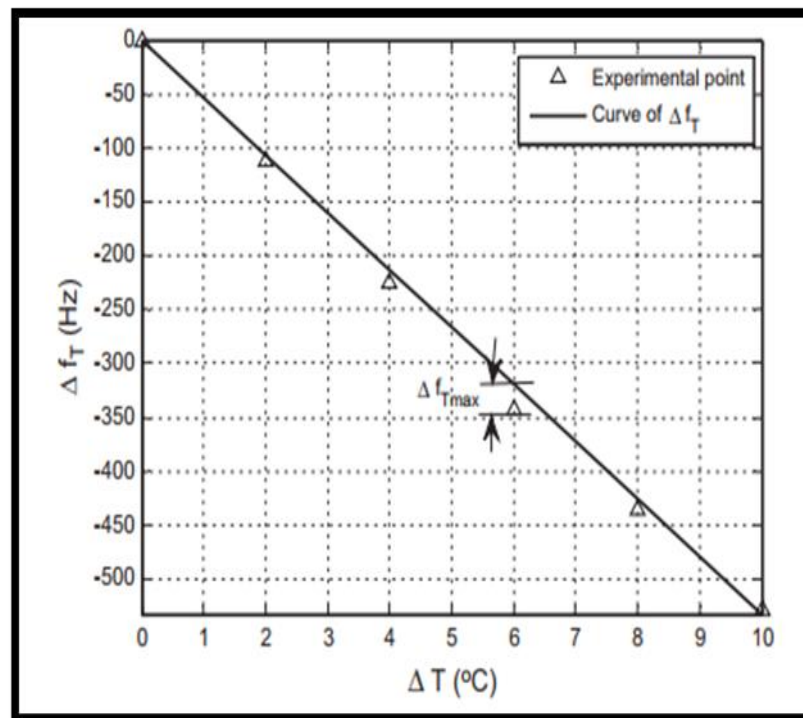


**Figure 2.39.** The curve between temperature change  $\Delta T$  and oscillation frequency  $\Delta f_T$  (Lu et al. 2017)

Another method for yarn tension measurement was studied and developed by Chifu (1970) where he tried to develop a high frequency responsive transducer to be used as a yarn tension sensor, the transducer was based on the principle of changing frequency shifts of a quartz crystal resonator when subjected to a force. According to the researcher, the yarn tension sensor has to have the following properties;

- Has a frequency response of 0-10KHz.
- Measure 200-300 gr in full scale.
- to be stable under temperature fluctuations.

An experimental apparatus (Figure 2.40 a) was used to double the tensile force caused by the yarn and press the resonator. The load is applied to the lever which in return transmits it to the quartz plate. The quartz plate is shown in Figure 2.40 b. Its diameter is 14mm, thickness 0.33mm and has a frequency of 5MHz. Then it is connected to an oscillator circuit. To keep natural frequency high, the lever was built from a metal which had a high Young's modulus, went through heat treatment and kept small in size. The measurements were conducted at a speed of 10 m/sec. The yarn tensile deformation was formed by a compressed-air piston.

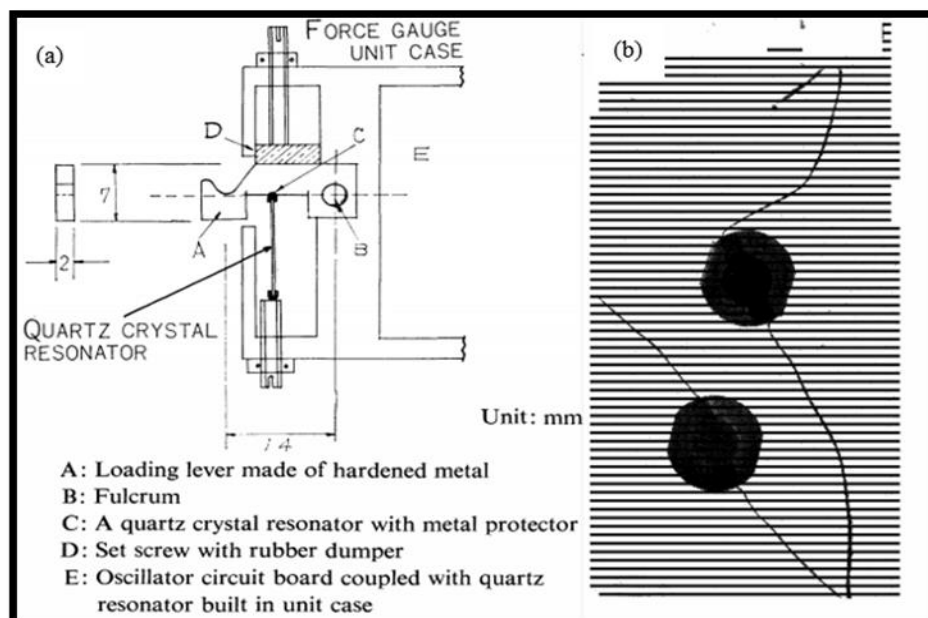


**Figure 2.40.** (a) The developed measuring apparat (b) Quartz Crystal Resonator (Chifu 1970)

In their patent, Hartel et al. (1994) invented a sensor to measure yarn tension. The sensor is using the magnetic field fluctuations to measure the tension of the yarn. The magnetic field changes continuously according to the change in tension. The developed sensor is suitable for high speed yarns and high-frequency tension changes. And it can detect the periodic and nonperiodic changes of the tension and has a wide area of applications. Figure 2.41 shows a schematic of the developed yarn tension measuring system.

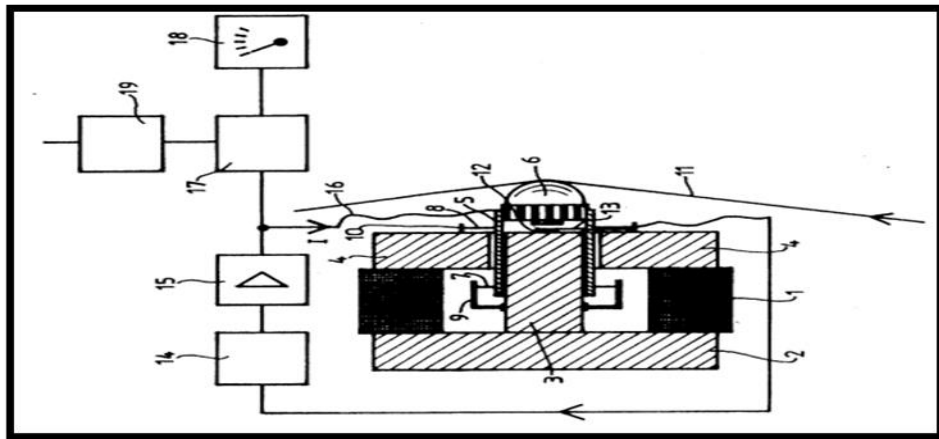


**Figure 2.41.** A detailed schematic of the developed yarn tension measuring system (Hartel et al. 1994)

A detailed description of the system and its elements in the figure above can be explained as follows. The ring magnet (1) which has pole disk (2) on its axial side and a pole ring (4) on the other side. In the center opening of the pole ring a plunger coil (5) which protrudes axially forming an annular air gap. The magnet parts, the pole disk, the core and the pole ring are made from a ferro-magnetic material. The plunger coil is connected to the diaphragms (7) (8) so it can move in an axial motion. (9) (10) are diaphragm retainers and they are connected to the core and the pole ring. The yarn (11) goes through the yarn guide (11) which is connected to the end of the plunger coil. Every small change in the position of the plunger coil is observed by (12) an analog Hall sensor. Then the signal is transmitted to the controller (14) and amplifier (15). After that it is fed to the winding of the plunger coil by a line (16). This causes a change in coil current. This change is related to the axial force of the plunger coil which is caused by the movement of the yarn. Finally, the tension signal is fed to the Evaluation device (17) and Display device (18).



Another tension measuring unit by Nakayama et al. (1980), it is capable of detection changes in yarns tension with high accuracy using a rotary guide driven by a motor and strain gauge force transducer. Figure 2.42 shows a detailed schematic of the invented yarn tension meter. When a yarn (1) gets through the fixed guides (1) (2) and presses on the guide (4) that is connected to the elastic element (5) which is a part of the force transducer (7), this force transducer has also strain gauges (6) installed on it. And its connected to the casting (13). (8) present a signal processing unit and (9) a meter. The rotary guides (11) are connected to a motor (12) that fluctuates the yarn between the guides (2) and (3). Figure 2.43 shows different rotary guides can be used in the sensor.

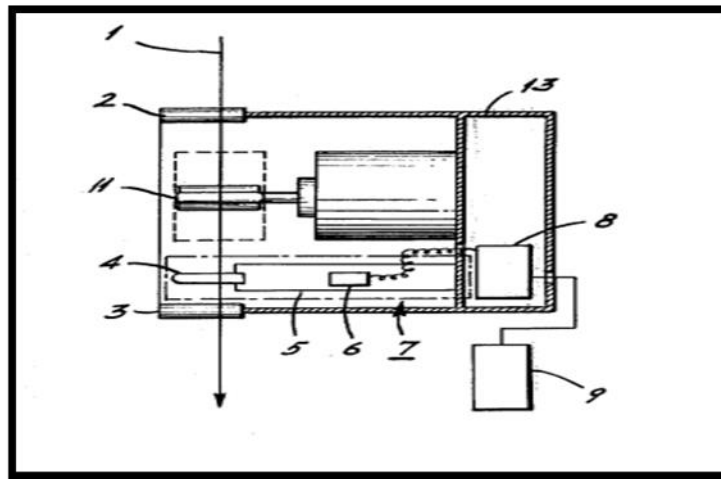


**Figure 2.42.** A schematic of the invented yarn tension meter (Nakayama et al. 1980)

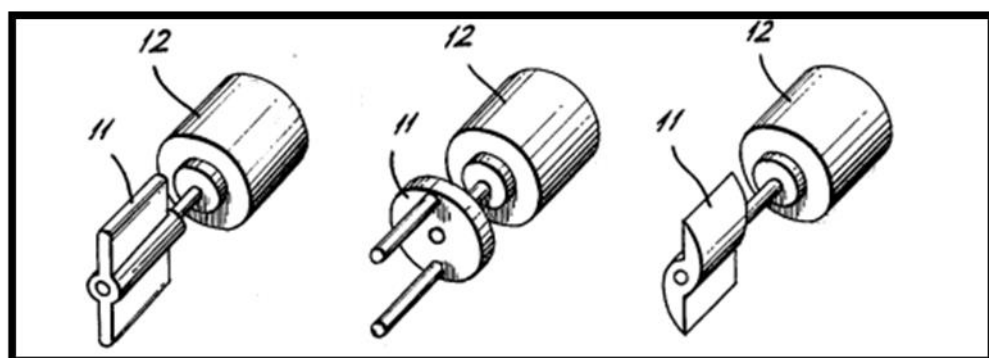


**Figure 2.43** Different rotary guides can be used in the sensor (Nakayama et al. 1980)

Barat and Salles (1996) developed a sensor to measure the filament yarn tension and speed without any contact. The sensor was based on converting the changes in capacitance due to filament vibration into voltage signals that were filtered, amplified and then converted into tension and speed values. Figure 2.44 shows a schematic of the developed sensor. The main parts of the system are the flat conductors (2, 4) and between them an air gap (6) that acts as a dielectric layer. All of them forms an air capacitance. The yarn's (8) path goes through the yarn guides (10a, 10b) through the conductors. Because of the movement and fluctuation of the yarn through the air gap, a change in capacitance value of the flat conductors accrues. The conductor (4) consists of two electrodes which allow to sense limited relative capacitance changes. When the yarn vibrates, its position alternates between the electrodes in every half cycle of the yarn vibration. For the speed measurement, the capacitive dipoles (13, 17) have two flat conductors, 12 and 14 for the dipole (13), 16 and 18 for the dipole (17). They are separated by air gaps (15 and 19).

The conductors (14) and (18) have two electrodes which are perpendicular to the yarn direction, and each conductor has two electrodes (a and b) which are raised to a potential +V and -V. The random signal  $x(t)$  caused by the yarn going through the first dipole (13) is the same as the random signal  $y(t)$  which comes from the second dipole (17) but there is a time shift ( $\Delta T$ ). By calculating the time shift, yarn speed is calculated as  $Speed = \frac{D}{\Delta T}$  where D is the distance between the dipoles. Similarly, yarn tension is calculated by analyzing signal variations due to yarn vibrations based on signal analysis (contactless method).

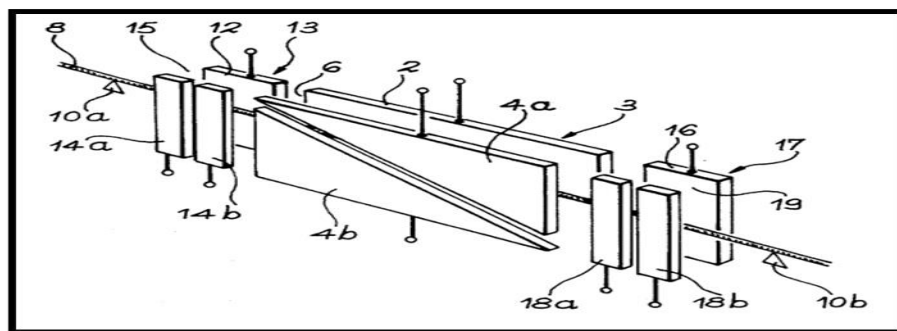


**Figure 2.44.** The schematic of the developed sensor (Barat and Salles 1996)

Wessolowski et al. (1987) developed a tension sensor with high natural frequency that could be used to measure the tension in yarn processing machines by overcoming the effect of vibration of the machine. Figure 2.45 shows an illustration of the developed sensor. The yarn tension sensor (1) has two parallel spring plates (2) which are connected by blocks (3 and 4) and they are fixed to the frame (7) by a mounting spacer (6). The yarn (10) goes over the yarn guide surface (8) and causes the force (11). A damping piston (9) is fixed to the free end of the spring from one side and the other side is placed in a magnetic fluid (ferrofluid) (13) which is hold in a cup shape receptor (12) placed on a magnet (14). Both the receptor and the magnet are fixed to the frame. The end of the spring arm has a hollow casing (16) with a rectangular shape. This casting has two opposite walls (22) (22'). Each wall has elongate openings (17) and each opening has edges that elongate along the casting. A support element (23) is fixed on the deflection instrument that is mounted in the casing. The displacement caused by the yarn is followed by a mounting head (19) and the deflections are scanned by a radiation source (29) and a receiver (30). Elongated spring arm is fixed from one end and its free end is subjected to deflection. This free end is connected to a guide that holds the running yarn. This tensioned running yarn causes deflection in the free end of the arm. To include a damping factor, a section of the spring element was immersed in a magnetic fluid which is hold in place by a permanent magnet. To measure the deflection of spring element an optical signal transmitter and receiver is used. This signal is converted to tension signal and used as tension sensor after calibration.

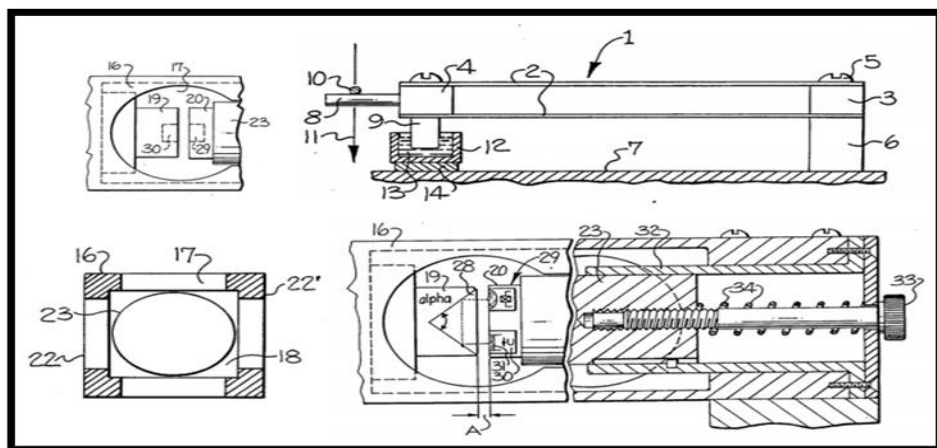


**Figure 2.45.** The developed optic sensor (Wessolowski et al. 1987)

In their patent Bandara (2007) developed a contactless sensor to measure tension of yarn and other elongating elements. Figure 2.46 shows (a) the yarn and the optical device, (b) and the optical device schematic, (c) the complete developed system. The tension measurement was done by an optical sensing device (14) and signal conditioning circuits. The moving yarn (11) runs over the two yarn support guides (12, 13) which help guiding the yarn into the desired path and define the distance Lambda.

The optical sensor is a charge couple device (CCD) linear array type (20). The radiation or lighting (21) is provided by high power LEDs (30) and it is focused by the lens (22) on the (CCD) array (20) which generates a signal (24) that is transmitted to the detection circuit (23). This provides another signal (25) that corresponds the transverse place of the targeted yarn. Finally, a signal processing unit samples the sensor output and conduct a frequency analysis of the signal and calculates the yarn tension.

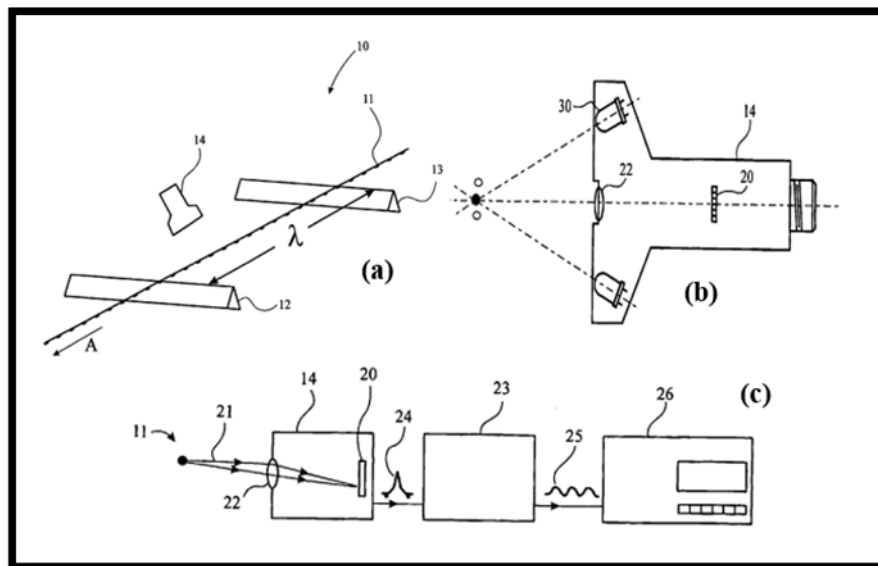


**Figure 2.46.** (a) The yarn and the optical device (b) The optical device schematic (c) The complete developed system (Bandara 2007)

### 3. MATERIALS AND METHODS

#### 3.1. Materials

In this chapter, the tools used in this thesis were presented. The tools and materials used in the designing process, analysis, signal conditioning, data acquisition and yarn winding system.

The used software for designing the yarn tension sensor prototypes is a computer-aided design software named SOLIDWORKS. It is a widely used CAD program and has a user-friendly interface. It allows the researcher to prototype and test different designs quickly, drawing sketches, 3D shapes, and assembling multiple parts. Figure 3.1 shows SOLIDWORKS interface.

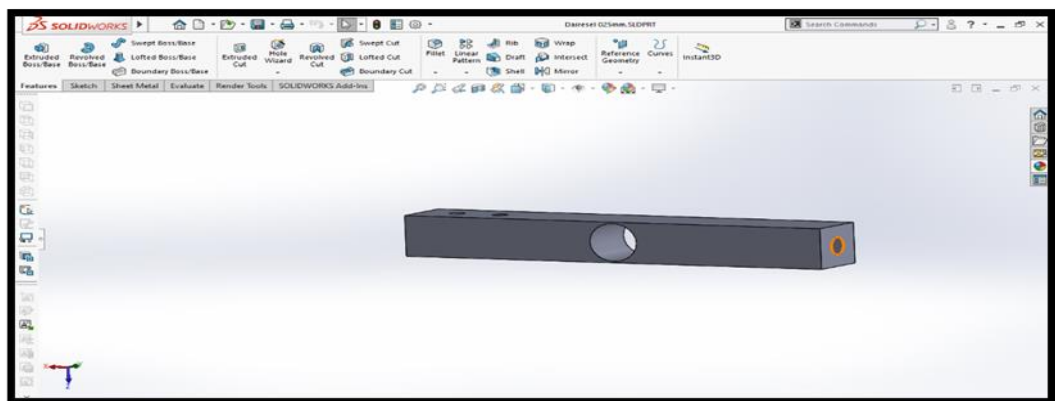


**Figure 3.1.** SOLIDWORKS user interface

The used software for analyzing the designed yarn tension sensor prototypes is an engineering simulation and finite element analysis software named ANSYS. It is one of the most used analysis programs due to its functionality and many analysis tools. Figure 3.2 shows the user interface of the software. ANSYS helps to conduct different analysis on the system and simulates it under conditions similar to the real life applications. Some of the analysis that can be done in ANSYS are:

- Static Structure Analysis
- Modal Analysis
- Harmonic Response Analysis
- Explicit Dynamics and Flow Analysis

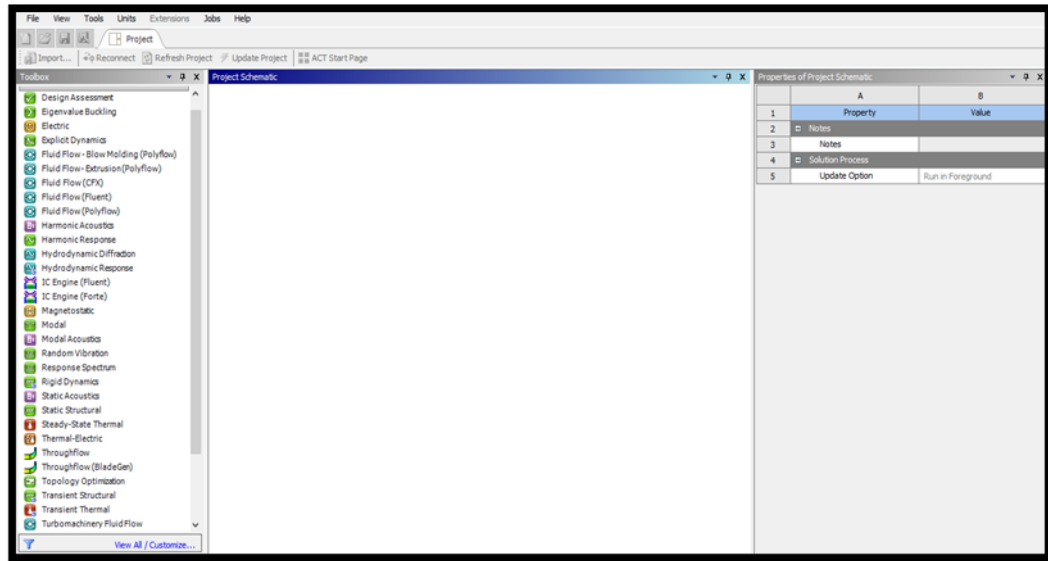


**Figure 3.2.** ANSYS user interface

For manufacturing the yarn tension sensor, a widely available Aluminum alloy, has a low price and suitable properties were chosen. Aluminum 6013 alloy is a wrought alloy type with high strength and widely used in aerospace applications. Table 3.1 shows Aluminum alloy 6013 properties.

**Table 3.1.** Aluminum alloy 6013 properties (Anonymous 2020c)

Density	2.8 g/cm <sup>3</sup>
Elastic Modulus	69 GPa
Poisson's Ratio	0.33
Shear Modulus	26 GPa
Fatigue Strength	98 to 140 MPa

For the strain gauges, a strain gauge with 350  $\Omega$  was chosen to endure higher supply voltage. With the minimal possible dimensions to fit on the load cell maximum strain areas.

The strain gauge properties:

- Gauge factor: 2.1
- Strain gauge resistance: 350  $\Omega$
- Strain gauge dimension: 3\*5 mm

For the amplification circuit, SGA/A from Mantracourt was chosen. It is an analog strain gauge signal conditioner. It provides a stable 5 and 10 V excitation voltage to the strain gauges. Furthermore, the output signal can be selected from a range of outputs like  $\pm 10$  V,  $\pm 5$  V, 0-10 V, 0-5 V, 0-20mA, or 4-20 mA. Figure 3.3 shows the SGA/A amplifier. Figure 3.4 shows the connection between the bridge and the amplifier. The SGA/A offers a bridge sensitivity of 60 steps for a span from 0.06 mV/V to 30.30 mv/V. Moreover, it has a potentiometer for fine-tuning. For the offset, it is capable of scaling 79% of the voltage.

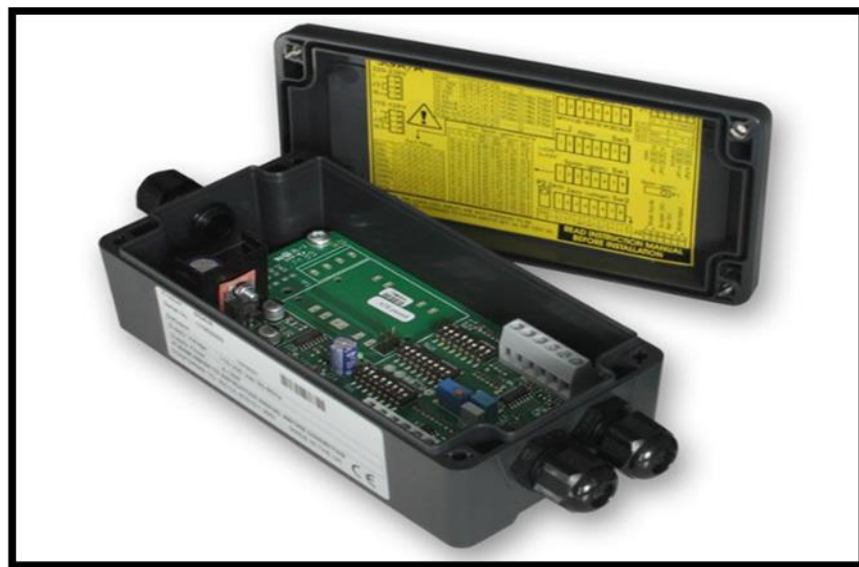


**Figure 3.3.** SGA/A analog strain gauge signal conditioner (Anonymous 2016b)

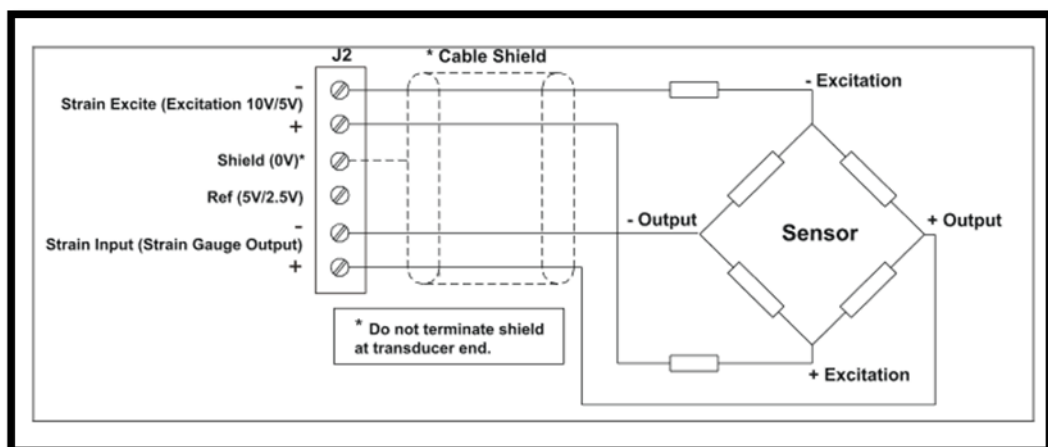


**Figure 3.4.** Strain gauge – amplifier connections (Anonymous 2016b)





The measurement system used for testing the yarn tension sensor is a winding unit shown in Figure 3.7. The sensor positioning can be seen in Figure 3.8.

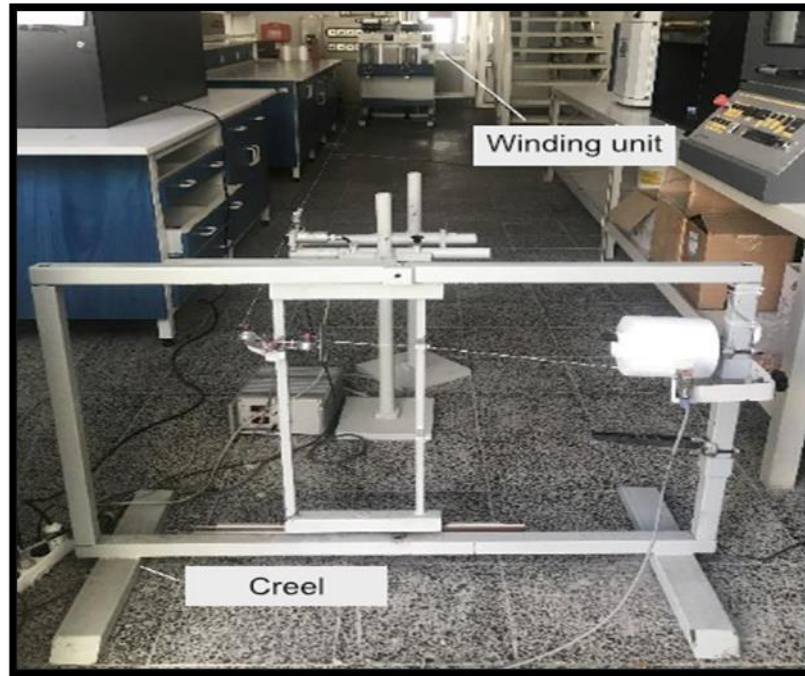


**Figure 3.7.** The creel and winding unit (Çelik 2018, changes were made)



**Figure 3.8.** The sensor positioning

Figures 3.9, 3.10, and 3.11 show the manufactured sensors, Sensor #1, Sensor #2, and Sensor #3, respectively. Figure 3.12 shows the complete yarn tension sensor.



**Figure 3.9.** Sensor #1

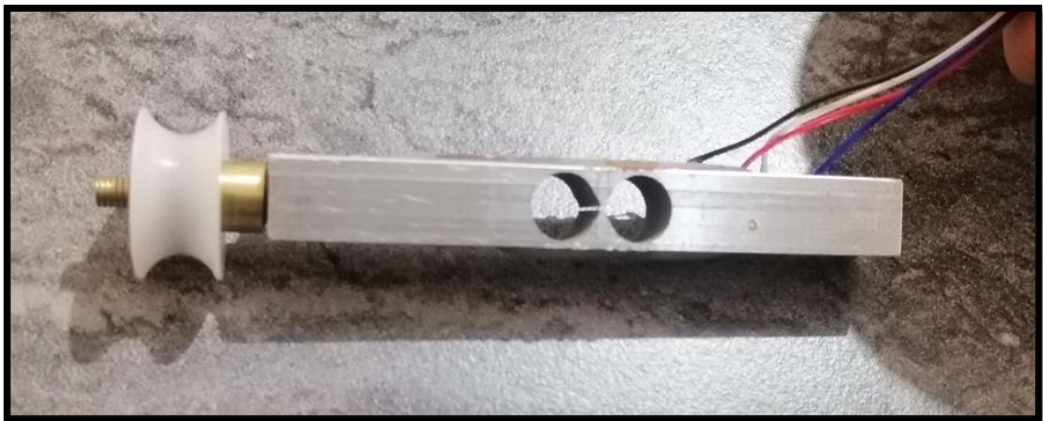


**Figure 3.10.** Sensor #2



**Figure 3.11.** Sensor #3



For the frequency analysis, FFT (Fast Fourier Transform) was performed, The FFT or fast Fourier transform is a mathematical technique that transforms a function of time  $F(t)$  into a function of frequency  $F(f)$ , and it is widely used in digital signal processing to find the frequency components of a signal. Figure 3.14 shows an illustration of the Fourier Transform.

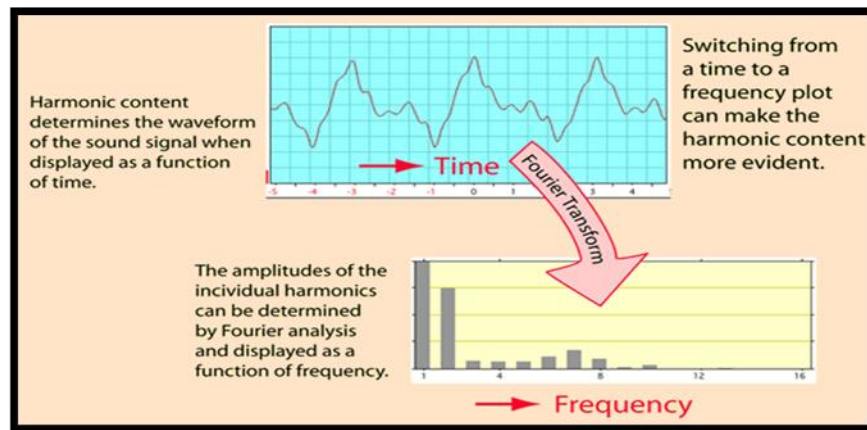


**Figure 3.14.** Fourier Transform (Anonymous 2018b)

For the frequency filtering, FIR (Finite Impulse Response) filter was used. Finite Impulse Response filter is one of the primary filters in digital signal processing. In MATLAB, the function `fir1` uses a Hamming window to design  $n$ th-order filters. The filter can be a lowpass, bandpass, or multi-band filter. It calculates the desired filter's impulse response, and by convoluting it with the signal, the filtered signal would be acquired. The `fir1` has two parameters ( $n$ ,  $W_n$ ). The first parameter  $n$  is selected according to the desired order of the filter. Where the second parameter  $W_n$  is the normalized cut-off frequency. The normalized cut-off frequency ranges from 0 to 1 (Nyquist, half of the sample rate).

### **3.2. Methods**

In the design and analysis stage, two steps process was conducted. In the first step, different sensor shapes were designed and studied. In the second step, the chosen designs were extensively analyzed. Different design parameters were changed, and the effect of every parameter was observed. Some of the tested parameters:

1. High strain zone length

The high strain zone length was changed, and its effect on the strain and natural frequency was studied.

2. High strain zone thickness

The high strain zone thickness was changed, and its effect on the strain and natural frequency was studied.

3. Place of the high strain zone

The high strain zone place was changed, and its effect on the strain and natural frequency was studied.

4. Different size rollers

Different size rollers with different weights were added to the sensor, and their effect on the strain and natural frequency was studied.

5. Sensor dimensions

Different dimensions were changed, and the effect of changing them on the strain and natural frequency was studied.

## 6. High strain zone shape

Different high strain zone shapes were studied, and the effect of changing them on the strain and natural frequency was studied.

In conducting the analysis in ANSYS, the following steps were followed. Figure 3.15 shows the design in ANSYS.

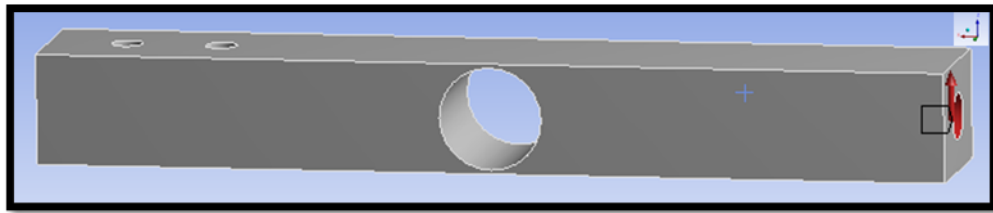


**Figure 3.15.** The design in ANSYS

1. Selecting and adding the analysis, Modal and Static Structure analyses were chosen (Figure 3.16) (Figure 3.17).

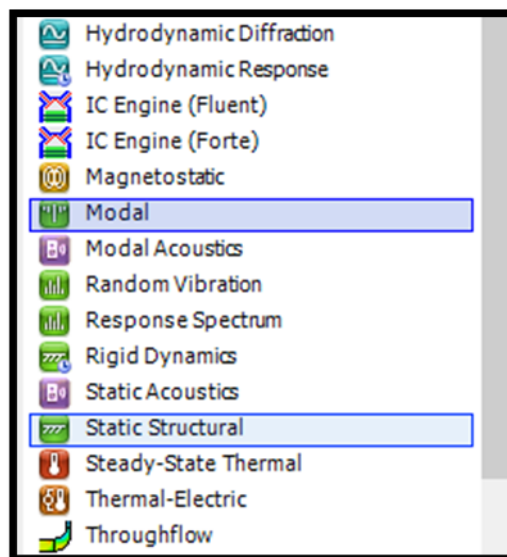


**Figure 3.16.** Selecting the analysis

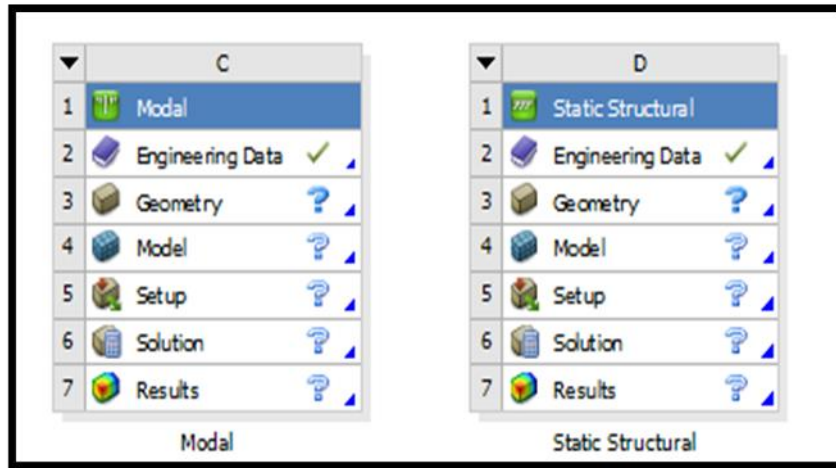


**Figure 3.17.** Adding Modal and Static Structural analyses

2. Adding the sensor material and properties (Figure 3.18).

Engineering Data Sources				
	A	B	C	D
1	Data Source		Location	Description
2	Favorites			Quick access list and default items
3	Granta Design Sample Materials			More than 100 sample datasheets for standard engineering materials, including polymers, metals, ceramics and woods. Courtesy of Granta Design.
4	General Materials			General use material samples for use in various analyses. Additive manufacturing material samples for use
Outline of General Materials				
	A	B	C	D
1	Contents of General Materials	Add	Source	Description
2	Material			
3	Air		General_Materials.:	General properties for air.
4	Aluminum Alloy		General_Materials.:	General aluminum alloy. Fatigue properties come from MIL-HDBK-SH, page 3-277.
5	Concrete		General_Materials.:	
6	Copper Alloy		General_Materials.:	
Properties of Outline Row 4: Aluminum Alloy				
	A	B	C	
1	Property	Value	Unit	
2	Density	2770	kg m <sup>-3</sup>	
3	Isotropic Secant Coefficient of Thermal Expansion			
5	Isotropic Elasticity			
6	Derive from	Young's Modulu...		
7	Young's Modulus	7.1E+10	Pa	
8	Poisson's Ratio	0.33		
9	Bulk Modulus	6.9608E+10	Pa	
10	Shear Modulus	2.6692E+10	Pa	

**Figure 3.18.** Material and material properties selection

3. Selecting the sensor design (Figure 3.19).

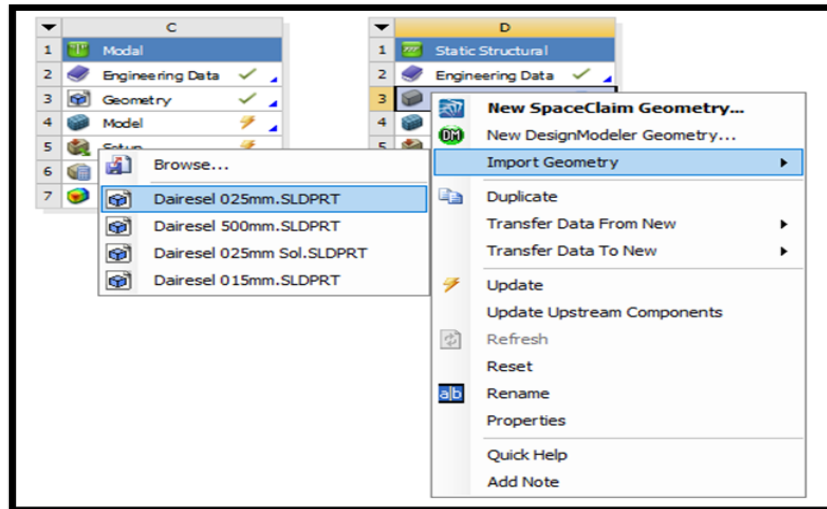


**Figure 3.19.** Selecting the sensor design

4. Choosing the material (Figure 3.20).

The used Material Properties:

- Aluminum Alloy
- Density = 2770 (Kg/m<sup>-3</sup>)
- Young's Modulus = 7.1\*10<sup>10</sup> (Pa)
- Poisson's Ratio = 0.33
- Bulk Modulus = 6.9608\*10<sup>10</sup> (Pa)
- Shear Modulus = 2.6692\*10<sup>10</sup> (Pa)

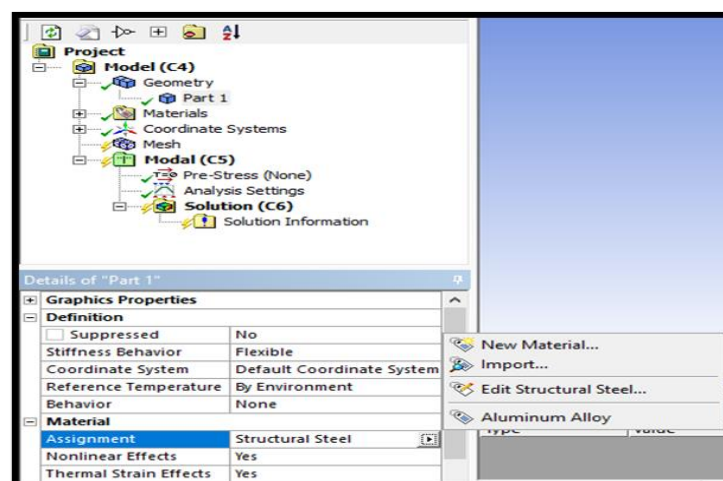


**Figure 3.20.** Selecting the sensor material



5. Choosing Meshing properties and creating the Mesh (Figure 3.21) (Figure 3.22).

Ansys Meshing Settings:

Meshing Method: Automatic

Behavior: Soft

Smoothing: Medium

Element Size: 1.0 mm

Transition = Slow

Span Angle Center: Medium

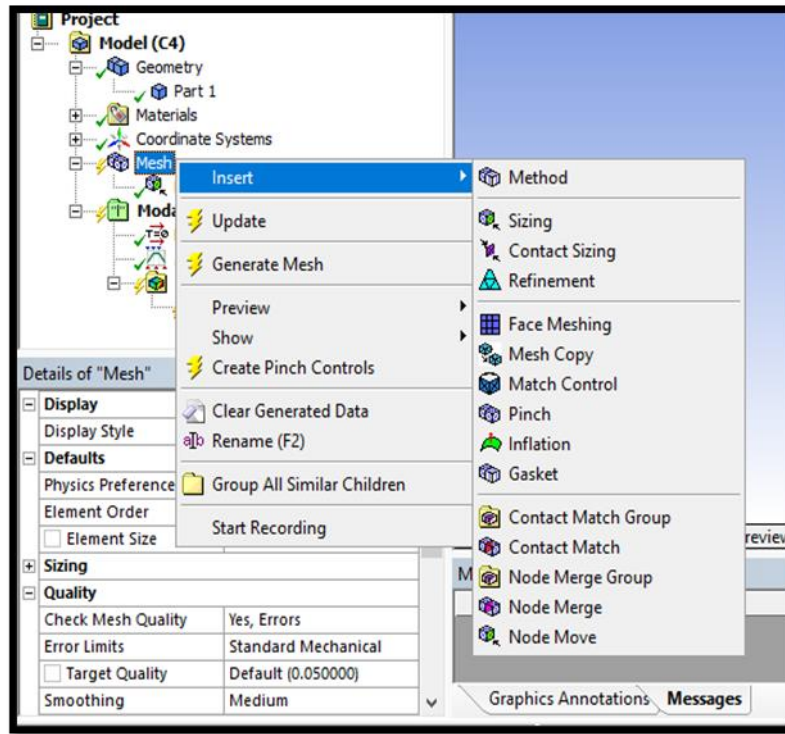


Figure 3.21. Meshing and selecting mesh properties

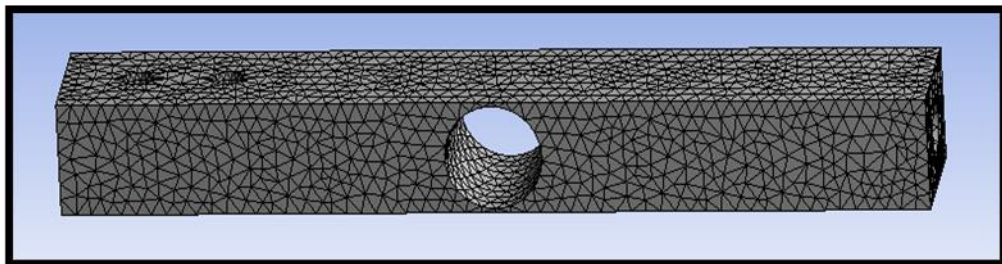
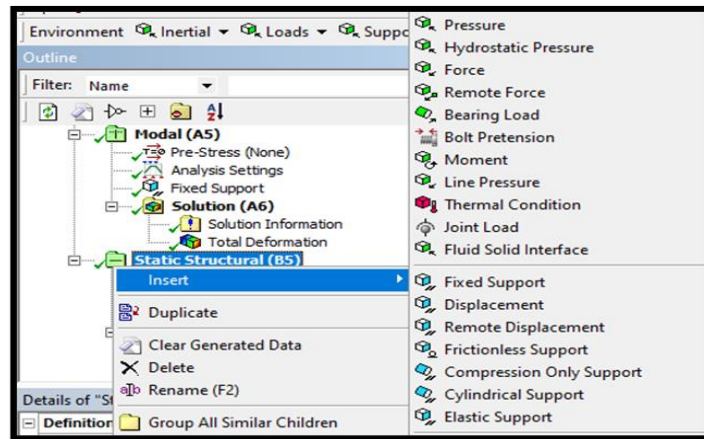


Figure 3.22. The sensor after the mesh process

6. Selecting the boundary conditions of the analysis and adding the force (Figure 3.23).

- The used force for the strain and stress analysis: 1, 10 (N)
- Force Direction: Z-direction. (see Figure 3.15)
- Applied place: The Red area seen in Figure 3.15.
- Fixed Support: The two screw holes



**Figure 3.23.** Adding the boundary conditions

7. Adding the analyses to solve (Figure 3.24).

The Used Ansys analysis:

- Modal analysis
- Normal Elastic Strain, X-Axis

8. Solving

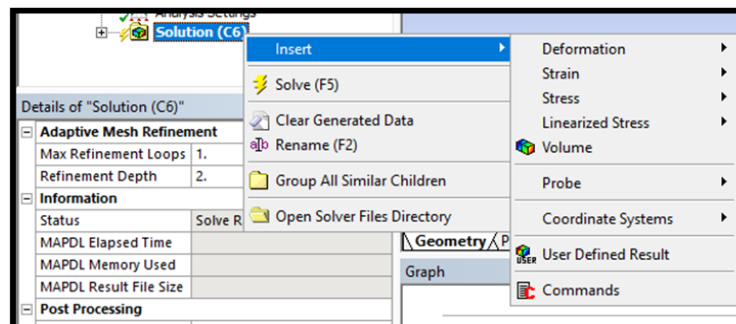


**Figure 3.24.** Adding the solutions

After the analysis process, three yarn tension designs were chosen. Figure 3.25 shows the selected designs. Then they were manufactured from aluminum alloy 6013 in a CNC machine to get the possible accurate manufacturing. Moreover, a Wire electrical discharge machine was used to cut some profiles that were not possible in the CNC machine. Figure 3.26 shows the sensor assembly.

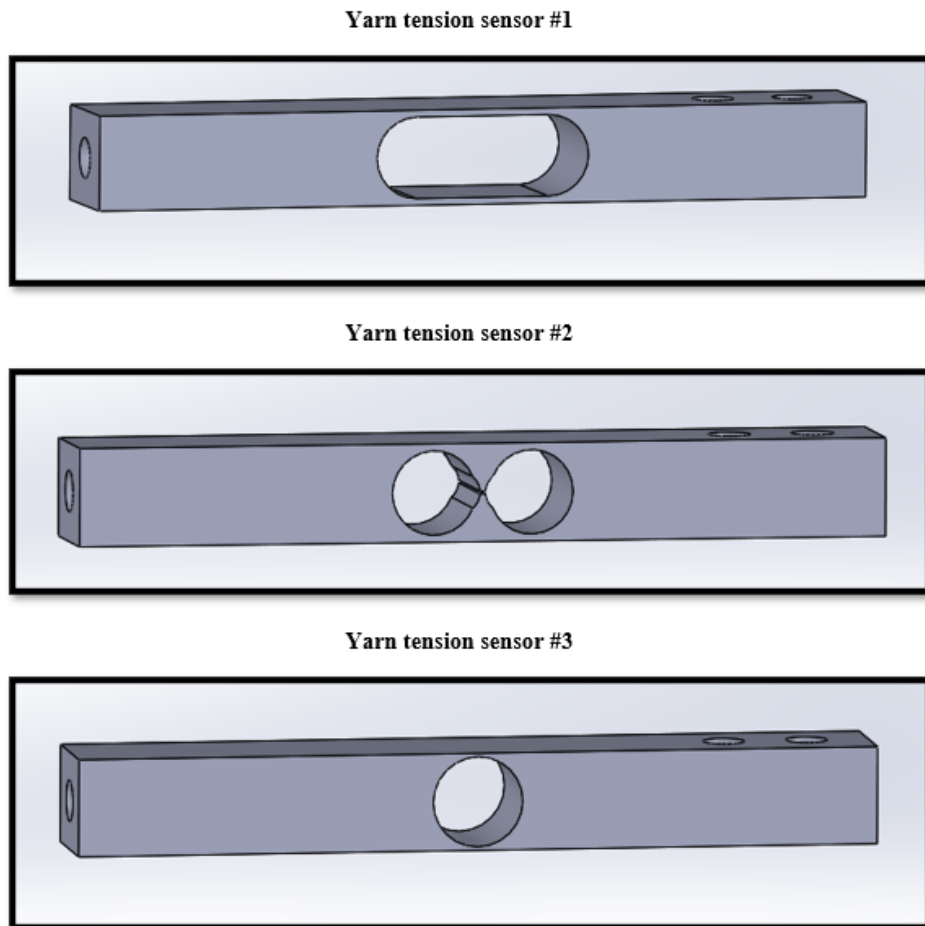


**Figure 3.25.** The designed sensors

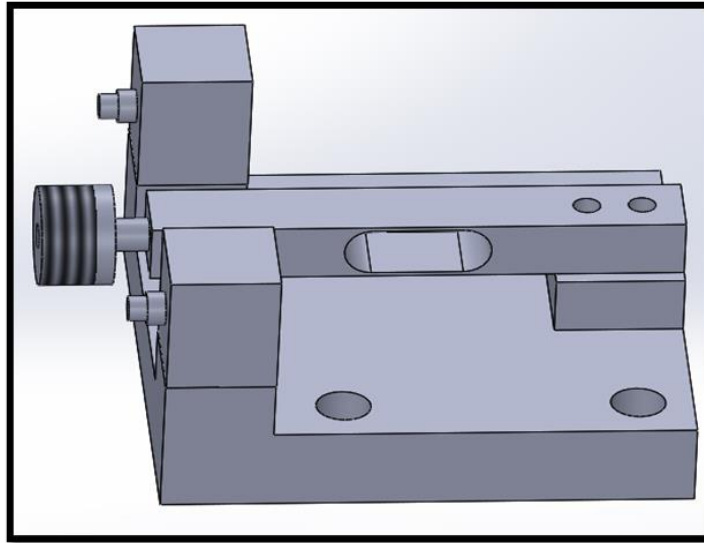


**Figure 3.26.** The sensor assembly

After manufacturing the yarn tension sensors, they were prepared for the strain gauge installment. The maximum strain zones were marked. Figure 3.27 shows the strain levels of the manufactured sensors. The bridge circuits were created (Figure 3.28 and 3.29). Finally, the sensors were sent to PULS ELEKTRONIK for bonding and installing the strain gauges.

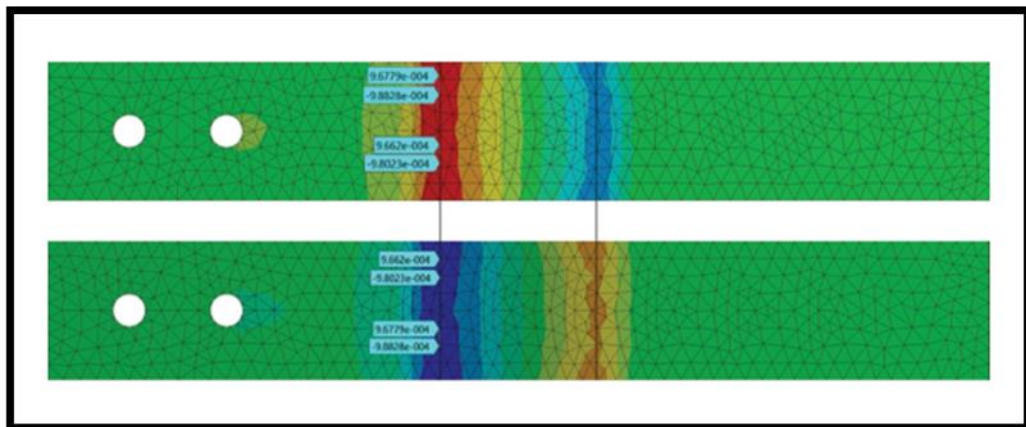


**Figure 3.27.** The maximum strain zones

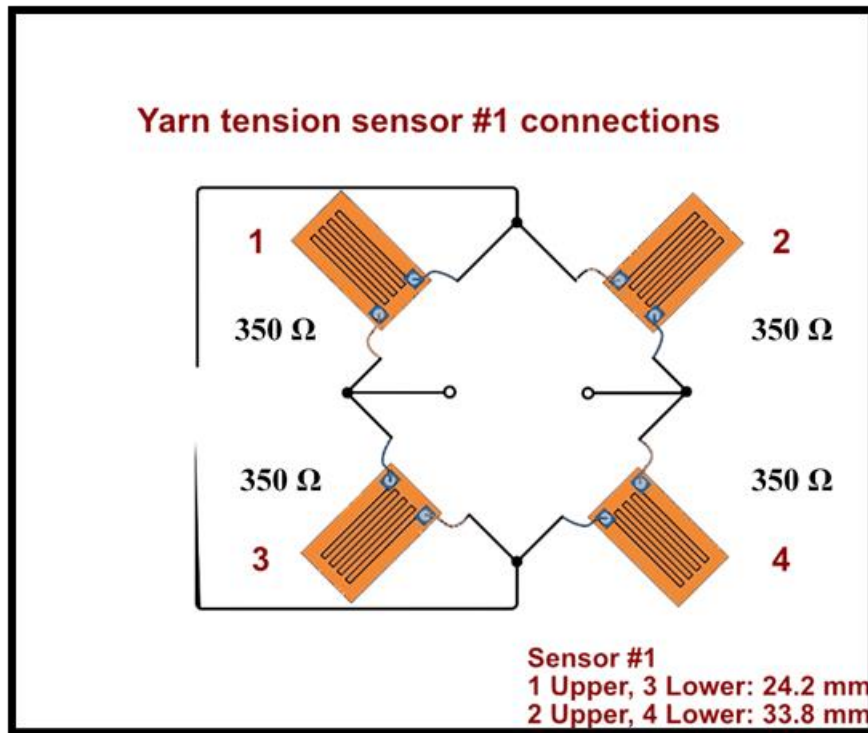


**Figure 3.28.** The bridge connection of the sensor #1

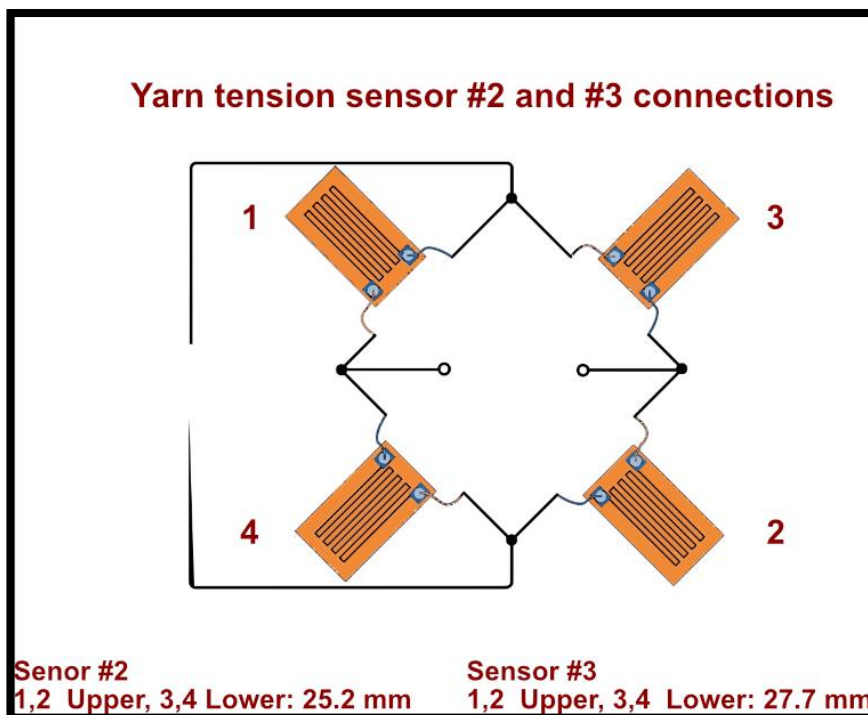


**Figure 3.29.** The bridge connection of the sensor #2 and #3

The used Arduino code is a simple code that reads the analog signal from the analog port and performs the Analog to digital converting process, and prints the ADC value to the serial port. The writing speed was measured, and it equals 1470 sample per second Figure 3.30 shows the analog read code.

```

void setup()
{
  Serial.begin(115200);
}

void loop()
{
  float value0 = 0;      // Defining the initial value
  value0 = analogRead(0); // Reading the signal from the sensor
  Serial.println(value0); // Printing the signal to the serial port
}

```

**Figure 3.30** The analog reading code

The used codes in MATLAB for the FFT and the FIR filter can be seen in Figure 3.31 and Figure 3.32.

```

%%Fast Fourier Transform Code

n = length(R800F100Hz);      % The length of the data
srate=1470;                  % The Sampling Rate
timevec = (0:n-1)/srate;    % The Time Vector
R800F100Hz1 = R800F100Hz - mean(R800F100Hz); % To minimize the effect of the Dc component

%% Computing the amplitude
FFT = fft(R800F100Hz1)/n; % Fast fourier transfer function
ampspect = 2*abs(FFT);      % The amplitude spectrum
hz = linspace(0,srate/2,floor(n/2)+1); % The frequency spectrum (From, To, Spacing)

%% Plotting
figure(2), clf
% Plotting the time domain signal
subplot(211)
plot(timevec(1000:3000),R800F100Hz(1000:3000),'k')
xlabel('Time (sec.)'), ylabel('Amplitude')
title('Time domain signal')

% Plotting the Frequency domain
subplot(212)
plot(hz,ampspect(1:length(hz)),'k','linewidth',1)
xlabel('Frequency (Hz)'), ylabel('Amplitude')
title('Frequency domain')
set(gca,'ylim',[0 5])
sgt = sgtitle('Sensor #1, 100Hz analog cut-off, 800 m/min','Color','red');
sgt.FontSize = 10;

```

**Figure 3.31.** The Fast Fourier Transform (FFT) code

```

%% FIR Filter Code
srate=1470; % The Sampling Rate
Cut_offF = 100/(srate/2); %Cutoff frequency,"srate/2" To normalize frequency to nyquist
order = 20; % The order of the filter
Lpfl= fir1(order,Cut_offF); %FIR Filter function
conT800 = conv(T800F1000Hz1,Lpfl); % Convolution of the singal with the FIR low pass filter impulse response
conT8001=conT800+ mean(T800F1000Hz);% Adding the mean to remove the detrending effect
conB=conT8001 (1:8196);

%% Fast Fourier Transform Code
n = length(conB); % The length of the data
timevec = (0:n-1)/srate; % The Time Vector
% Computing the amplitude
FFT1 = fft(conB)/n; % Fast fourier transfer function
ampspect = 2*abs(FFT1); % The amplitude spectrum
hs = linspace(0,srate/2,floor(n/2)+1); % The frequency spectrum (From, To, Spacing)

%% Plotting
figure(3), clf
% Plotting the time domain signal
subplot(311):
plot(timevec(1000:3000),T800F1000Hz(1000:3000),'r'); %- Plotting the original signal
xlabel('Time (sec.)'), ylabel('Amplitude')
title('Time domain signal before filtering')
subplot(312):
plot(timevec(1000:3000),conB(1000:3000),'r'); % Plotting the signal after filter
xlabel('Time (sec.)'), ylabel('Amplitude')
set(gca,'ylim',[0 100])
title('Filtered Time domain signal')
% Plotting the Frequency domain
subplot(313):
plot(hs,ampspect(1:length(hs)),'k','linewidth',1)
xlabel('Frequency (Hz)'), ylabel('Amplitude')
title('Filtered Frequency domain')
set(gca,'ylim',[0 5])
sgt = sgttitle('Sensor #3, 100Hz Digital cut-off,order 20, 800 m/min','Color','red' );
sgt.FontSize = 10;

```

Figure 3.32. The FIR filter code

Yarn tension sensors calibration curves can be seen in Figure 3.33.

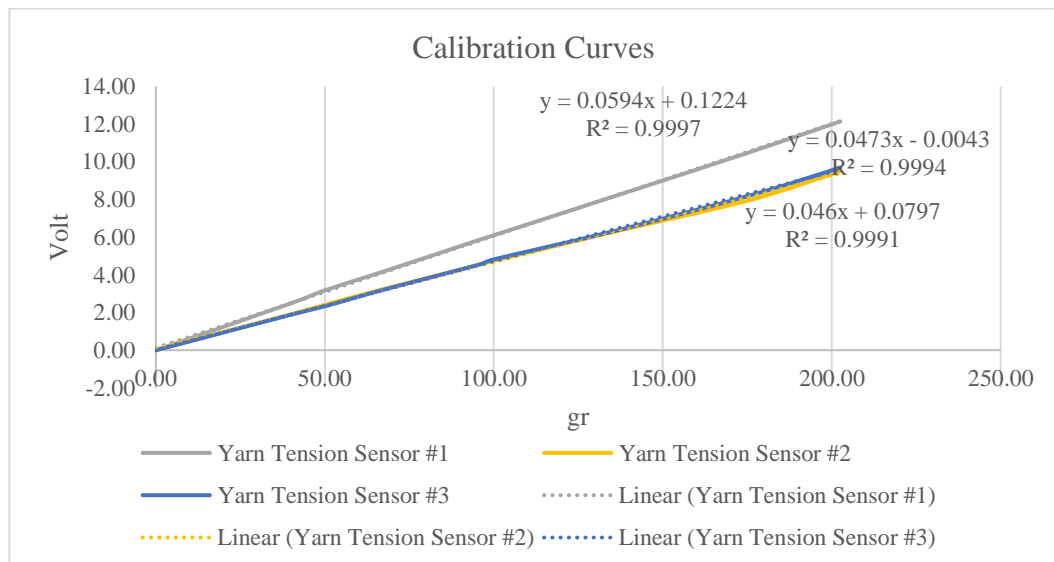
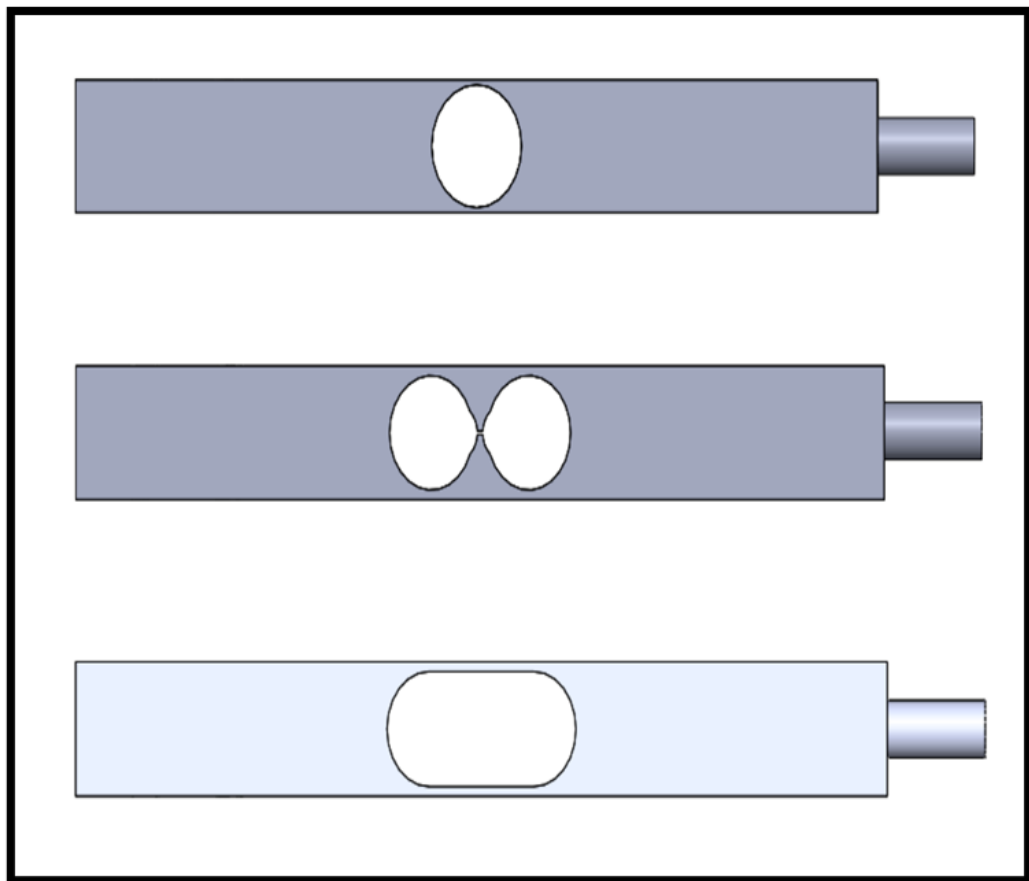


Figure 3.33. Sensors calibration curves

#### 4. RESULTS AND DISCUSSION

For choosing the shape and dimensions of the spring element of the load cells, extensive optimization study was conducted. The effects of changing multiple sensor parameters were studied. For every variable, a new design and analysis were done. Figure 4.1 shows tested sensor designs. The main focus was on the natural frequency and strain levels of the sensors. The natural frequency has to be about ten times higher than the maximum frequency of the applied force to get an acceptable measurement accuracy, as it has been deduced in the mathematical study of the sensor. On the other hand, the strain levels have to be higher than a certain level to get a detectable output voltage.



**Figure 4.1.** Tested yarn tension sensors shapes



The effect of most of the parameters on analysis results has been shown on Sensor #1 as similar results would be shown on other sensors. To study the effect of the sensor's length, width, and height on the natural frequency and strain, three different values for every dimension was taken. It was seen from the analysis results that the effect of increasing sensor width is minimal on the natural frequency; however, it has a significant effect on the strain (Table 4.1). With the decrease in the sensor's height, both the natural frequency and the strain increase (Table 4.2). Regarding the sensor length, increasing the length has a small effect on the strain while affecting the natural frequency noticeably (Table 4.3).

**Table 4.1.** The width effect on strain and natural frequency

<b>Width</b>	<b>7 mm</b>	<b>8.5 mm</b>	<b>10 mm</b>
<b>Natural Frequency (Hz)</b>	724	728	732
<b>Total strain (1N)</b>	476	392	331
<b>Weight (gr)</b>	6.1	7.4	8.8

**Table 4.2.** The height effect on strain and natural frequency

<b>Height</b>	<b>6 mm</b>	<b>7 mm</b>	<b>8 mm</b>
<b>Natural Frequency (Hz)</b>	775	728	685
<b>Total strain (1N)</b>	400	392	380
<b>Weight (gr)</b>	6.5	7.4	8.3

**Table 4.3.** The length effect on strain and natural frequency

<b>Length</b>	<b>50 mm</b>	<b>58 mm</b>	<b>66 mm</b>
<b>Natural Frequency (Hz)</b>	818	728	655
<b>Total strain (1N)</b>	381	392	398
<b>Weight (gr)</b>	6.1	7.4	8.8

The effect of the weight of the yarn guide roller was studied, a model with just a rod and two models with different rollers were designed and analyzed. It was observed that by increasing the weight, the natural frequency decreases distinctly with small effect on the strain (Table 4.4).

**Table 4.4.** The rollers effect on strain and natural frequency

<b>Rollers</b>	<b>Without a roller</b>	<b>With a roller</b>	<b>With a bigger roller</b>
<b>Natural Frequency (Hz)</b>	728	668	592
<b>Total strain (1N)</b>	392	395	400
<b>Weight (gr)</b>	7.4	8	9

Some variations in designs can be seen in Figure 4.2.

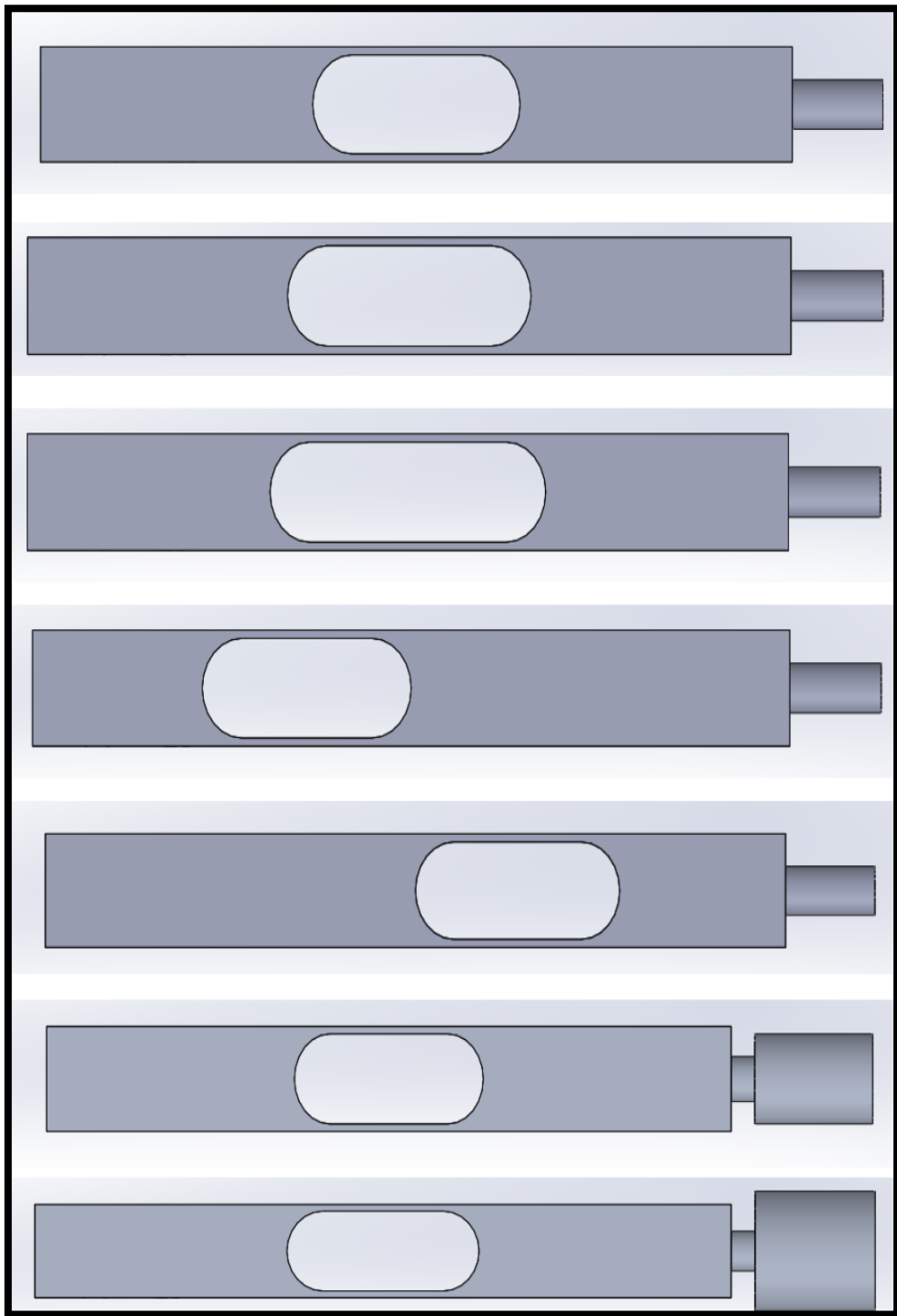


**Figure 4.2.** Variation in designs for studying different specifications

The high strain zone in the middle of the yarn tension sensor has a considerable effect on its characteristics. The effect of offsetting this zone from the center was studied. When it was moved 8 mm to the left end side of the center, the natural frequency decreases noticeably and vice versa and only a small amount of strain change occurs (Table 4.5).

**Table 4.5.** Offsetting the high strain zone effect

<b>Offsetting the high strain zone</b>	<b>Without offsetting</b>	<b>8 mm to the right</b>	<b>8 mm to the left</b>
<b>Natural Frequency (Hz)</b>	728	896	628
<b>Total strain (1N)</b>	392	379	410
<b>Weight (gr)</b>	7.4	7.4	7.4

The effect of the length of this zone was also studied. The tested zone lengths were varied between 2.5 and 15 mm. It was seen that natural frequency decreases with the increment in zone length. But the strain increases with the increase in zone length. While 2.5 mm zone length produced a very high natural frequency, its strain levels were significantly low. Increasing the zone length to 7.5 mm almost halved the natural frequency but doubled the strain. Table 4.6 and Table 4.7 show the results in detail.

**Table 4.6.** The high strain zone length effect 1

<b>High strain zone length</b>	<b>2.5 mm</b>	<b>5 mm</b>	<b>7.5 mm</b>
<b>Natural Frequency (Hz)</b>	1742	1293	954
<b>Total strain (1N)</b>	152	231	313
<b>Weight (gr)</b>	8.5	8.2	7.8

**Table 4.7.** The high strain zone length effect 2

<b>High strain zone length</b>	<b>10 mm</b>	<b>12.5 mm</b>	<b>15 mm</b>
<b>Natural Frequency (Hz)</b>	728	578	474
<b>Total strain (1N)</b>	392	428	567
<b>Weight (gr)</b>	7.4	7.1	6.7

The effect of the high strain zone thickness was studied. Three different thicknesses were tested, which are 0.25, 0.5, and 1 mm for the single hole sensor (Sensor #3). While a very high natural frequency was obtained with 1 mm thickness, its strain was very small, which may not be suitable for the measurement. With the thickness's decrement, the strain levels started to increase with an expected decrease in natural frequency. However, when reaching thicknesses less than 0.25, it became harder for manufacturing. Therefore, it was taken as the lowest thickness because more precise manufacturing was needed for lower thicknesses. Table 4.8 shows the results in detail.

**Table 4.8.** The High strain zone thickness effect

<b>High strain zone thickness</b>	<b>1 mm</b>	<b>0.5 mm</b>	<b>0.25 mm</b>
<b>Natural Frequency (Hz)</b>	2328	2131	1843
<b>Total strain (1N)</b>	51	95	183
<b>Weight (gr)</b>	9.1	8.9	8.7

Finally, the chosen three yarn tension sensor spring elements were in the middle of the analysis spectrum, having good natural frequency while maintaining acceptable strain levels, all in consideration with the manufacturing feasibility.

Models dimensions:

- Width: 8.5
- Length: 58
- Height: 7

For Sensor #1 and #2, 0.5 mm high strain zone thickness was used to balance high natural frequency with high strain. However, in sensor #3, 0.25 mm was chosen.

Table 4.9 shows the developed sensors analysis results. These designs were manufactured to convert to a load cell for yarn tension measurements.

**Table 4.9.** Yarn tension sensors properties.

<b>Summery</b>	<b>Sensor #1</b>	<b>Sensor #2</b>	<b>Sensor #3</b>
<b>Natural Frequency (Hz)</b>	764	1156	1988
<b>Total strain (1N)</b>	321	225	147
<b>Weight (gr)</b>	6.98	7.7	8.3

Figure 4.3 shows the ANSYS report for Sensor #1.

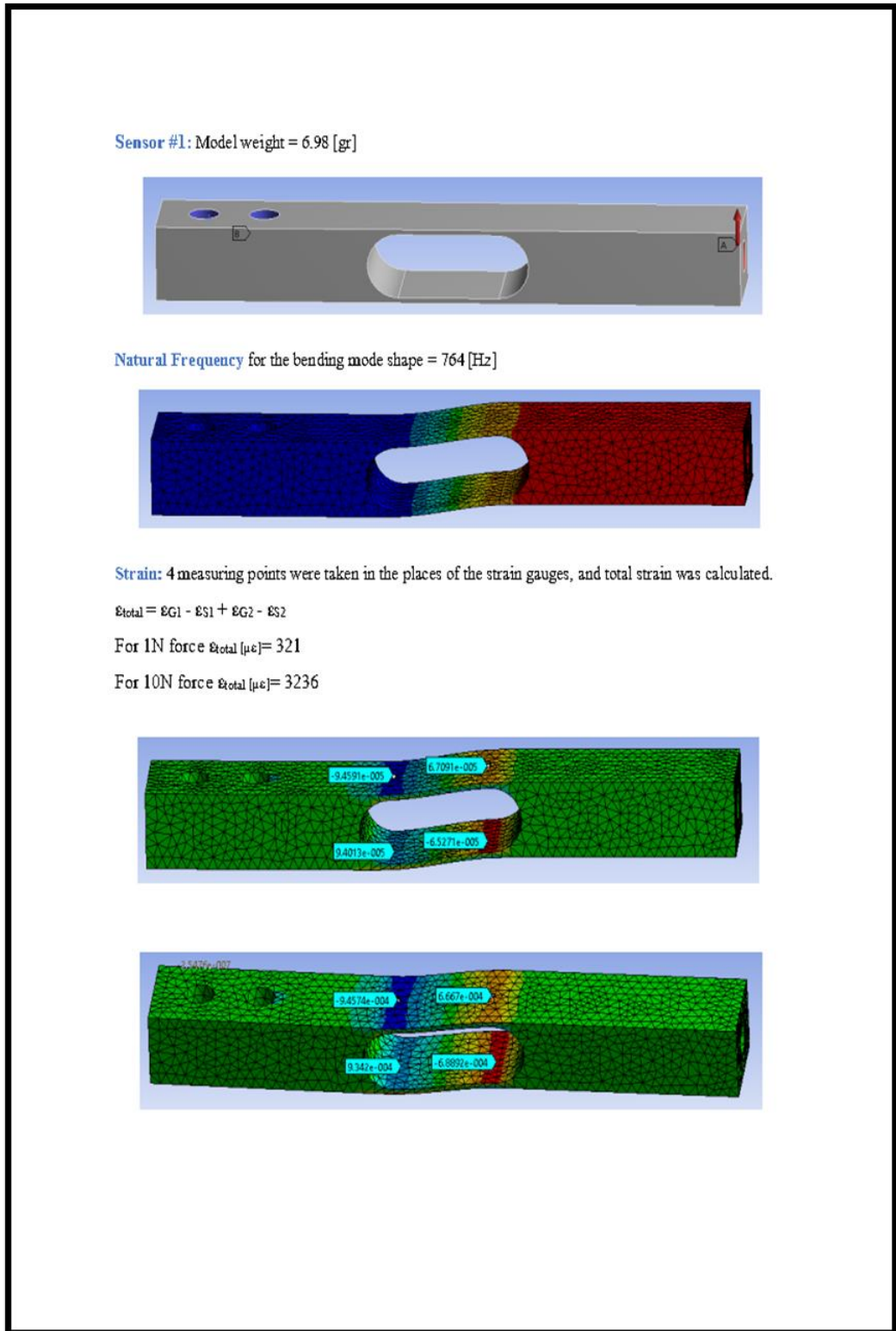


Figure 4.3. ANSYS report for Sensor #1

Figure 4.4 shows the ANSYS report for Sensor #2.

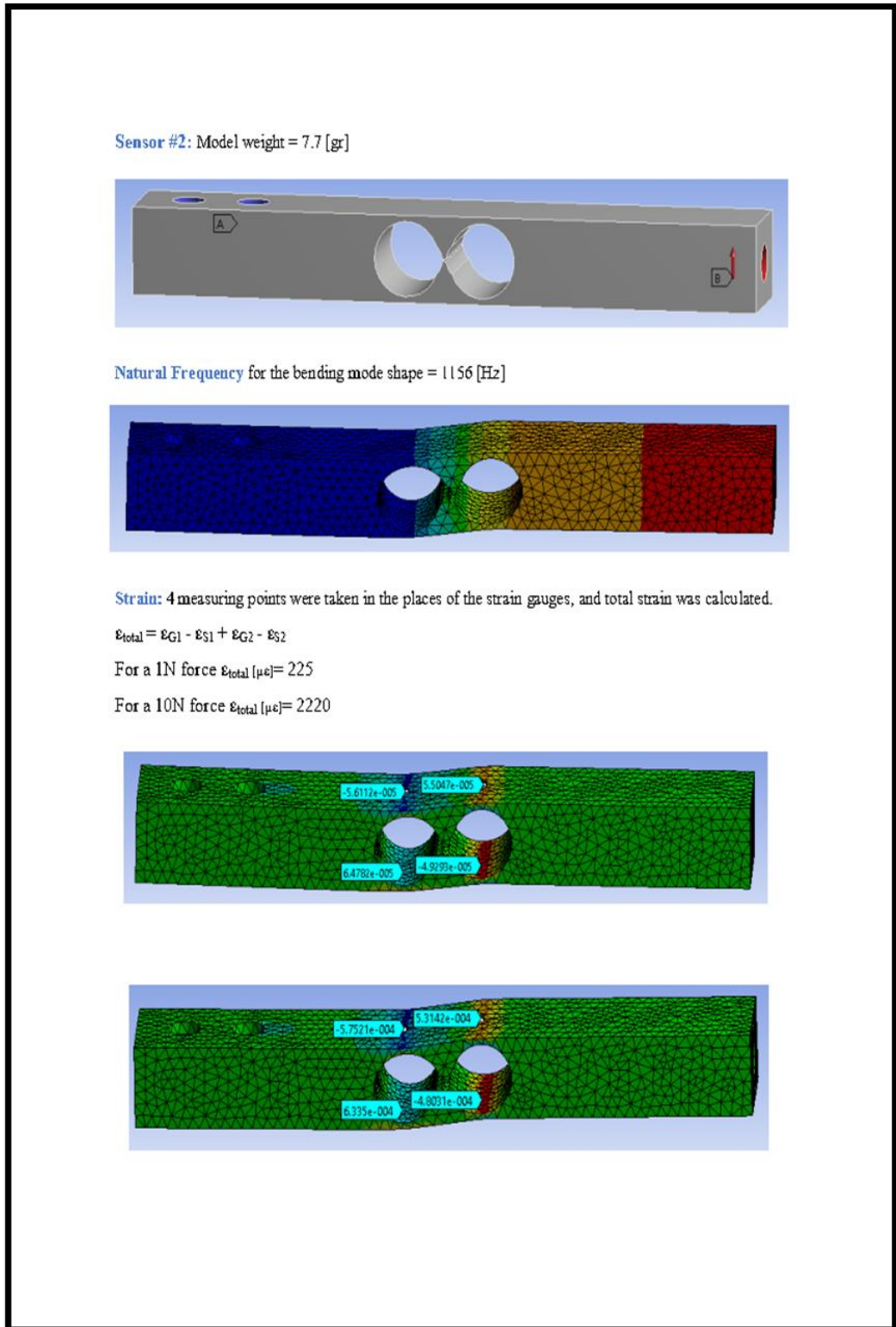
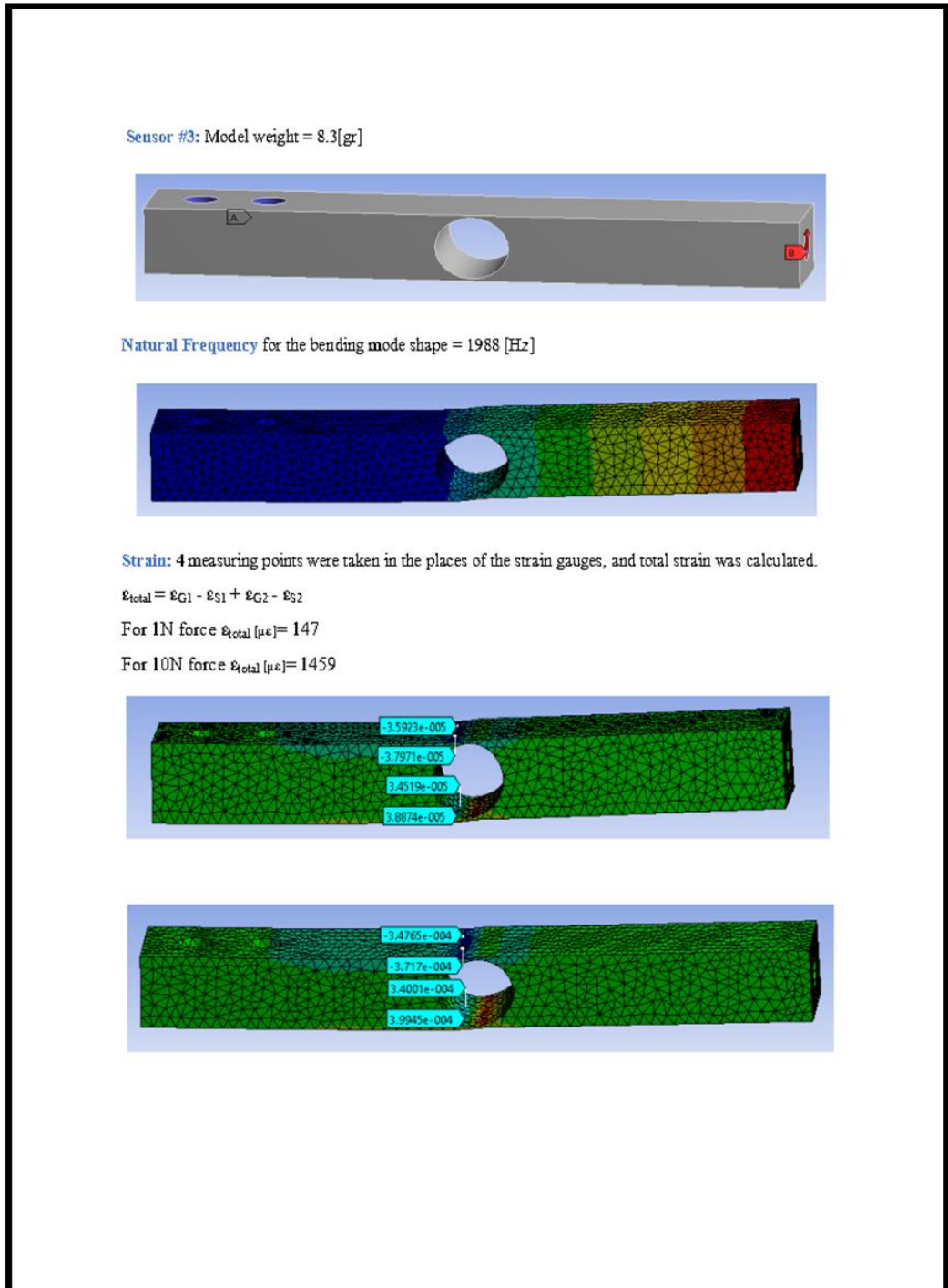


Figure 4.4. ANSYS report for Sensor #2



Figure 4.5 shows the ANSYS report for Sensor #3.



**Figure 4.5.** ANSYS report for Sensor #3

The analyses were done for all the parameter changes in this report form, but only the final sensor shape analyses were shown to avoid repetition.

Strain gauges were bonded on the high strain regions of the manufactured spring elements and then they were used in manufacturing of yarn tension sensors. After calibration, they were prepared for yarn tension measurement tests. Yarn tension measurement test results are presented below.

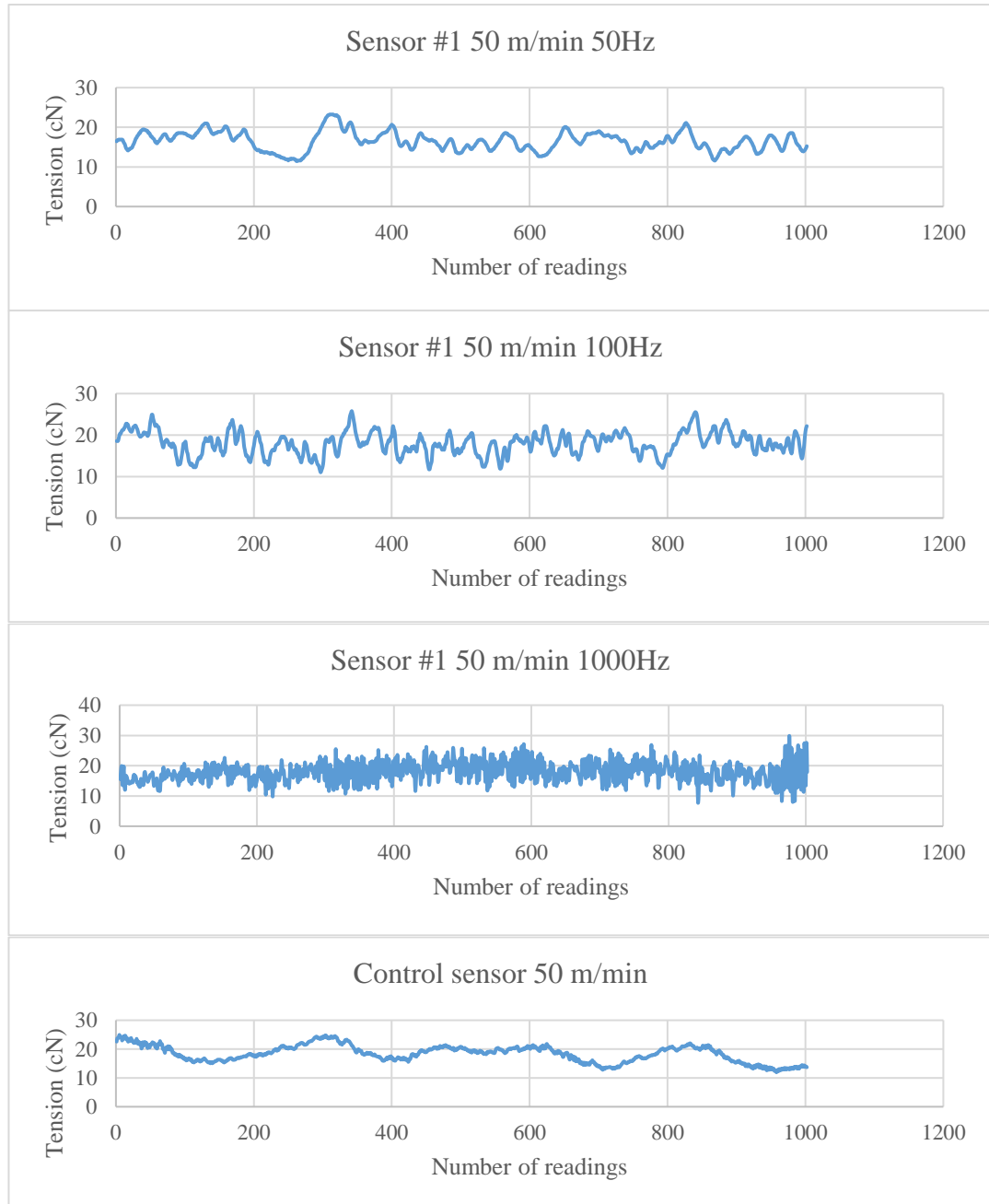
*Experimental work with tension measurements*

The yarn tension tests were conducted for the three designed sensors in addition to a control sensor to compare the results. Ten thousand samples were taken with a time interval of 0.68 ms (millisecond). The tests were done at four different speeds namely 50, 200, 500, 800 m/min, and at three filter cut-off frequencies which are 50, 100 and 1000 Hz. It should be mentioned here that tension measurements were not carried at the same time. Rather measurements were conducted successively to prevent the interaction between sensor measurements. Also filter cut-off frequency was not known for the control sensor. Despite all these, the results were found to be comparable. Sensor #1 and Sensor # 2 measured very close average tension values but higher than Sensor #3 measurements. This was seen to be due to calibration difference between the sensors. Sensor #3 average tension measurements were found to be closer to the control tension sensor. As the cut-off frequency of the control tension sensor was not available no precise comparison became possible (Table 4.10).

**Table 4.10.** The averages of 1000 sample for the sensors

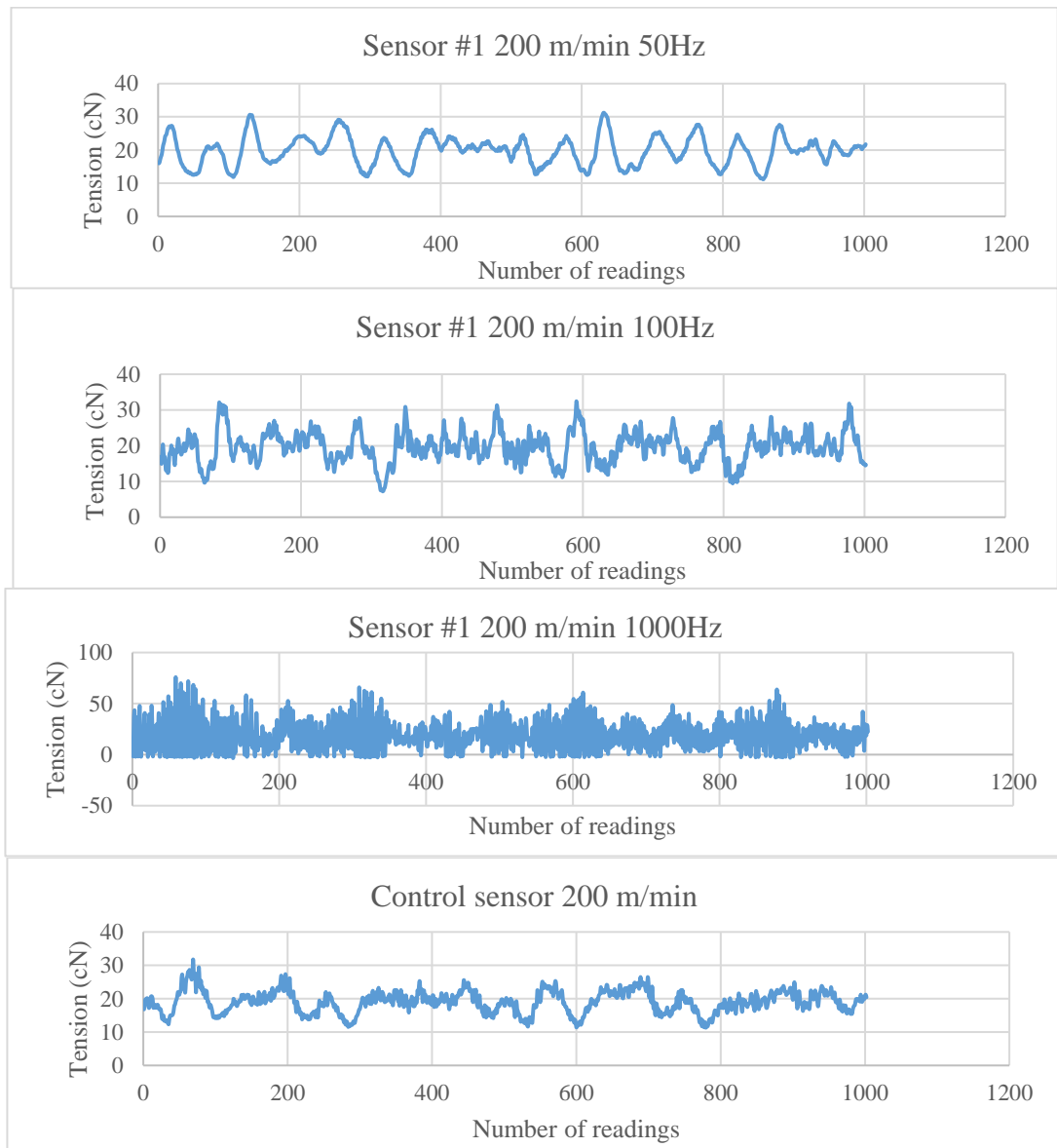
<b>Tension measurements 1000 average 100Hz</b>	<b>Sensor #1</b>	<b>Sensor #2</b>	<b>Sensor #3</b>	<b>Control sensor</b>
<b>50 m/s</b>	18.0	18.8	17.8	18.4
<b>200 m/s</b>	19.7	21.9	20.6	19.1
<b>500 m/s</b>	28.3	29.3	27.7	25.9
<b>800 m/s</b>	41.1	41.0	37.2	35.6

Figure 4.6 shows yarn tension measurements recorded with 0.68 ms at 50 m/min unwinding speed with 50, 100 and 1000 Hz amplifier filter cut-off frequencies. Tension measurement of control sensor at 50 m/min was also included for comparison purpose. The effect of the cut-off frequency on the signal shape can be observed clearly.



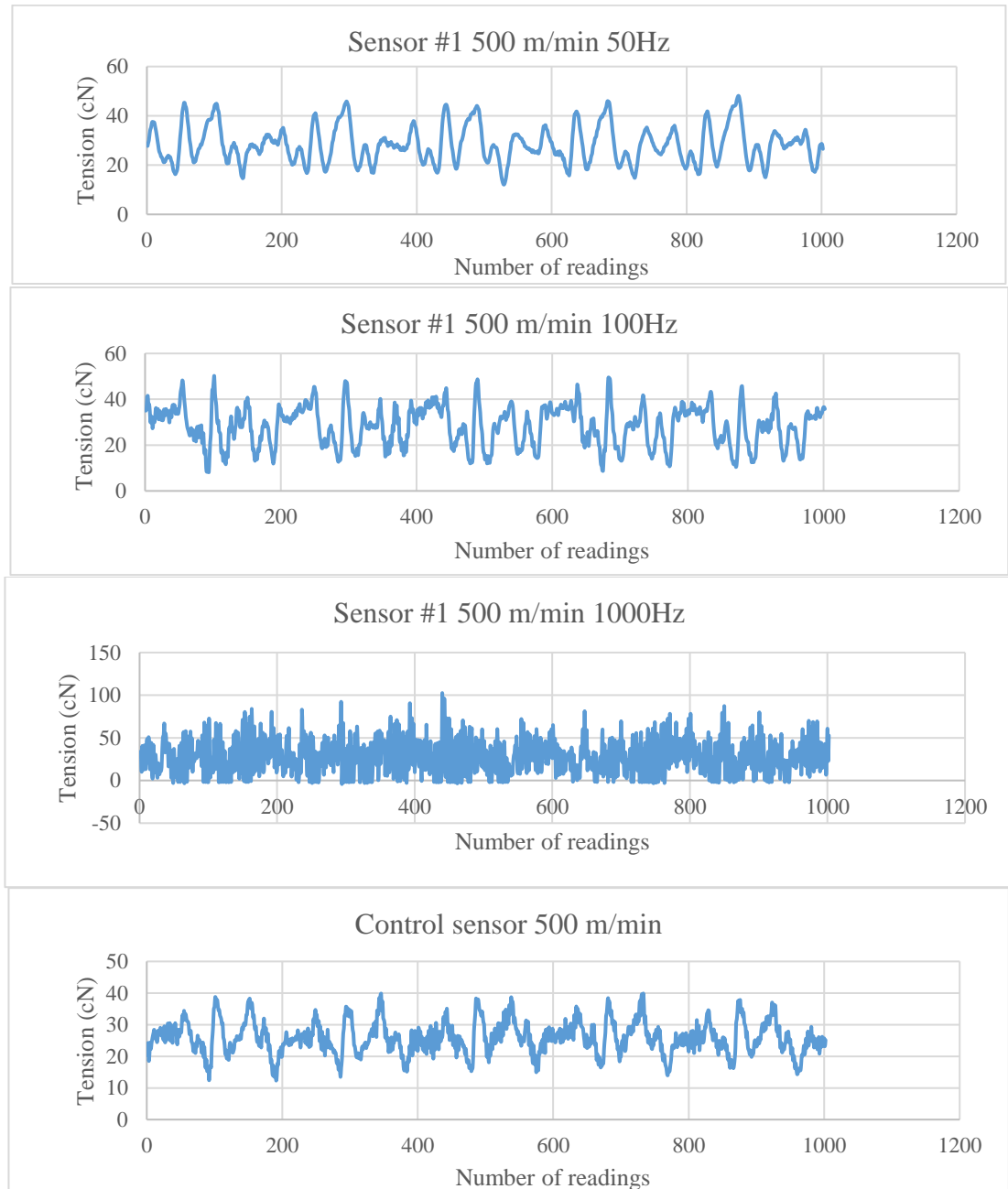
**Figure 4.6.** The effect of amplifier filter cut-off frequency on the signal shape at a speed of 50 m/min

The effect of amplifier filter cut-off frequency on yarn tension variations is seen in Figure 4.7 at the speed of 200 m/min. The filtering effect is observed on tension curves and higher frequency variations are clearly seen in 100 Hz but specially at 1000 Hz. A very similar tension variation indicates that the tension sensors designed in this study produces similar measurements to control sensor already used commercially. At 1000 Hz cut-off frequency signal is too much fluctuating as high frequency noise up to 1000 Hz is also included in the signal.



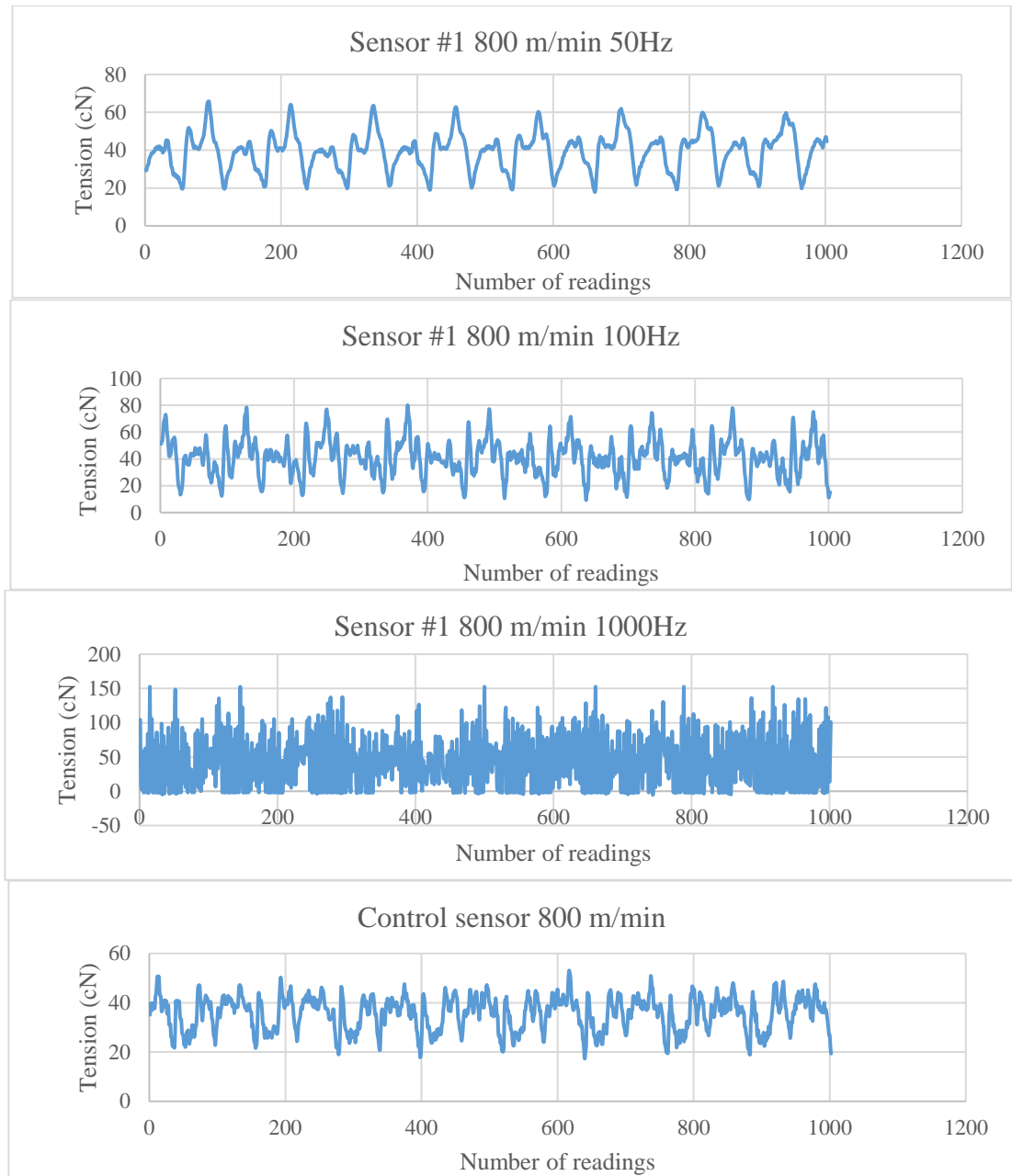
**Figure 4.7.** The effect of amplifier filter cut-off frequency on the signal shape at a speed of 200 m/min

Similar tension variations are obtained at 500 m/min in all cut-off frequencies. Here again tension variation is very similar to control sensor tension measurement at both 50 and 100 Hz cut-off frequencies (Figure 4.8).



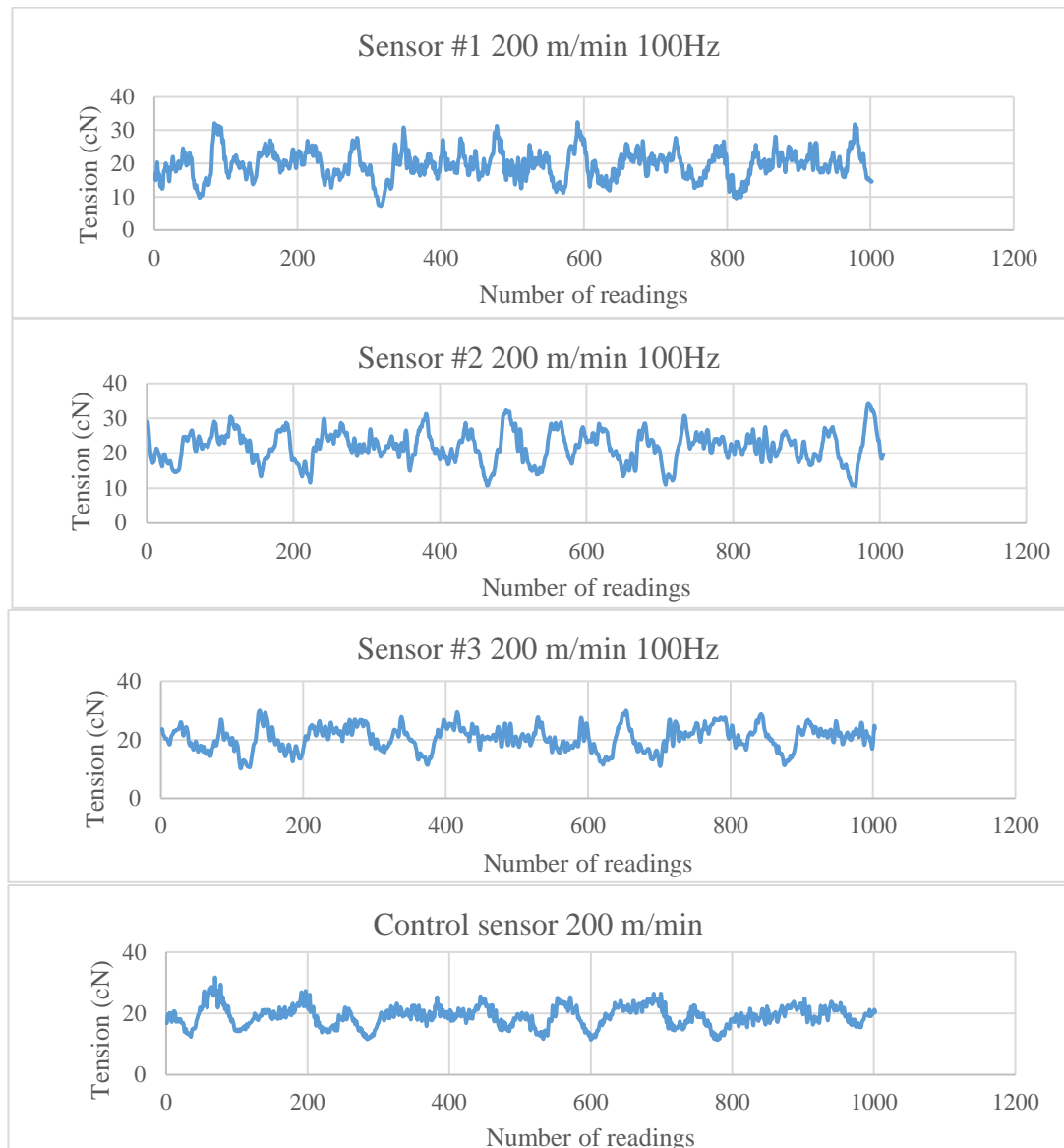
**Figure 4.8.** The effect of amplifier filter cut-off frequency on the signal shape at a speed of 500 m/min

Figure 4.9 shows tension variation during unwinding from bobbin at 800 m/min at 50, 100 and 1000 Hz cut-off frequencies along with control sensor tension measurements. Tension measurements with 50 and 100 Hz show very similar variation to control sensor tension measurement with a higher tension peak. This is observed at all speeds and thought to be due to the filtering frequency of control sensor.



**Figure 4.9.** The effect of amplifier filter cut-off frequency on the signal shape at a speed of 800 m/min

To get a better comparison of the different sensor signal shapes, 1000 sample was taken at three different speeds recorded with 100 Hz filter cut-off frequency. Tension measurement of control sensor was also included for comparison purpose. Figure 4.10 shows tension signal variations during unwinding at 200 m/min. The tension variations of all sensors including the control sensor are very similar to each other in shape and magnitude except some higher peaks in sensor #1 and sensor #2. As measurements were taken at different times, this can be due to bobbin surface structure.



**Figure 4.10.** The developed sensors and control sensor signal shapes at a speed of 200 m/min

The measurements taken at 500 m/min are presented in Figure 4.11. As it was mentioned above, sensor #1 and sensor #2 produced a similar tension variation to tension sensor #3 and the control sensor but with a higher peak. This difference might be because of strain distribution in the area of spring element where strain gauges are bonded.

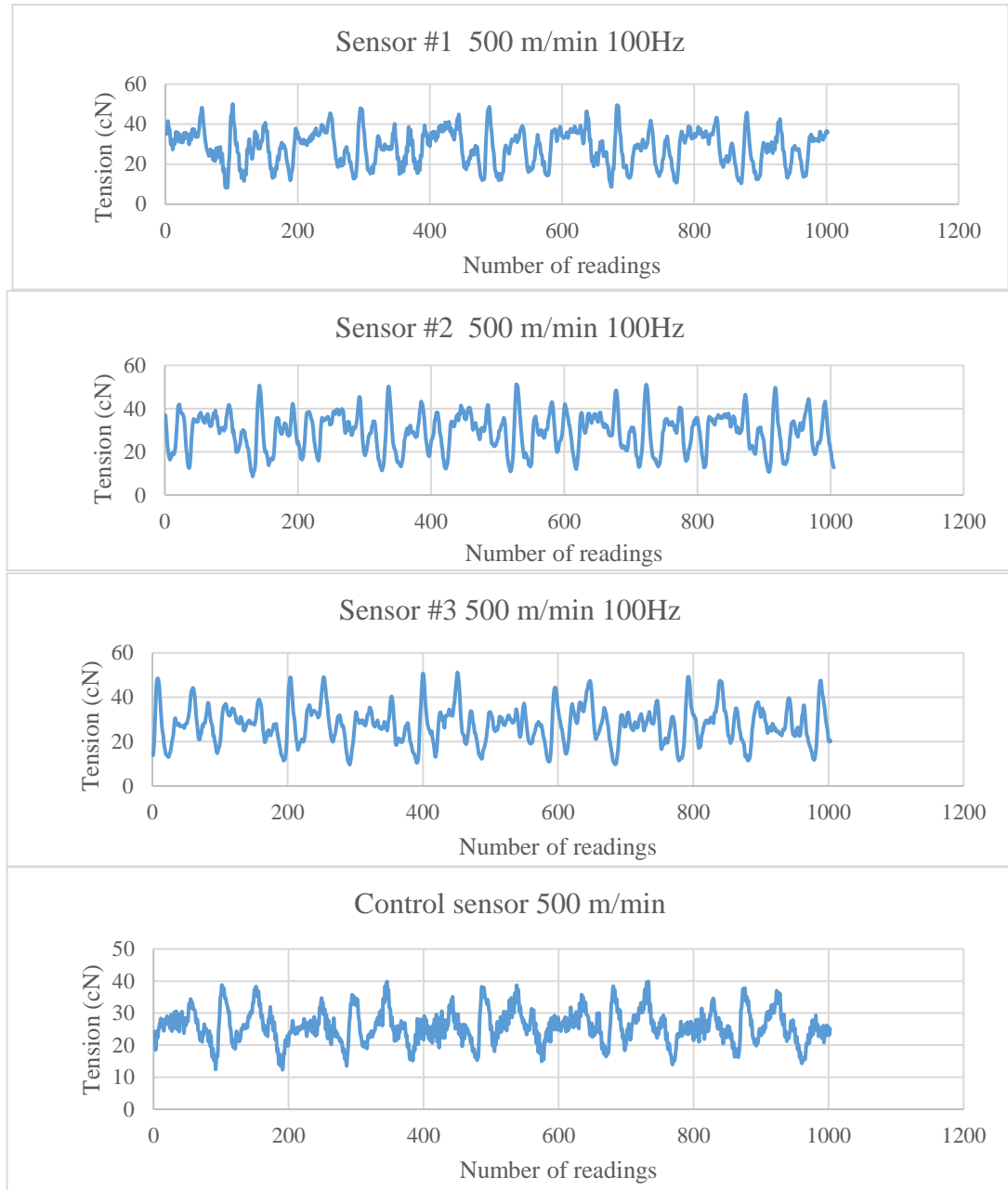


**Figure 4.11.** The developed sensors and control sensor signal shapes at a speed of 500 m/min



Similar tension measurement traces were recorded at 800 m/min yarn unwinding speed. The above mentioned results also occurred at 800 m/min speed and the same interpretation can be made at 800 m/min speed as well (Figure 4.12).

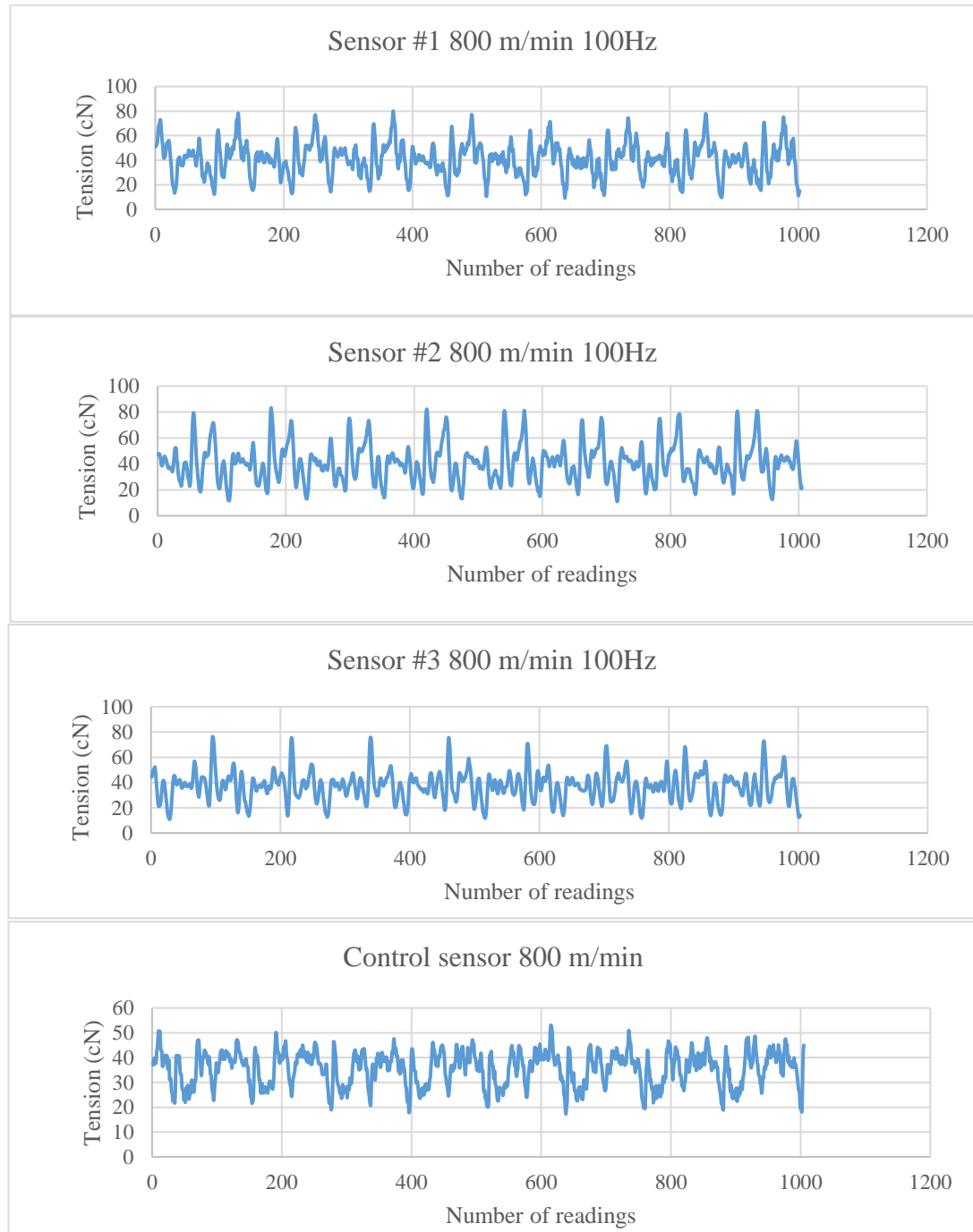


**Figure 4.12.** The developed sensors and control sensor signal shapes at a speed of 800 m/min

The tension measurement samples with a 1000 Hz filter cut-off frequency were taken specially to process them by using a Fast Fourier Transform in MATLAB and get a better understanding of the acquired signals. Figures below show the frequency domain analysis for Sensor #1 and #3 with a 1000 Hz analog filter cut-off frequency along with the control sensor all at a speed of 800 m/min. The analysis of the control sensor can be seen in Figure 4.13.

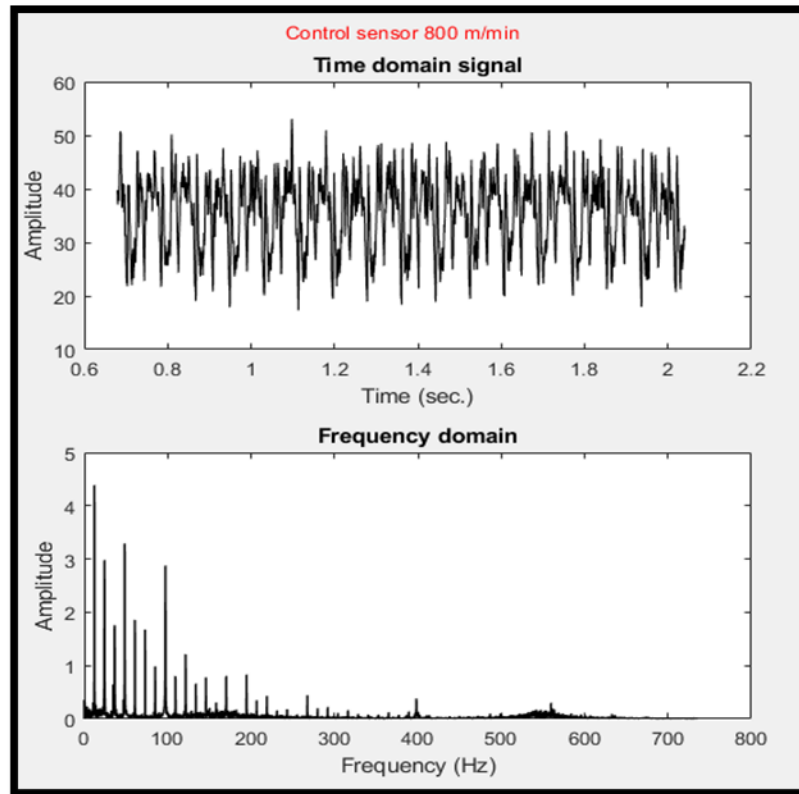


**Figure 4.13.** Frequency and time domains for the control sensor at a speed of 800 m/min

The Figure 4.14 shows the time and frequency domains of the tension signals from Sensor #1 and Sensor #3 at 1000 Hz analog filter cut off frequency. As high frequency signals are passed by the filter, tension signals look very much fluctuating. Frequency domain analysis shows high level of frequency signals between 400 and 500 Hz which are irrelevant to textile technology.

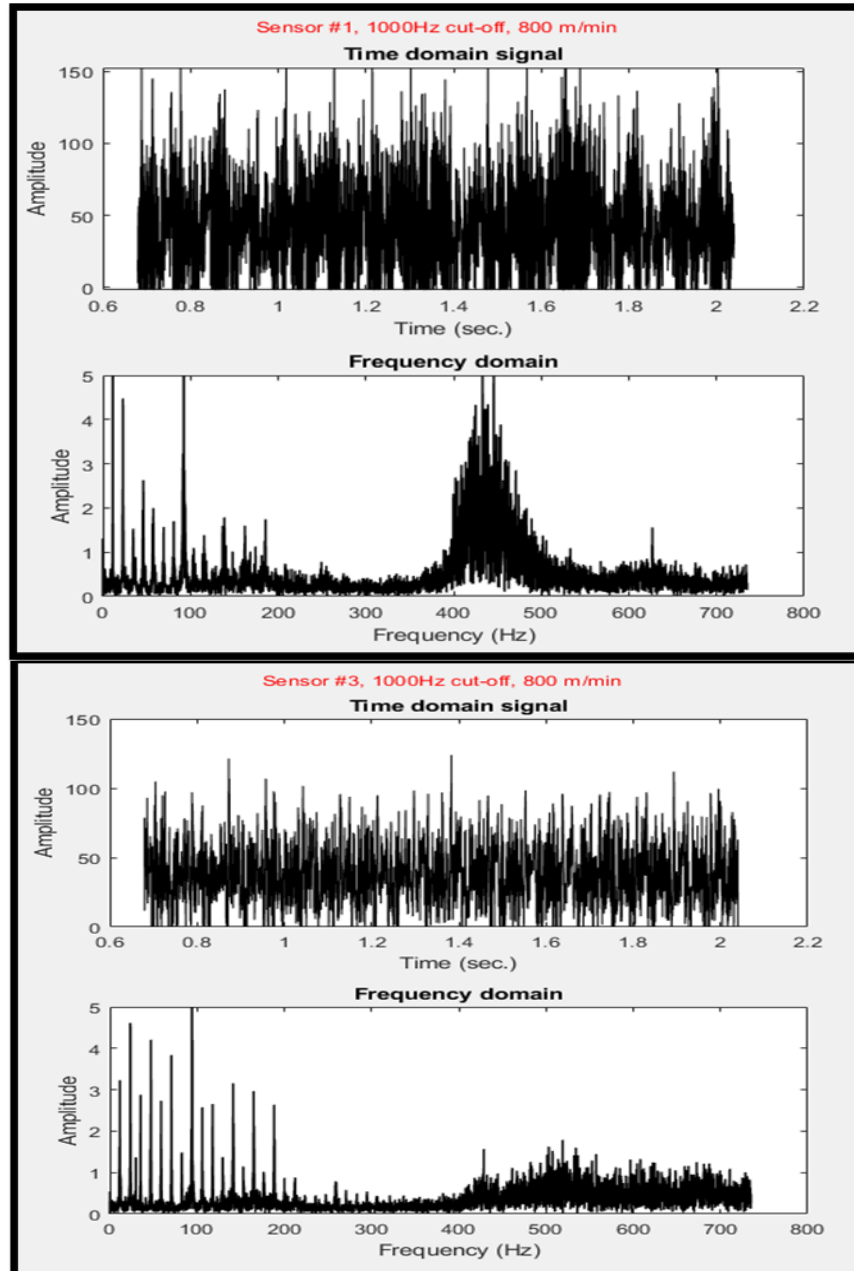


**Figure 4.14.** Frequency and time domains for sensors #1 and #3 with a 1000 Hz analog filter, at a speed of 800 m/min

Tension measurements of Sensor #1 and Sensor #3 with 100 Hz analog filter cut-off frequency are shown in Figure 4.15 for both time and frequency domains. As seen from the figures high frequency variations are cleared with filtering effect. This shows itself in both time domain and frequency domain curves.

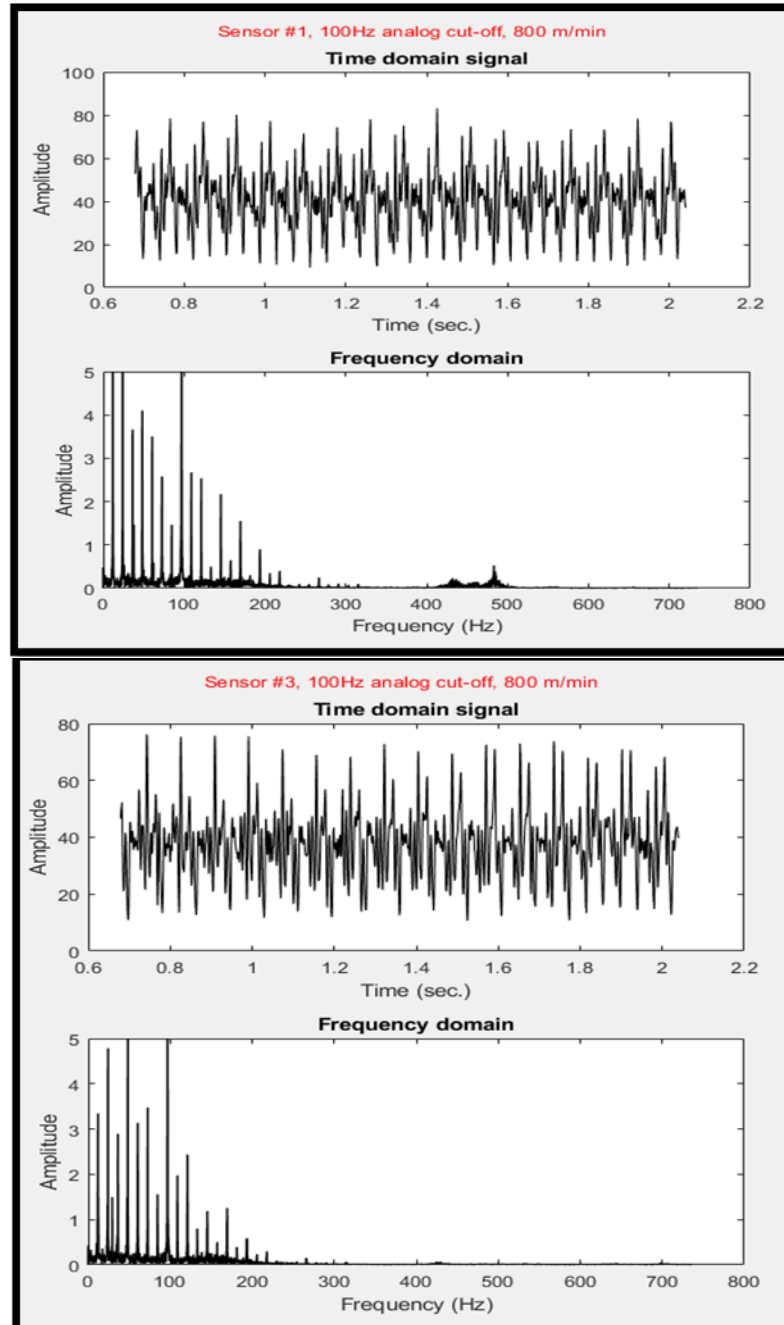


**Figure 4.15.** Frequency and time domains for the sensor #1 and #3 with a 100 Hz analog filter at a speed of 800 m/min

Fourier analysis was applied to tension signals measured with 1000 Hz analog filter cut-off frequency. Digital signal processing (DSP) was applied to produce a filtering effect at 100 Hz cut-off frequency and with filtering order of 20 for both sensor #1 and sensor #3 measurements. Results are shown in Figure 4.16 As seen from figures, tension signals at 100 Hz with digital filtering match mostly with those of analog filtering at 100 Hz. Higher peaks at 100 Hz analog filtering cut-off frequency measurements are thought to be due to lower filtering order with analog filter.

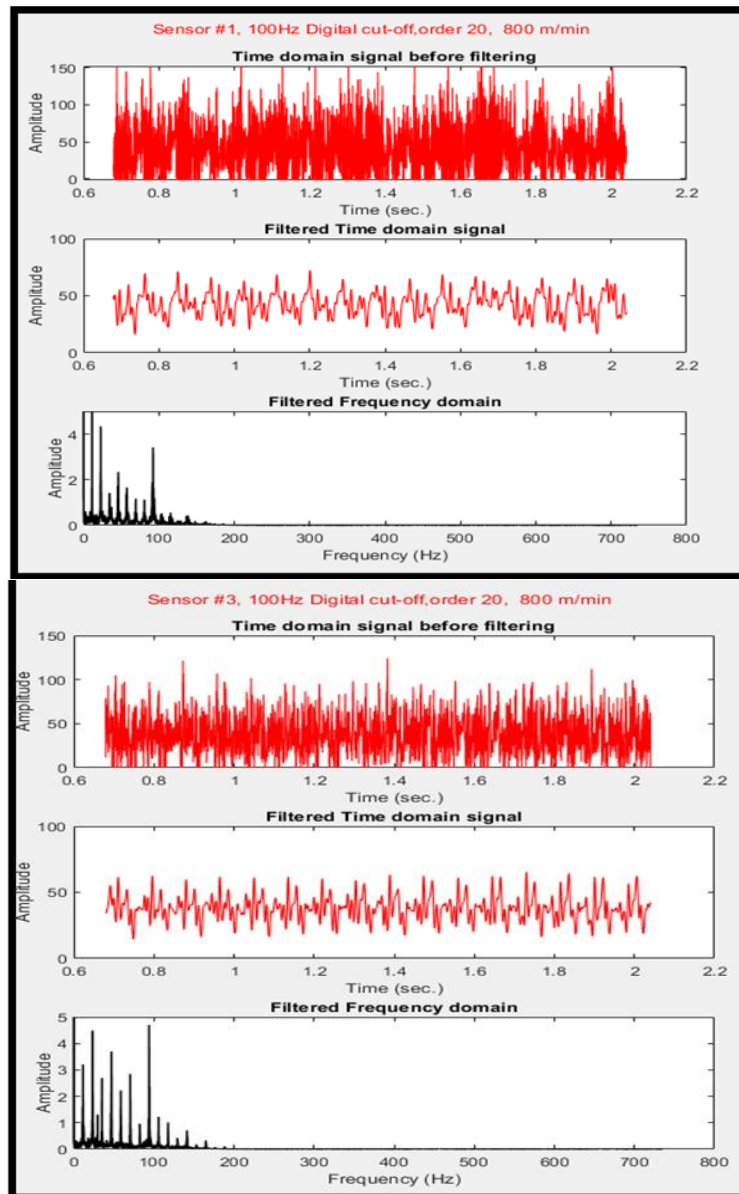


**Figure 4.16.** Frequency and time domains for the sensor #1 and #3 with a 100 Hz digital filter at a speed of 800 m/min

## 5. CONCLUSION

In this MSc thesis, we studied and investigated strain gauge based yarn tension sensors thoroughly. Firstly, design specifications for yarn tension sensors were determined. These specifications were measuring intervals and yarn tensions measuring frequencies. Then mechanical design of tension sensor was conducted using SOLIDWORKS. Different shapes of tension sensor spring elements were analyzed in ANSYS program. Strain distributions under forces of different intervals (100 cN, 1000 cN) were obtained and maximum strain regions were determined. Also, natural frequency of each design was calculated.

Among different design trials, three designs were selected and a detailed analysis was carried out on this design to see the effect of the cut-shapes location, geometry of the shape and thickness on strain distributions and natural frequency. Based on this analysis three different spring elements were chosen and manufactured. Strain gauges were bonded on maximum strain regions and load cells were produced for yarn tension sensors in this way. Yarn tension sensors were constructed using these load cells and an analog amplifier with filtering unit, and then they were tested in a single unit bobbin unwinding system. A commercial yarn tension sensor (control sensor) was also used in the tests to compare the newly designed yarn tension sensor performance.

Despite some slight differences in tension peak values, the designed tension sensors measurement results matched mostly with each other and control sensor measurements. Differences in the results of the designed tension sensors and the control sensor can be due to difference between filter cut-off frequencies and order of filter used in amplification circuits.

Static calibration was used in this study and dynamic tension measurements were conducted. It would be more precise approach to calibrate the sensor by applying dynamic forces at different frequencies. This could not be done because of the absence of such a calibration unit. Also, more spring element designs with different strain distributions should be tested to obtain higher sensitivity at Wheatstone bridge level as the designed

sensors in this study had lower sensitivity compared to some commercial load cells at same or near measuring interval. A commercial amplifier with an analog variable filtering frequency capability was used in this research although an amplifier was designed without filtering capability. It was thought to continue with digital filtering rather than analog ones. As this required a detailed study, it was left to another research.

## REFERENCES

**Anonymous, 1992.** Vishy Measurement Student Manual for Strain Gauge Technology. [http://www.egr.unlv.edu/~bj/MEG\\_302L\\_web/Student\\_strain\\_gage\\_Manual-001.PDF](http://www.egr.unlv.edu/~bj/MEG_302L_web/Student_strain_gage_Manual-001.PDF)-(Date of access:12.11.2020).

**Anonymous, 1998.** National Instruments Application Note 078 - Strain Gauge Measurements. [http://elektron.pol.lublin.pl/elekp/ap\\_notes/NI\\_AN078\\_Strain\\_Gauge\\_Meas.pdf](http://elektron.pol.lublin.pl/elekp/ap_notes/NI_AN078_Strain_Gauge_Meas.pdf)-(Date of access:29.11.2020).

**Anonymous, 2008.** Strain gauges. <https://www.allaboutcircuits.com/textbook/direct-current/chpt-9/strain-gauges->(Date of access:15.11.2020).

**Anonymous, 2014.** What is the load cell? <https://www.locosc.com/What-is-the-load-cell-id6733376.html>-(Date of access:19.11.2020).

**Anonymous, 2015a.** How does a load cell amplifier work? <https://www.futek.com/store/instruments/analog-amplifier->(Date of access:19.11.2020).

**Anonymous, 2015b.** Getting Started with Load Cells. <https://learn.sparkfun.com/tutorials/getting-started-with-load-cells/all->(Date of access:14.11.2020).

**Anonymous, 2016a.** Load cell working principle. <https://instrumentationtools.com/load-cell-working-principle->(Date of access:15.11.2020).

**Anonymous, 2016b.** Mantracourt SGA / A & SGA / D Strain Gauge / Load Cell Amplifier / Signal Conditioner. 7. [https://www.mantracourt.com/userfiles/documents/sga\\_manual.pdf](https://www.mantracourt.com/userfiles/documents/sga_manual.pdf) -(Date of access:25.11.2020).

**Anonymous, 2018a.** Typical Bonding Procedures and Dampproof Treatment. [https://www.kyowa-ei.us/eng/file/download/technical/notes/bonding\\_procedure/pdf\\_bonding\\_procedure\\_001\\_eng.pdf](https://www.kyowa-ei.us/eng/file/download/technical/notes/bonding_procedure/pdf_bonding_procedure_001_eng.pdf)-(Date of access:15.12.2020).

**Anonymous, 2018b.** Fourier Analysis and Synthesis. <http://hyperphysics.phy-astr.gsu.edu/hbase/Audio/fourier.html#c1>-(Date of access:29.11.2020).

**Anonymous, 2019.** Load cell types and uses. <https://www.800loadcel.com/white-papers/383.html>-(Date of access:18.11.2020).

**Anonymous, 2020a.** What is a tension load cell, and how does it work. <https://www.flintec.com/weight-sensors/load-cells/how-does-a-tension-load-cell-and-how-does-it-work->(Date of access:25.11.2020).



**Anonymous, 2020b.** What is a beam load cell, and how does it work. <https://www.flintec.com/weight-sensors/load-cells/how-does-a-beam-load-cell->(Date of access:25.11.2020).

**Anonymous, 2020c.** 6013 (AlMg1Si0.8CuMn, A96013) Aluminum. <https://www.makeitfrom.com/material-properties/6013-AlMg1Si0.8CuMn-A96013-Aluminum->(Date of access:20.11.2020).

**Bandara, P. 2007.** *Tension measurement by optical means.* U.S. Patent Application No: 10/575,371.

**Barat, E., Salles, A. 1996.** *Method and contactless measuring device for the tension of a filament.* U.S. Patent No: 5,493,918.

**Çelik, Ö. 2018.** Bobin sağımında iplik gerginliğine etki eden faktörlerin deneysel araştırılması. *Doktora Tezi*, Bursa Uludağ Üniversitesi Fen Bilimleri Enstitüsü, Tekstil Mühendisliği Anabilim Dalı, Bursa.

**Chifu, M. 1970.** Load Cell for High-speed Tensile Testing of Yarns. *Journal of the Textile Machinery Society of Japan*, 16(3), pp.100-107.

**Gee, S. W., L. Conder, 1984** A Strain Gauge Manual. No. ARL/STRUC-TM-378. *Aeronautical research labs Melbourne* (Australia).

**Hamed, A. M. S., Abdullah, M. Q. 2017.** Evaluation of stress concentration factor in steel elastic element of load cell. *Journal of Scientific and Engineering Research*, 4(5): 157–161.

**Hartel, R., Hoehne K.J., Hermanns, J., Henze, H., Knors, H., Engelhardt, D., Zitzen, W., Veyes, M., Merckens, H., Weissenfels, W., Ruetten, H., Jaegers, D., Pommer, B. 1994.** *Yarn tension sensor for a textile machine.* U.S. Patent No: 5,329,822.

**Lei, B., Lu, W., Mian, Z., & Bao, W. 2020.** Effect of IDT position parameters on SAW yarn tension sensor sensitivity. *Measurement and Control*, p.0020294020965620.

**Lei, B., Lu, W., Zhu, C., Liu, Q., Zhang, H. 2014.** A novel optimal sensitivity design scheme for yarn tension sensor using surface acoustic wave device. *Ultrasonics*, 54(6): 1649–1655.

**Lei, B., Lu, W., Zhu, C., Liu, Q., Zhang, H. 2015.** Optimization of sensitivity induced by substrate strain rate for surface acoustic wave yarn tension sensor. *IEEE Sensors Journal*, 15(9): 4769–4776.

**Lu, W., Feng, Y., Zhu, C., Zheng, J. 2017.** Temperature compensation of the SAW yarn tension sensor. *Ultrasonics*, 76: 87–91.

**Lu, W., Lü, X., Zhu, C., Liu, Q., Zhang, H. 2012.** Solving three key problems of the SAW yarn tension sensor. *IEEE Transactions on Electron Devices*, 59(10): 2853–2855.

**Nakayama, T., Yamazaki, C., Ohno, M. 1980.** *Yarn tension meter*. U.S. Patent No: 4,182,167.

**Shankam, V. P., Oxenham, W., Seyam, A. M., Grant, E., Hodge, G. 2009.** Wireless yarn tension measurement, and control in direct cabling process. *Journal of the Textile Institute*, 100(5): 400–411.

**Ștefănescu, D. M. 2020.** Handbook of Force Transducers Characteristics and Applications. Springer Nature. ISBN: 978-3-030-35322-3.

**Wang, Q., Lu, C., Huang, R., Pan, W., Li, X. 2016.** Computer vision for yarn microtension measurement. *Applied Optics*, 55(9), pp.2393-2398.

**Wessolowski, B., Mink, W. 1987.** *Yarn tension sensor*. U.S. Patent No: 4,677,860.

**Xiang-lin, C. Xiao-ping, C. 2008.** Modal analysis for the elastic solid of the yarn- tension sensor. *Machinery Design Manufacture* No 6: 7-8.

## **RESUME**

Name Surname : Mohamad Yazan SADOON  
Place and Date of Birth : Aleppo/Syria 1993  
Foreign Languages : Arabic, English

Education Status  
High School : Ibn Hayyan High School (2011)  
Bachelor's : University of Aleppo  
Faculty of Mechanical Engineering  
Textile Engineering Department (2017)

Contact (e-mail) : Yznsadoun@gmail.com